8-2010

Characterizing the Role of DNA Repair Proteins in Telomere Length Regulation and Maintenance: Fanconi Anemia Complementation Group C Protein and 8-Oxoguanine DNA Glycosylase

David Beomjin Rhee
brhee@utk.edu

To the Graduate Council:

I am submitting herewith a dissertation written by David Beomjin Rhee entitled "Characterizing the Role of DNA Repair Proteins in Telomere Length Regulation and Maintenance: Fanconi Anemia Complementation Group C Protein and 8-Oxoguanine DNA Glycosylase." I have examined the final electronic copy of this dissertation for form and content and recommend that it be accepted in partial fulfillment of the requirements for the degree of Doctor of Philosophy, with a major in Life Sciences.

Yie Liu, Major Professor

We have read this dissertation and recommend its acceptance:

Brynn H. Voy, Mariano Labrador, Kurt H. Lamour

Accepted for the Council:

Carolyn R. Hodges

Vice Provost and Dean of the Graduate School

(Original signatures are on file with official student records.)

To the Graduate Council:

I am submitting herewith a dissertation written by David Beomjin Rhee entitled "Characterizing the role of DNA repair proteins in telomere length regulation and maintenance: Fanconi anemia complementation group C protein and 8-oxoguanine DNA glycosylase." I have examined the final electronic copy of this dissertation for form and content and recommend that it be accepted in partial fulfillment of the requirements for the degree of Doctor of Philosophy, with a major in Life Sciences.

Yie Liu
Major Professor

We have read this dissertation
and recommend its acceptance:

Brynn Voy

Kurt H. Lamour

Mariano Labrador-San Jose

Accepted for the Council:

Carolyn R. Hodges

Vice Provost and Dean of the
Graduate School

(Original signatures are on file with official student records.)

Characterizing the Role of DNA Repair Proteins in Telomere Length Regulation and Maintenance: Fanconi Anemia Complementation Group C Protein and 8-Oxoguanine DNA Glycosylase

A Dissertation Presented for
The Doctor of Philosophy
Degree
The University of Tennessee, Knoxville

David Beomjin Rhee
August 2010

Dedication

To my father Byong Chon Rhee, for his sacrifices and encouraging words.
To my mother Kee Ja Rhee, for her unconditional love and support.
To my brother John Rhee, for being the best brother anyone could ask for.

Acknowledgements

I would first like to thank my advisor, Dr. Yie Liu for giving me a number of amazing opportunities to both initiate and expand my research career. It is also necessary to acknowledge her unwavering support and guidance through some tough times I had to face during my Ph.D. training. I also thank the members of my dissertation committee, Drs. Brynn Voy, Kurt H. Lamour, and Mariano Labrador for their participation, guidance, and many discussions which played an integral part in this study. I would also like to thank Dr. Cynthia Peterson and the Graduate School of Genome Science and Technology (GST) for the financial support, which allowed me to finish my training in time. In addition, I like to thank Dr. Vilhelm Bohr for a unique opportunity to work at the National Institute on Aging (NIA) and financial support during my fellowship there. If it wasn't for their generous supports, this study would not have been possible. I would also like to acknowledge all of our collaborators who have contributed to this study. For that, I thank Drs. Laura Haneline, Melissa Mizesko, Birija S. Patro, Nadja C. de Souza-Pinto, Avik Ghosh, and Ms. Christina Bohr for providing technical assistance, tools, and expertise necessary to complete this study. Further, I would like to acknowledge Ms. Marla Gomez, Drs. Hyekyung Plumbley, Yisong Wang, and Yonglong Zhou whom I had the pleasure of working with at the Oak Ridge National Lab. In particular, I thank Drs. Yisong Wang and Hyekyung Plumbley for their guidance and sharing of many experimental techniques with patience. I would also like to acknowledge my fellow GST students for all the memorable crammed study sessions, moral support, and good times in Knoxville. I would especially like to thank my lab-mates and friends, Drs. Richard Gianonnes and Jun Wu for their support and most importantly their friendship. I would also like to thank all the members of the Laboratory of Molecular Gerontology at the NIA whom I had the pleasure of working with for the past three years. In particular, the members of the telomere group, Drs. Jian Lu, Haritha Vallabhaneni, Zhilong Wang, Jinhu Yin, and Fang Zhou. Finally, I would like to thank my family; because, without all the sacrifices you have endured, I would not be here today.

Abstract

Telomeres are the chromosome end structures consisting of telomere-associated proteins and short tandem repeat sequences, TTAGGG, in humans and mice. Telomeres prevent chromosome termini from being recognized as broken DNA ends. The structural integrity of DNA including telomeres is constantly threatened by a variety of DNA damaging agents on a daily basis. To counteract the constant threats from DNA damage, organisms have developed a number of DNA repair pathways to ensure that the integrity of genome remains intact. A number of DNA repair proteins localize to telomeres and contribute to telomere maintenance; however, it is still unclear as to what extent.

Telomere shortening has been linked to rare human disorders that present with bone marrow failure including Fanconi anemia (FA). FANCC is one of the most commonly mutated FA genes in FA patients and the FANCC subtype tends to have a relatively early onset of bone marrow failure and hematologic malignancies. Here, we studied the role of Fancc in telomere length regulation in mice. We demonstrated that deletion of Fancc did not affect telomerase activity, telomere length or telomeric end-capping in mice with long telomeres. We also showed that Fancc deficiency accelerates telomere shortening during high turnover of hematopoietic cells and promotes telomere recombination initiated by short telomeres.

Telomere shortening has also been linked to human aging and cancer development, with oxidative stress as a major contributing factor. 8-oxo-7, 8-dihydroguanine is among the most common oxidative DNA lesions, and is substrates for OGG1-initiated DNA base excision repair. Mammalian telomeres consist of triple guanine repeats and are subject to oxidative guanine damage. Here, we investigated the

impact of oxidative guanine damage and its repair by OGG1 on telomere integrity. We demonstrated that oxidative guanine damage can arise in telomeres where it affects length homeostasis, recombination, DNA replication, and DNA breakage repair. We also examined if telomeric DNA is particularly susceptible to oxidative guanine damage and if telomere specific factors affect the incision of oxidized guanines by OGG1. We showed that the GGG sequence context of telomere repeats and certain telomere configurations may contribute to telomere vulnerability to oxidative DNA damage processing.

Table of Contents

List of Figures

List of Tables

Chapter 1: Current Understanding of Telomere Biology

1.1 Introduction

All eukaryotic linear chromosomes consist of nucleoprotein complexes called telomeres. Telomeres are composed of extended tracts of short G-rich tandem repeat sequences, 5'-TTAGGG-3', and short terminal single-stranded DNA 3'-overhangs in both humans and mice (1,2). This nucleoprotein complex includes telomere-specific binding proteins and their associated proteins (Fig. 1.1). It has been widely accepted that one of the main functions of telomeres is to prevent the ends of linear chromosomes from being recognized as broken DNA ends, thus protecting the cells from unwarranted double strand break (DSB) DNA repairs (e.g. non-homologous end-joining (NHEJ) or homologous recombination (HR)) (3). On the other hand, dysfunctional telomeres, emanating from loss of telomere repeats or loss of protection by telomere-associated proteins, can trigger a DNA damage response and subsequently lead to genome instability, cell proliferation defects, and cell death(4). To date, a number of human diseases and premature aging syndromes are frequently associated with telomere shortenings (5-7). This chapter will summarize the advancements made in the telomere field in recent years and discuss the significance of telomere maintenance in genome stability, cancer and aging in mammals.

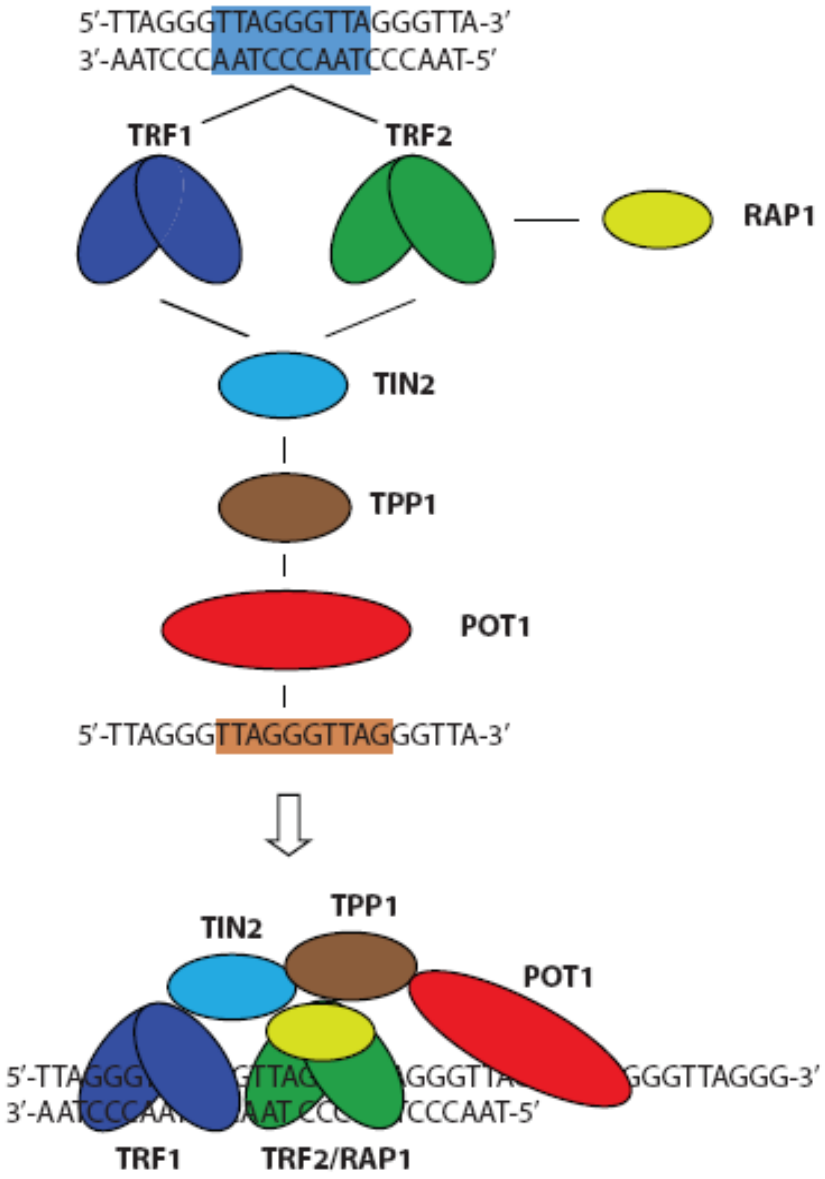

Figure 1.1 – The Shelterin Complex
The proposed assembly of shelterin complex is illustrated; six core members associate with telomeric DNA either directly or indirectly through protein-protein interactions

1.2 Shaping and Protecting the Human Telomeres – the Shelterin Complex

To date, a number of proteins have been found to localize at telomeres; however, only six have been identified as components of the shelterin complex in humans and mice. These include telomere repeat binding factor 1 (TRF1), telomere repeat binding factor 2 (TRF2), TRF interacting protein 2 (TIN2), repressor activator protein (RAP1), adrenocortical dysplasia homolog (TPP1), and protection of telomeres 1 (POT1) (Fig. 1.1). They meet the conditions, as described in a recent review article, to be components of the shelterin complex, whereas the non-shelterin proteins found at telomeres often fail to meet the following criteria. "*Shelterin is abundant at chromosome ends but does not accumulate elsewhere; it is present at telomeres throughout the cell cycle, and its known function is limited to telomeres*" (3). The complex is assumed to consist of six core members; recent attempts to expand the list of shelterin complex via mass spectrometry have failed to add additional members (8,9). Shelterin-like complexes are also found in other eukaryotes, which suggest that the complex is functionally conserved (10-13).

The functional significance of the shelterin complex depends, in part, on its components to directly bind and associate with telomeric DNA. However, not all members of the complex share this feature; only three out of the six components TRF1, TRF2 and POT1 are able to directly bind to telomeric DNA, whereas RAP1, TPP1, and TIN2 associate with telomere through protein-protein interactions as shown in **Figure 1.1**. TRF1 and TRF2 directly bind to double-stranded telomeric DNA as homodimers and serve as the basis of the complex (14,15). TIN2 plays an important role by forming a bridge between TPP1/POT1 to TRF1 and TRF2, connecting them together (8,16,17).

RAP1 associates with the telomere through TRF2 (18,19). Interestingly, POT1 not only associates with telomeres by directly binding to single-stranded telomeric DNA, but it can also associate by interacting with TRF1 or TRF2 through TPP1 (16,20,21).

When members of the shelterin complex were gradually identified and characterized, it was anticipated that shelterin complex provides protection at telomeres. Evidence now indicates that such protection occurs through members of the shelterin complex modulating/shaping the telomere's unique landscape in three ways: the t-loop formation, generation and protection of 3'-overhang, and maintenance of the telomere length. T-loop formation was initially discovered by analyzing purified telomeric DNA using electron-microscopy-based analysis (22). Briefly, the t-loop is generated by allowing single-stranded telomeric DNA of the 3'-end of the G-strand to displace the upstream G-strand and then base pair with the C-strand creating a displacement loop or D-loop, which creates a circular structure where the 3'-end of the telomeric DNA is safely tucked in (Fig. 1.2). Interestingly, the size of this circular loop varies from 1kb to 25kb in human cells, suggesting that the size of the structure is not functionally significant (3). Studies show that TRF1 and TRF2 may be involved in the formation of the t-loop since they are able to bend and modify telomeric DNA into different formations *in vitro* (15,23-25). However, it is anticipated that other shelterin proteins may also participate in the formation of the t-loop since TRF1's ability to generate t-loop *in vitro* was inefficient and addition of TIN2 seemed to increase this ability (26,27). It is also plausible that non-shelterin proteins found at telomeres (e.g. WRN, BLM, and MRN complex) may participate in the formation of the t-loop (3).

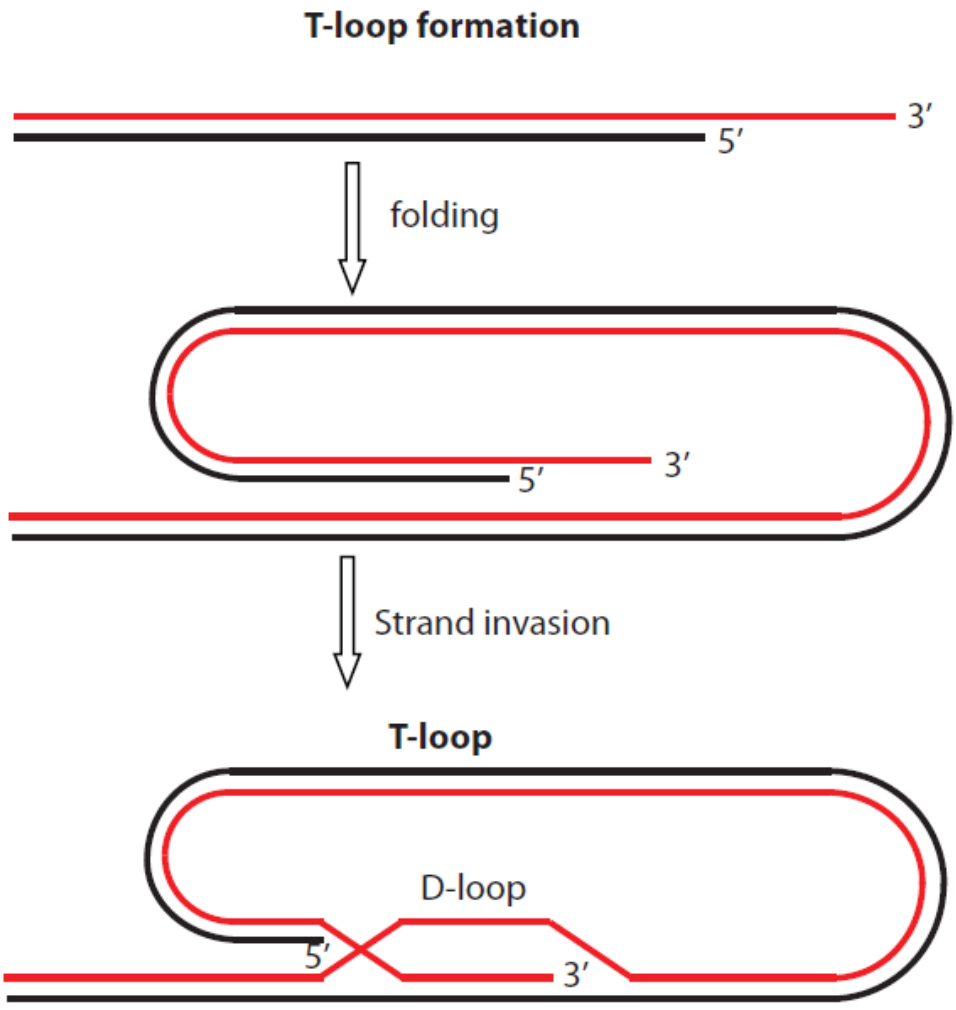

Figure 1.2 – The t-loop formation
T-loop structure is formed via strand invasion of 3'-overhang that displaces the G-strand, creating a D-loop.

The generation of the t-loop relies on strand invasion of 3' end of G-strand, which requires invading strand to be single-stranded. Studies suggest that the shelterin complex may also have a hand in shaping this part of the telomere. For instance, TRF2 has been shown to protect the junction between double-stranded and single-stranded telomeric DNA by binding and blocking the cleaving of the 3'-overhang of G-strand by ERCC1/XPF, a 3' flap endonuclease, and MRE11 nuclease, a part of MRN complex. It is hypothesized that safely-tucked in t-loops can also indirectly protect the 3'-overhang by blocking the access of nucleases (28-30). In addition, inhibition of POT1 results in a significant reduction of single-stranded 3'-overhang of G-strands in human cells, thus it is speculated that single-stranded 3'-overhang is protected from nucleolytic degradation via the binding of POT1 (31-33). POT1 is also implicated in the generation of 3'-overhang. Briefly, as a result of leading strand DNA synthesis, telomere blunt ends may require nucleolytic processing on the newly synthesized daughter strand (3). It is hypothesized that POT1, which prefers to occupy the 3'-overhang just two nucleotides from the junction of double-stranded telomeric DNA, may simply block the 5' exonuclease from further processing the terminal structure (3,31,34). However, the nuclease responsible for the processing of 5' strand is still unclear.

The maintenance of telomere length has proven to be a dynamic process in which cooperation between the members of shelterin complex and telomerase, a reverse transcriptase responsible for telomere extension (covered in next section), dictates the outcome. Briefly, it was demonstrated that shelterin proteins can either inhibit or promote (negative or positive feedback loops, respectively) the access of telomerase to telomeric

DNA. In terms of negative regulation, long telomeres most likely trigger a cis-acting mechanism that inhibits the access of telomerase since a large quantity of shelterin is available at telomeres (35). In contrast, short telomeres trigger the relaxation of this inhibition mechanism imposed by shelterin at telomeres; this is most likely due to limited quantity of telomeric DNA available for shelterin proteins to bind (Fig. 1.3). A mutant version of POT1, which can not bind to single-stranded telomeric DNA, caused extremely long telomeres, possibly as a result of its inability to inhibit the telomerase accessing telomeric DNA (36,37). Additional studies demonstrating a similar effect in TRF1, TRF2 and RAP1 further supports the view that the shelterin complex has a role in controlling the length of telomere (38,39).

In eukaryotes, disruption of the t-loop and subsequent exposure of the 3'-overhang (telomere uncapping) can lead to destabilized telomeres. Consequently, destabilized telomeres (dysfunctional or uncapped telomeres) are known to elicit DNA damage response pathways since the "capped" telomere normally inhibits such events from taking place (3,4). For instance, introduction of a dominant-negative form of TRF2 inhibits the binding of endogenous TRF2 to telomeric DNA by heterodimerizing with the endogenous protein (28); this results in the activation of ATM kinase pathway and the subsequent up-regulation of p53-dependent and p21-mediated G1/S arrest (40-42). Furthermore, when other shelterin components POT1 and TIN2 were inhibited or the length of telomeres is shortened, DNA damage response markers such as 53BP1, γ-H2AX, MRN complex, and ATM-Ser-1981-P accumulate at telomeres and form a structure now known as the Telomere dysfunction Induced Foci (TIF) (26,31,43). Studies

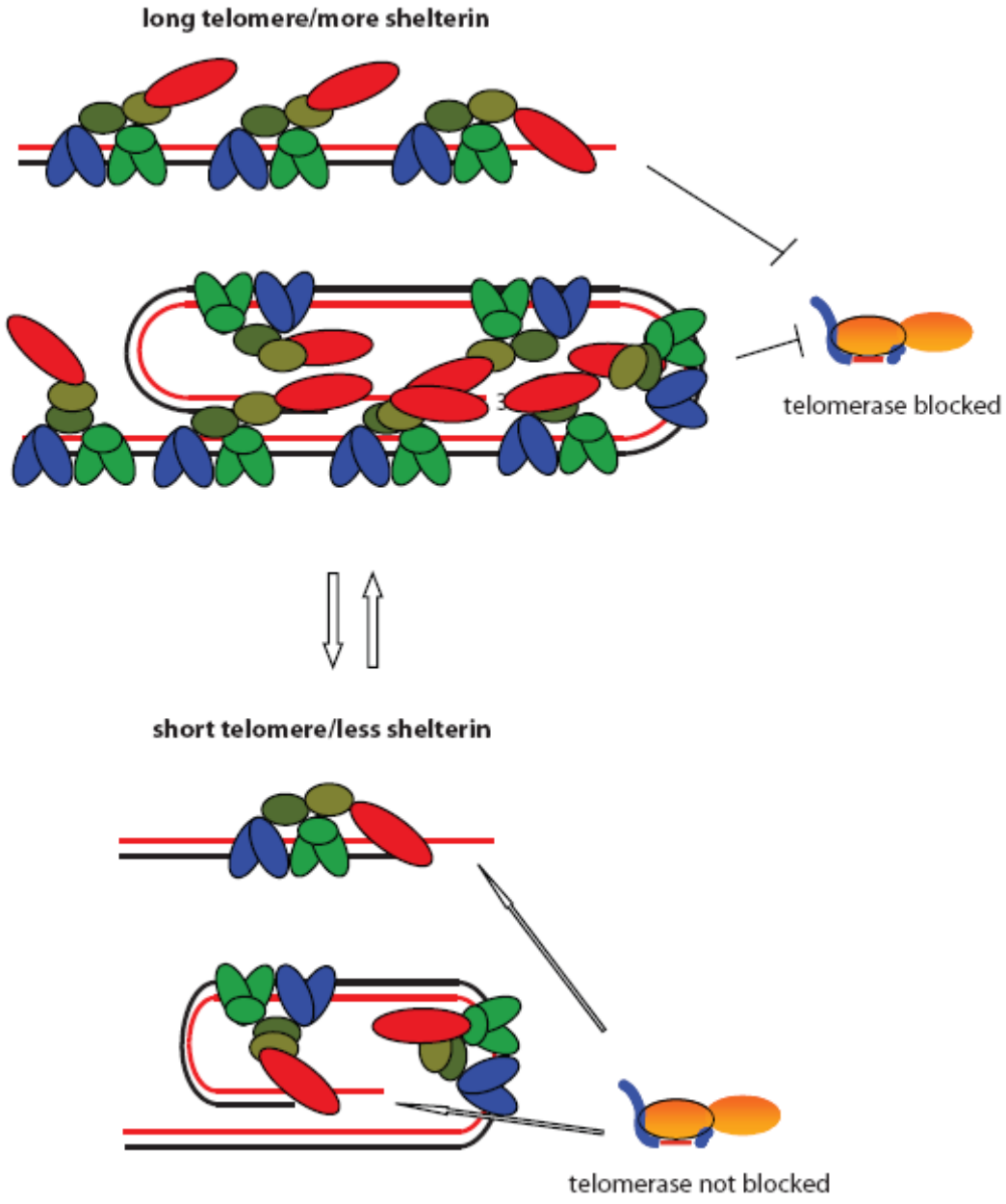

Figure 1.3 – The telomere length regulation via shelterin
The accessibility of telomerase to telomeric DNA depends on the amount of shelterin proteins available at telomeres.

using ATM-deficient cells and caffeine, inhibitors of ATM and other PI3-like kinases, lead to a decrease in TIF formation, which suggest that DNA damage response at the telomere is dependent on ATM and PI3-like kinase pathways (43). However, it is still unclear how functional telomeres prevent ATM activation at telomeres. It is thought that TRF2 can directly interact with ATM and inhibit its phosphorylation at serine-1981, which is required for its activation (44,45).Overall, it appears that DNA damage response at telomeres is a general damage response that is not specific to telomeres.

Aided by the shelterin complex, functional telomeres not only protect the ends of linear chromosomes from DNA damage response but also from undesirable recombination repairs such as nonhomologous end-joining (NHEJ) and homologous recombination (HR). These repairs are known to create problems at telomeres. For instance, NHEJ between two ends of telomere causes abnormal chromosome end-to-end fusions resulting in a circular or a dicentric chromosome. These events could lead to chromosome segregation defects during cell division, thus forming a characteristic chromatin bridge of dicentric chromosome in anaphase cells; this could result in chromosome breakage or cytokinetic failure leading to aneuploidy and eventually apoptosis or cancer (Fig. 1.4A) (4). The shelterin components (e.g. TRF2 and POT1) protect telomeres from aberrant NHEJ since a lack of function results in fusion between two telomeres (31,33). More over, critically short telomeres (i.e. uncapped telomeres) can trigger NHEJ at telomere ends (4). Interestingly, the 3' overhang poses an obstacle to telomeric NHEJ since the process requires two blunt ends. In mammals, ERCC1/XPF endonuclease is implicated in removing the 3' overhang in telomeres before NHEJ

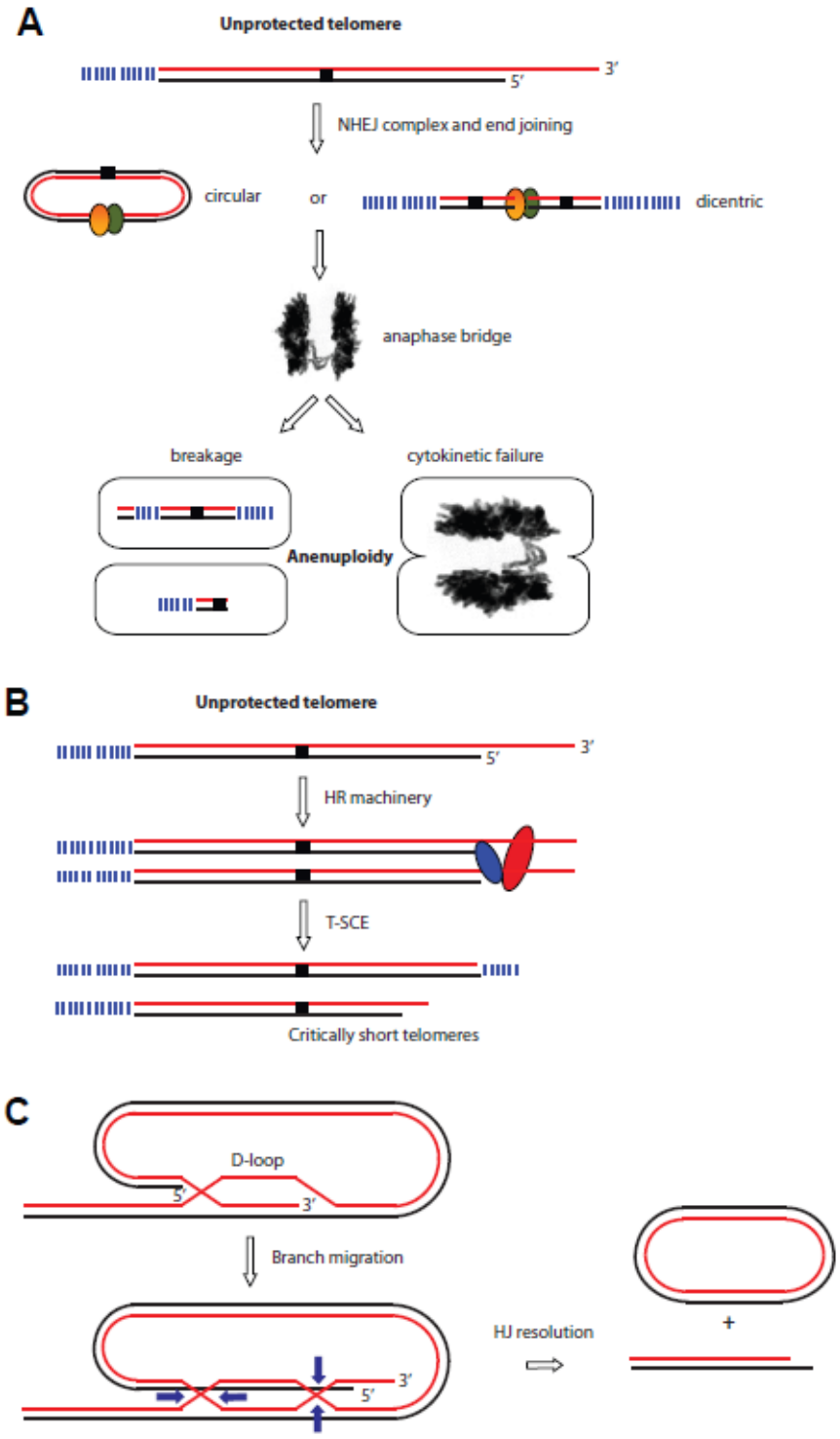

Figure 1.4 – DNA repairs such as NHEJ and HR can create havoc to telomere integrity
A) Chromosome end-to-end fusion from NHEJ could result in aneuploidy. B) HR between two sister chromatids through T-SCE could have severe consequences as a result. C) T-loop HR could shorten telomeric DNA by truncating the circular part of t-loop.

machinery can fuse the two telomeres (29). However, the events leading up to recruitment of nucleases and activation of NHEJ is still unclear. Nonetheless, it is thought that functional telomeres prevent NHEJ through t-loop formation since its circular structure can hide the 3' ends from being accessible to ERCC1/XPF endonuclease that NHEJ machinery depends on (3,41).

Telomeric homologous recombination is another aberrant repair that is known to be detrimental; it can lead to abnormal telomere length and collapse of the t-loop. For instance, branch migration of the t-loop toward the centromere can result in double holiday-junction and if the resulting structure is resolved by crossover, the entire loop segment can be lost, leaving critically shorten telomeres (Fig. 1.4C) (46). The shelterin protein TRF2 protects telomeres from such events since a loss of function results in sudden truncation of telomeres and appearance of circular extrachromosomal telomeric DNA (47,48). Further examination revealed that these truncations were dependent on proteins implicated in HR, the MRN complex and XRCC3, a protein involved in holiday-junction resolution (49). However, an exact mechanism of TRF2 suppressing the t-loop HR is not well understood. The telomere sister chromatid exchange (T-SCE) is another telomere-specific recombination event, in which one of the sister chromatids maintains its telomere length by using the other as a template (50). Thus, if the length of two sister chromatids were different, one could be lengthened at the expense of the other, risking the possibilities of acquiring critically short telomeres via HR (Fig. 1.4B) (51). These two HR events are closely related since relaxation of repression can be observed in alternative lengthening of telomere (ALT) cells (52), suggesting that tight control of telomeric HR is

strictly enforced via shelterin complex under normal circumstances; thus strengthening the importance of the shelterin complexes' role in providing protection of telomeres.

1.3 Telomere Length Regulation – Telomerase or Alternative Lengthening of Telomere (ALT)

In living organisms, DNA is replicated in a "semi conservative" fashion where the complementary strands are synthesized using each parental strand as a template. This process is mainly carried out by DNA polymerase enzymes which are only able to synthesize DNA in the 5' to 3' direction. In cells with linear chromosomes, the leading strand can be replicated in a continuous manner, whereas the lagging strand is replicated in a discontinuous manner by the use of Okazaki fragments. The Okazaki fragment typically cannot bind to the very tip of the 3' end of lagging strand for further replication, which means that chromosomes will gradually get shorter after each successive round of DNA replication (Fig. 1.5A). This is known as the "end-replication problem" which could compromise the integrity of the genome due to loss of genetic information at the end part of the chromosomes (53). Eukaryotic cells have evolved to counteract the "end-replication problem" by using telomeres as a buffer zone and extending it through the enzyme telomerase. Telomerase is ribonucleoprotein complex composed of telomere reverse transcriptase, TERT, with its own RNA molecule, TERC, and dyskerin. The template region of TERC is 3'-CAAUCCCAAUC-5', which telomerase uses to extend new telomeric DNA repeat (5'-GGTTAG-3') sequence by using the first few nucleotides of the template at the 3' end of the leading strand (Fig. 1.5B). As discussed in **Section 1.2**,

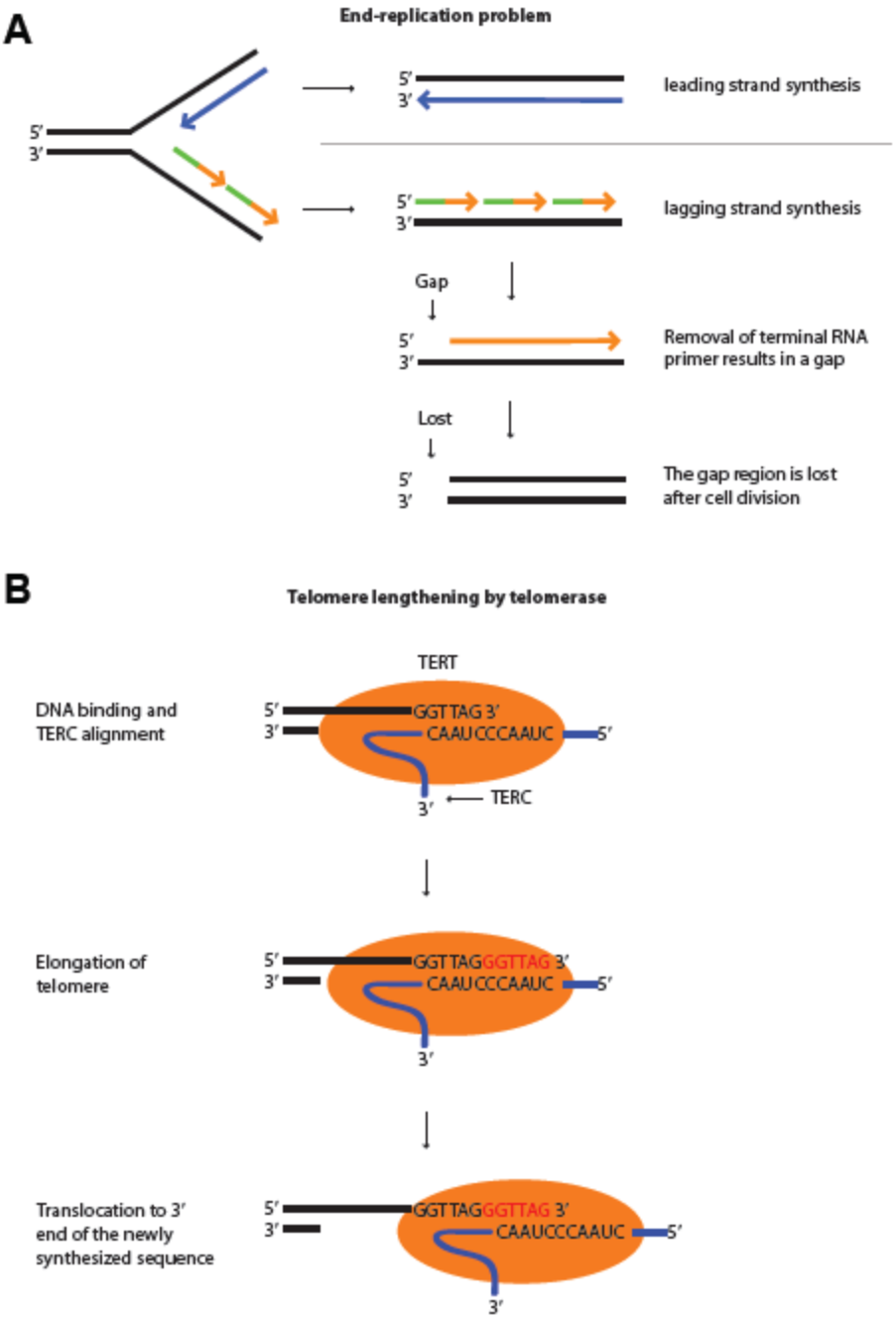

Figure 1.5 – Telomere length regulation via Telomerase
A) The end-replication problem; inability to replicate part of the lagging strand could lead to genetic information loss at the ends of linear chromosomes. B) Telomeres are elongated by telomerase, a holoenzyme which consist of a reverse transcriptase (TERT) and RNA molecule (TERC).

the members of shelterin complex and telomerase collaborate through carefully choreographed *cis/trans* mechanism to ensure that the telomere length is maintained above a critical level (54).

L. Hayflick made an observation that human fibroblasts, when cultured, had a life span of ~50 population doublings before succumbing to cellular senescence. This phenomenon is widely known as the Hayflick limits. It was later discovered that adult stem cells and somatic cells, such as primary fibroblasts, lack the ability to regenerate telomeric DNA since they either have low or no telomerase activity, therefore contributing to cellular senescence. However, not all cell types share this characteristic; germ cells have high telomerase activity, and are thus believed to go on dividing for the lifetime of the organism. In addition, another class of cells that has high telomerase activity and have unlimited potential to divide are cancer cells. Most cancer cells are known to reactivate telomerase, which is an important feature of the cellular immortalization process (55). Indeed, there is a technique used to immortalize primary cells involves transfecting them with telomerase; thus demonstrating that telomerase activity and maintenance of telomere length allow for long term cellular survival (56). This suggests that cellular immortalization has high correlation with reactivation of the telomerase enzyme, and prior studies have also shown that about 85-90% of all cancers have active telomerase (57). Interestingly, about 10-15% of all cancers do not have active telomerase (57), and studies have shown that these cells utilize a mechanism known as the alternative lengthening of telomere (ALT) to maintain their telomere length (58).

The initial discovery of ALT was made when human cell lines, without any noticeable telomerase activity, were found that are able to uncharacteristically maintain their telomere length over many cell divisions (59). These ALT cells have a unique set of phenotypic characteristics different from that of telomerase positive cells (52). One of the most important features of ALT cells is that they have long and heterogeneous telomeric DNA ranging from 2kb to 50kb in length along with few ends with a little or no visible telomeric DNA, also known as the telomere signal free ends (60). Furthermore, ALT-associated promeylotic leukemia nuclear bodies (APBs) are often found in ALT cells. These APBs can be easily identified using a standard indirect immunofluorescence technique since they contain extrachromosomal telomeric DNA in both linear or circular form (termed t-circles), shelterin proteins (i.e. TRF1 and TRF2), PML protein, and DNA repair proteins (46,61-63). It has been suggested that one of APB's function is to act as a garbage collector for extrachromosomal telomeric DNA to prevent unnecessary DNA damage responses (61). Also, there is evidence suggesting that APBs are the sites of ALT activity. The frequency of APB-positive cells is much higher during G2 phase when ALT is thought to take place; HR, a key mechanism in ALT, is also most active during this phase (64,65). Interestingly, not all ALT cells share these unique phenotypic characteristics since some ALT cell lines without telomerase were shown to lack some of these characteristics (58); therefore it is still unclear how these phenotypic characteristics are associated to the ALT mechanism.

A number of studies suggest that ALT cells maintain their telomere length through a HR-dependent mechanism. For instance, ALT cells characteristically have

increased levels of two different types of telomere-specific HR events when compared to non-ALT cells; HR-dependent telomeric DNA replication and post-replicative T-SCE (Fig. 1.6) (66). Earliest evidence to support the occurrence of HR-dependent telomeric DNA replication in ALT cells was uncovered by performing recombinational telomere extension (RTE). Briefly, when a DNA tag was inserted within telomeric DNA repeats, ALT cells were able to duplicate the tags into other telomeres whereas no duplication was made in telomerase-positive cells; it failed to duplicate in a sub-telomeric region when subjected to similar treatment (67). Although an exact mechanism is not established, studies indicate adjacent telomeres in addition to extrachromosomal telomeric DNA (i.e. linear and t-circles) can be used as a template in HR-dependent telomere replication in ALT cells (66). Accumulating evidence demonstrates that there is significant increase in the frequency of T-SCE in ALT cells compared to non-ALT cells. Simultaneously, there is no significant increase in the rate of recombination frequencies at the genomic regions in ALT cells as compared to non-ALT cells, which indicates that increased recombination events in ALT cells are telomere-specific (68,69). The mechanism behind T-SCE is still unclear. It is thought that repair of a broken replication fork at telomere can initiate telomeric-HR, thus leading to T-SCE (66).

The relationship between proteins involved in HR-dependent telomere maintenance and ALT-related activities remains to be a complex issue. It appears to require the usual proteins involved in functional telomere maintenance (66). To date, only two protein complexes, MRN and SMC5/6, have been shown to participate in telomere length maintenance in ALT cells; inhibition of these proteins led to significant reduction

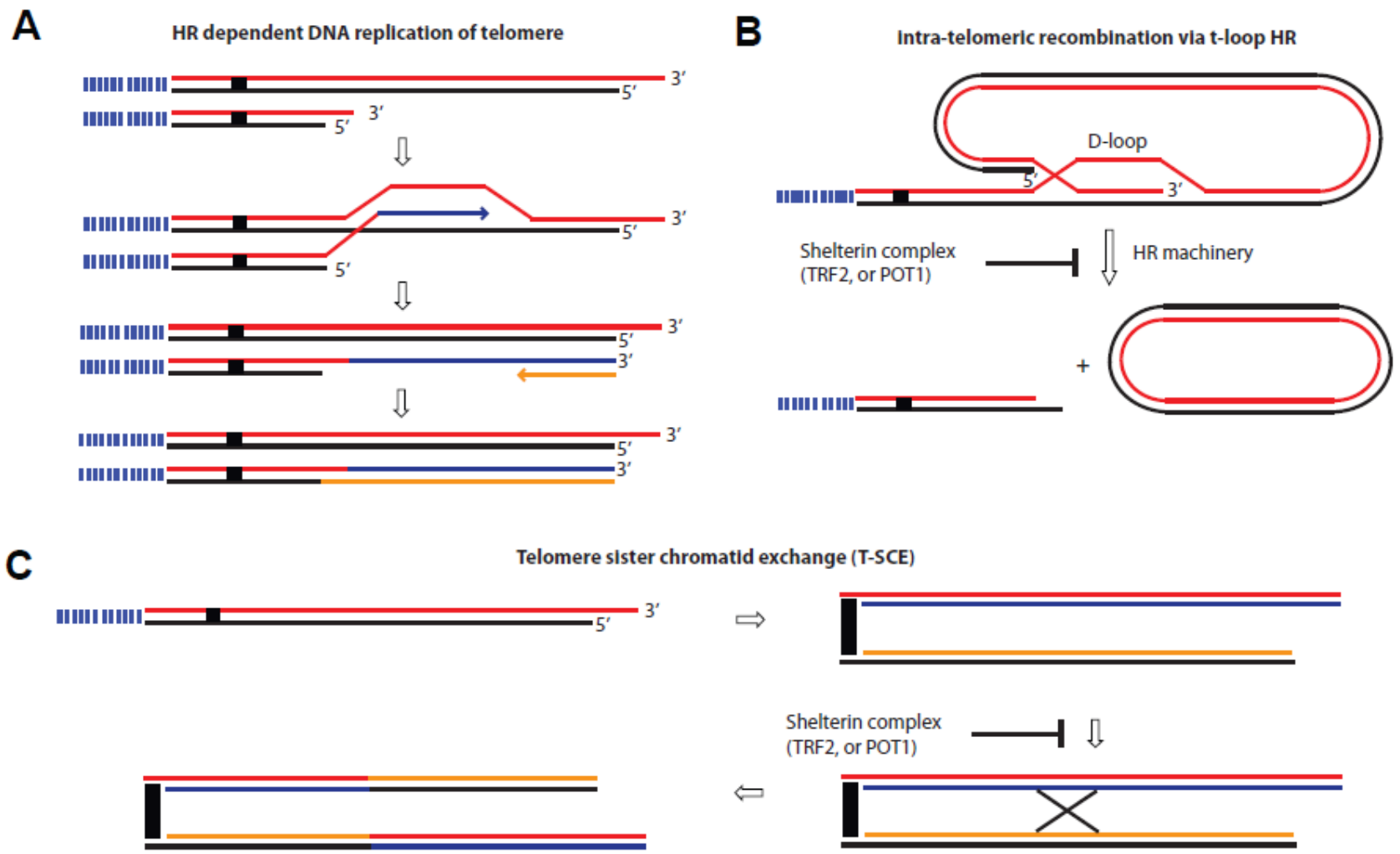

Figure 1.6 – HR-dependent telomere maintenance in ALT cells
A) HR-dependent DNA replication. B) T-loop resolution C) Telomere recombination via T-SCE.

in amount of APB-positive cells (70,71). The accumulation of shelterin and its associated proteins in APB also suggest that they are involved in ALT activity but it is still unclear as to what extent. How the ALT mechanism is suppressed and/or initiated and which proteins are involved is still being debated, however, it has been considered that a loss of protection by the shelterin complex could serve as one of the possible starting points as discussed in **Section 1.2**.

1.4 Telomeres and Disease

As discussed in **Section 1.3**, somatic and adult stem cells have little or no telomerase activity as compared to germ cells, and, as a result, this eventually leads to progressive telomere shortening with age. Depending on the cell type, short telomeres could ultimately contribute to cellular senescence (fibroblast) and apoptosis (epithelial), which can be detrimental to an organism's well-being (42). In fact, short telomeres are frequently observed in a number of late stage cancers, premature ageing syndromes and human diseases that are associated with ageing (72-74). For instance, human diseases of various origins that are associated with ageing, such as heart disease, liver cirrhosis and atherosclerosis are characterized as having short telomeres when compared to healthy individuals (75-77). In addition, a correlation between the risk of death from heart disease and telomere length has been recently demonstrated (78). Taken together, these observations suggest that there is a correlation between telomere length maintenance and the manifestation of human diseases associated with short telomeres. However, it is still

unknown if the diseases are caused by short telomeres or accelerated telomere attrition is the result of the disease itself.

A number of human premature ageing syndromes have been instrumental in providing our current knowledge of telomere loss and its consequence due to their accelerated rate of telomere shortening with age. One such syndrome is dyskeratosis congenita (DC). It is a rare but genetically diverse and age-associated disease that is frequently identified by the triad of classical symptoms of dysplastic nails, oral leukoplaskia and hyperpigmentation of skin. DC is the quintesential form of the inherited bone marrow failure syndrome (IBMFS) that represents a clinical consequence of short telomeres, many cases of disease exhibit mutations in the shelterin component, TIN2, or the components of telomerase: *Tert, Terc*, or dyskeratosis congenita 1 (*DKC1*) genes. Mutations in any one of these genes in telomerase have shown to reduce telomerase activity and result in accelerated telomere loss along with elevated incidence of chromosomal instabilities in DC patients (79,80). Additionally, other forms of IBMFS such as acquired aplastic anemia (AA) and idiopathic pulmonary fibrosis (IPF) have also been shown to possess mutations in the telomerase components, resulting in accelerated telomere attrition and ultimately premature death (81,82). In contrast, however, a number of human premature ageing syndromes associated with accelerated telomere loss and chromosomal instability do not have mutations in genes encoding the telomerase complex. Instead, these syndromes have mutations in genes that encode DNA repair proteins, e.g., Nbs1 (Nijmegen breakage syndrome), Mre11 (Ataxia telangiectasia–like disorder), WRN (Werner syndrome), BLM (Bloom syndrome), ATM (Ataxia

telangiectasia) and proteins encoded by *FANC* (Fanconi anemia complementation group proteins) genes. However, many of these proteins are known to play a role at telomeres, thus may contribute to telomere length maintenance (83).

Ever since the practice of employing a knock-out mouse model has been popularized, it has become instrumental in examining gene functions in the context of the whole organism. The telomerase knock-out model, generated by eliminating the mouse *Terc or Tert* genes, has helped in illustrating the consequence of aberrant telomere length maintenance (84-87). Studies indicate that the telomerase-deficient mouse model is characterized with atrophies of various tissues and a loss of long-term viability where only a limited number of generations can be obtained (88-91). More importantly, the phenotypes of the telomerase knock-out model emulate some of pathologies illustrated in age-related human diseases and premature ageing syndromes (92). For instance, recent studies have shown that the telomerase knock-out mouse model partially showed symptoms similar to DC patients, such as short stature, infertility, premature death, and, most importantly, defective hematopoietic system and bone marrow defect. Interestingly, DC patients have increased occurrences of spontaneous cancer, whereas *Terc*-deficient mice showed elevated resistance to cancer. A possible rationale for this difference could be that some DC patients still have intact telomerase function which could be unexpectedly up-regulated during tumorigenesis; *Terc*-deficient mice have no telomerase activity (92-94). The phenotype discrepancy between knock-out mouse model and its representative human disease extends to other age-related diseases with short telomeres. For instance, fanconi anaemia (FA) mouse models have normal telomeres and do not

fully reproduce the human disease phenotype (95). Similarly, knock-out mouse models for human premature ageing syndromes such as BLM and WRN do not emulate the full-blown human manifestation of the disease and, more importantly, do not reproduce premature ageing pathologies (96,97).

Inbred mice have unusually longer telomeres and higher telomerase activities than humans. Therefore, it is believed that some human-disease mouse models' inability to manifest the pathological phenotypes is probably due to lack of critically short telomeres. In agreement with this idea, mouse-model deficient in *Terc* and some DNA repair genes show an acceleration of the ageing phenotypes. For instance, Werner, Bloom and ATM mouse models in conjunction with telomerase deficiency featured some pathological phenotypes observed in human patients (98-100). This demonstrates that short telomeres contribute to the generation of, or may be required for, these premature ageing diseases. Taken together, these observations strengthen the notion that telomerase activity and telomere length maintenance play an important role in the manifestation of human diseases associated with accelerated telomere attrition.

1.5 Oxidative DNA Damage in Telomere Attrition and Aging

Telomere attrition is frequently associated with aging and premature aging syndromes, and it has been proposed that oxidative stress plays a role in telomere attrition in aging (101). High oxygen levels and mitochondrial dysfunction-induced reactive oxygen species (ROS) accelerate telomere shortening and reduce the proliferative lifespan of human somatic cells *in vitro*, whereas these phenotypes are delayed when

cells are grown in low oxygen or in the presence of antioxidant (101). Interestingly, human cells with long telomeres show increased sensitivity to hydrogen peroxide, but not to etoposide and bleomycin, supporting the notion that telomeres are particularly vulnerable to oxidative damage (102). High oxygen levels also severely limit the replicative lifespan of primary mouse embryonic fibroblasts (MEFs) (103), however, it is not known if oxidative stress causes telomere-shortening and telomere capping defects in MEFs. Nevertheless, primary MEFs with critically short telomeres display a premature senescence-like arrest as well as reduced spontaneous immortalization (104). These results suggest that oxidative stress associates with telomere defects, which, in turn, play a role in cellular senescence *in vitro*.

A number of reports demonstrate that oxidative DNA damage causes more single strand breaks (SSBs) in telomeric than in non-telomeric DNA, and it has been proposed that SSBs could be a major cause of telomere shortening (105). The telomeric G triplets are especially sensitive to cleavage by H_2O_2 or benzoyl peroxide plus Cu(II), UVA plus riboflavin, and H_2O_2 plus Fe^{2+} *in vitro* (106-108). Oxidative stress by prolonged culture in the presence of 20% oxygen or H_2O_2 increases the frequency of SSBs in telomeres, especially in the G-strand (109,110). Several studies have shown that oxidation also induces oxidative base damage preferentially at telomeric DNA *in vitro*. For example, oxidative damage is several fold more efficient in inducing 8-oxo-7,8-dihydroguanine (8-oxodG) in oligonucleotides containing telomeric repeats than non-telomeric repeats, even though the latter have similar G-content (106-108). Oxidized guanines occur at either the 5' or the middle G in GGG triplets (106-108). Thus, telomeric G triplets may act as sinks

for oxidative damage, and the presence of enough telomere repeats may serve as a buffer to protect the bulk genome from oxidative DNA damage. *In vitro* experiments show that the presence of 8-oxodG at single- or double- stranded telomeric nucleotides disrupts telomerase activity (111) and inhibits binding of TRF1 and TRF2 (112), respectively. 8-oxodG lesions at every telomeric repeat dramatically reduce binding of TRF1 and TRF2 (112). However, it is not clear whether 8-oxodG or other oxidized bases accumulate and have similar effects at telomeres *in vivo*. Thus, thorough investigation on this matter is warranted since evidence indicates that these shelterin proteins regulate telomerase extension, telomere capping, and efficient telomere replication (3,4).

1.6 Summary

The mammalian telomeres provide protection at the ends of linear chromosomes which is an essential aspect in maintaining overall genome stability. A number of factors contribute to this protective role, mostly through concerted efforts between core members of the shelterin complex and its associated proteins, and telomerase. Failure to cap the chromosome ends have shown to have devastating effects, which include, but are not limited; to cell death, cell proliferation defects and increased incidence of malignancies. The importance of telomere integrity can be observed in a number of age-related human diseases and pre-mature ageing syndromes. These disorders have mutations in genes regulating telomere maintenance, accompanied by accelerated telomere shortening. Studies indicate that the maintenance of telomere length is tightly regulated and that it requires a highly specialized group of proteins for its maintenance. Telomerase, a ribonucleoprotein complex, replenishes replication dependent-telomere repeat loss and is

essential in telomere length maintenance. However, ALT mechanism can provide length maintenance through HR-dependent DNA repair if necessary.

Although our current understanding of the telomere field has grown immensely, there are still many unanswered questions which need to be addressed. In particular, a clear picture of telomere maintenance and its relationship with DNA repair is warranted. This will help foster a better understanding of the functional significance of telomeres and could one-day lead to therapeutic solutions for a range of human disorders.

Chapter 2: Introduction to DNA Repair Proteins

2.1 Introduction

The structural integrity of DNA is continuously challenged by a daily assault from a variety of DNA damaging agents (both endogenous and exogenous). Exogenous DNA damages come from various environmental sources such as ultraviolet radiation (UV), ionizing radiation (IR) and chemicals, while endogenous DNA damages mostly come from reactive oxygen species (ROS) generated from cellular metabolism. It is estimated that roughly thousands of single strand breaks (SSB) and spontaneous base losses occur daily in the nuclear genome of every cell; inclusion of other types of spontaneous DNA damages generate a total number of DNA damages of approximately 100,000 lesions per day. When these staggering amounts of damages are not properly repaired, it can lead to genome instability, cell proliferation defects, and cell death. These effects have been known to cause embryonic lethality, accelerated ageing, cancer, and a number of premature ageing syndromes at the organism level (113).

To counteract the constant threats from DNA damage, organisms have developed a number of DNA repair pathways to ensure that the integrity of genome remains intact. These pathways include, but are not limited to the base excision repair (BER) pathway, the mismatch repair pathway, the nucleotide excision repair pathway, the homologous recombination pathway, and the non-homologous end joining pathway; each repair pathway specializing in specific types of DNA damage (Fig. 2.1). Although most of these

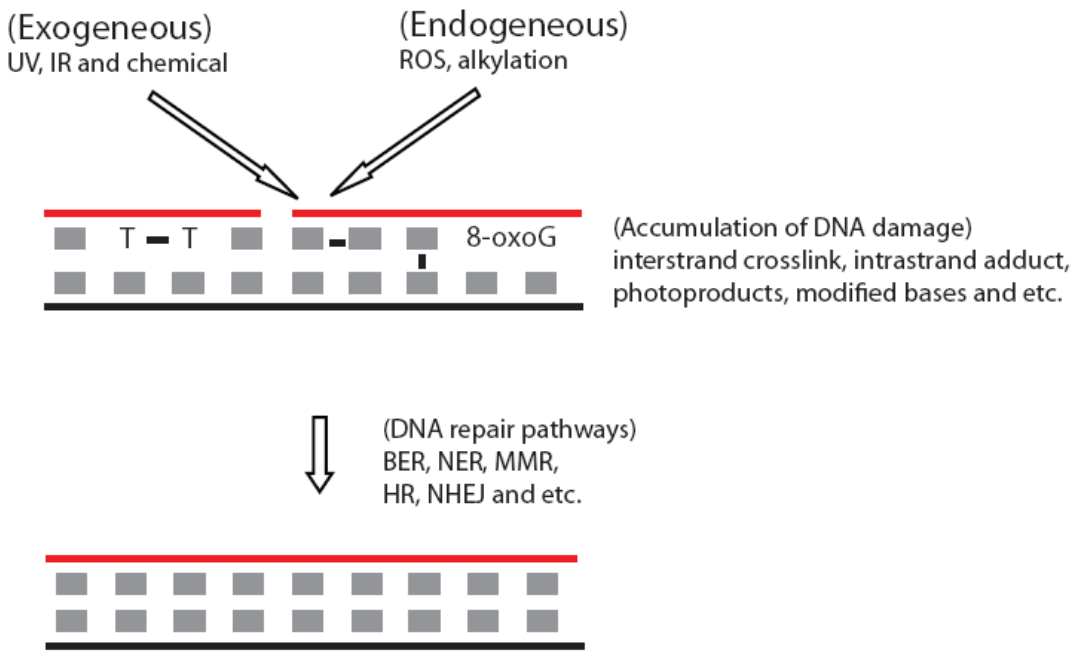

Figure 2.1 – The DNA repair pathways
The diagram demonstrates the consequence of DNA damage from a variety of damaging agents and subsequent DNA repair via multiple pathways.

repair pathways utilize a number of repair proteins, in some cases, loss of function of key repair proteins can have serious consequences. On the other hand, loss or inactivation of some repair proteins do not impact their respective repair pathways since they lack functional significance at both the cellular and organism level (114). These findings suggest that not all DNA repair proteins are created equal. Thus, careful examination of their roles in their respective repair pathways will expand our understanding and may play a crucial part in the development of treatment and drugs for various human diseases. In this chapter, two repair proteins will be examined; in particular, 8-oxoguanine DNA glycosylase-1 (OGG1) and Fanconi Anemia Complementation Group C (FANCC), and their role will be discussed in their respective DNA repair pathways.

2.2 OGG1 and the BER pathway

The BER pathway is one of the simplest yet most highly conserved pathways among other predominant DNA repair pathways in mammalian system. It is the primary DNA repair pathway that repairs non-bulky damaged bases, abasic sites, and SSBs induced by methylation, ROS, and spontaneous hydrolysis (115). Although it is one of the simplest among other repair pathways, there are two modes of repair as illustrated in **Figure 2.2** and described below.

The initial step in BER is base removal by a DNA glycosylase. The enzyme first recognizes a specific damaged base then cleaves the glycosylic bond that links the base to the sugar phosphate backbone. This creates an abasic site, also known as the apurinic/apyrimidinic (AP) site. The removal of the AP site is crucial since these sites can

also occur through spontaneous depyrimidination and depurination and is highly mutagenic (116,117). The subsequent repair steps involve either short patch repair, in which only one damaged nucleotide is replaced, or long patch repair, in which up to thirteen adjacent nucleotides are replaced along with the damaged one, both pathways involve the incision of the phosphodiester backbone by the abasic endonuclease (APE1). In the short patch pathway, mammalian polymerase beta's (Pol β) deoxyribophosphodiestrase (dRPase) activity removes the 5'-dRP terminus left by APE1. On the other hand, either mammalian Pol γ or Pol ε extends from the 3'-OH group created by APE1 for up to thirteen nucleotides by displacing the strand containing the 5'-dRP terminus in long patch repair. The resulting 'flap' structure in long patch repair is promptly removed by the structure-specific flap endonuclease (FEN1), producing a gap. Subsequently, the gap in both short and long patch repairs is filled in by Pol β, followed by either DNA ligase I or III, which seals the remaining DNA strand breaks.

Alternatively, subsets of DNA glycosylases possess additional AP lyase activity. For example, OGG1 and endonuclease VIII (Nei)-like protein 1 (NEIL1) can both excise the damaged base and then additionally incise 3' to the AP site, producing a SSB with either a 3'-α,β unsaturated aldehyde or a 3'-phosphate (118). The resulting 3' terminus is cleaned by 3' diestrase activity of APE1, followed by repair synthesis by Pol β, and nick sealing by DNA ligase I or III (Fig. 2.2). These DNA gylcosylases with additional functions are considered bifunctional while monofunctional glycosylases such as uracil DNA glycosylase (UNG) have only glycosylase activity. They require additional enzyme such as APE1 for the incision of subsequent AP sites (118). All DNA glycosylases can

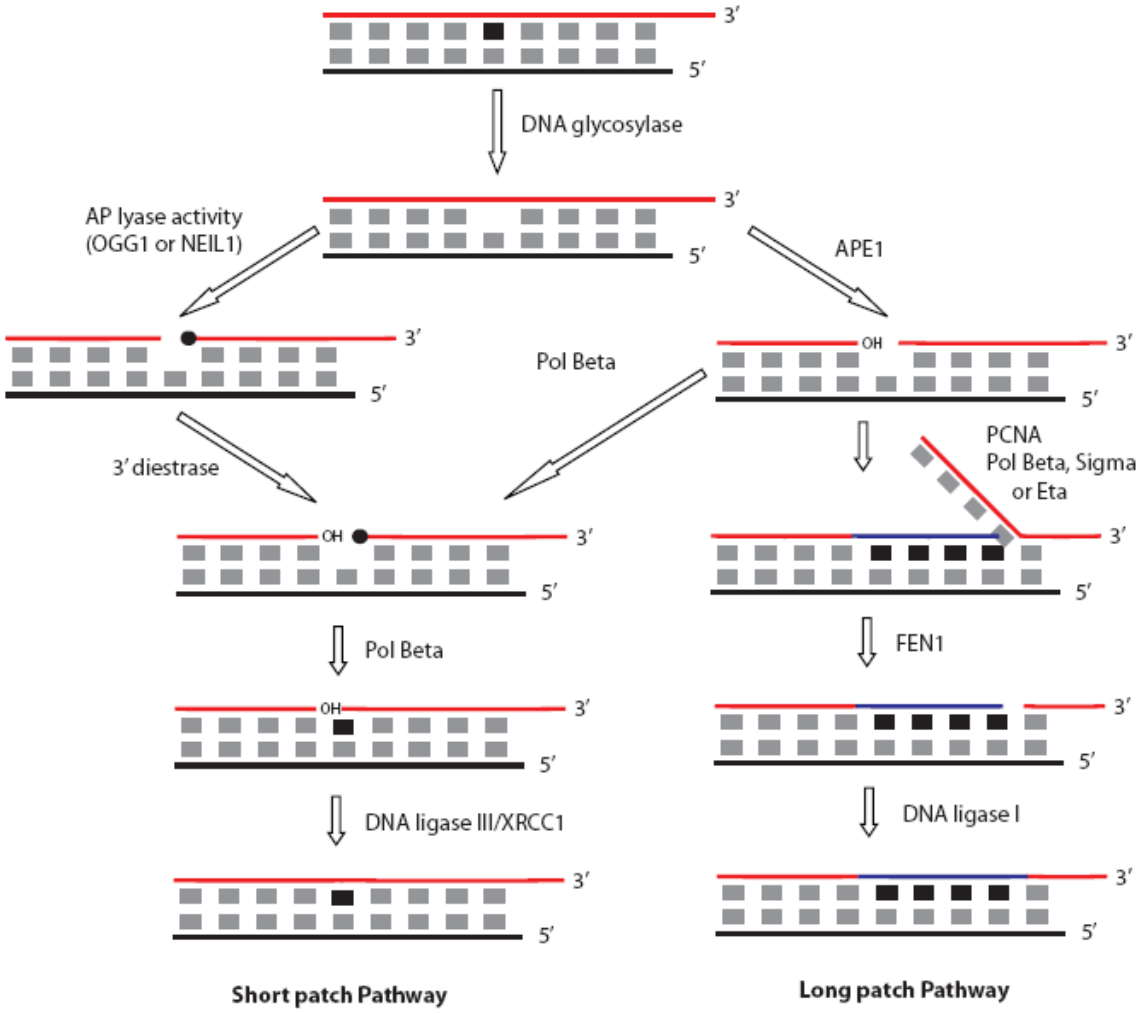

Figure 2.2 – The Base Excision Repair (BER) pathway
It divides into two pathways, short patch and long patch, and utilizes overlapping components with few exceptions.

cleave glycosylic bonds, however, each enzyme has its own preference to specific base substrates and reaction mechanisms. Several DNA glycosylases with distinct but overlapping substrate specificities have been characterized (Table 2.1). For example, DNA glycosylases such as OGG1 and NTH1, which belong to the *E. coli* endonuclease III (Nth) family, excise oxidized base lesions in double strand DNA. NEIL1 and NEIL2 DNA glycosylases, which belong to *E. coli* Fpg/Nei family, can also excise base lesions in double strand DNA, but their preferred DNA substrates are single strand DNA, bubble DNA, or forked DNA (119). The adenine-specific mismatch DNA glycosylase, MYH, removes the adenine opposite 8-oxodG (120,121).

BER pathways have been well-characterized for their role in repairing oxidative lesions which are produced at high rates via both endogenous and exogenous DNA damaging agents. The endogenous DNA damage is mainly caused by ROS attacks and guanines are particularly susceptible to ROS oxidation since they have a low redox potential (122). Particularly, it is estimated that approximately 100–500 8-oxodG lesions are formed in a cell everyday (123). 8-oxodG is one of the most frequent and widely-studied forms of DNA damage generated by ROS and is commonly used as a biomarker for oxidative stress level (124). 8-oxodG can be extremely harmful to cells because it is able to mimic thymine in the *syn* conformation by forming an 8-oxodG (*syn*) to adenine (*anti*) base pair. This structural modification is brought upon by addition of an oxo group on the 8^{th} carbon (C8) and a hydrogen atom on the 7^{th} nitrogen (N7) (Fig. 2.3). If not repaired, DNA polymerases can bypass 8-oxodG during DNA replication, and results in guanine-to-thymine transversion mutations as a consequence (122). To alleviate this high

Table 2.1 – DNA glycosylase substrate specificity

Enzyme	Type	DNA substrate	Preferred lesions*
OGG1	Bifunctional	dsDNA	8-OxoG, Fapy G; prefers lesion opposite C
NTH1	Bifunctional	dsDNA	5-OHU, 5-OHC, TG, Fapy G, Fapy A
NEIL1	Bifunctional	ssDNA, bubble, fork and dsDNA	5-OHU, 5-OHC, TG, Fapy G, Fapy A
NEIL2	Bifunctional	ssDNA, bubble, fork and dsDNA	5-OHU and 5-OHC
MYH	Monofunctional	dsDNA	A opposite 8-OxoG

*Fapy, formamidinopyrimidine; 5-OHC, 5-hydroxycytosine, 5-OHU, 5-hydroxyuracil; TG, thymine glycol; the list does not cover all the DNA glycosylases or substrates, especially poor substrates.

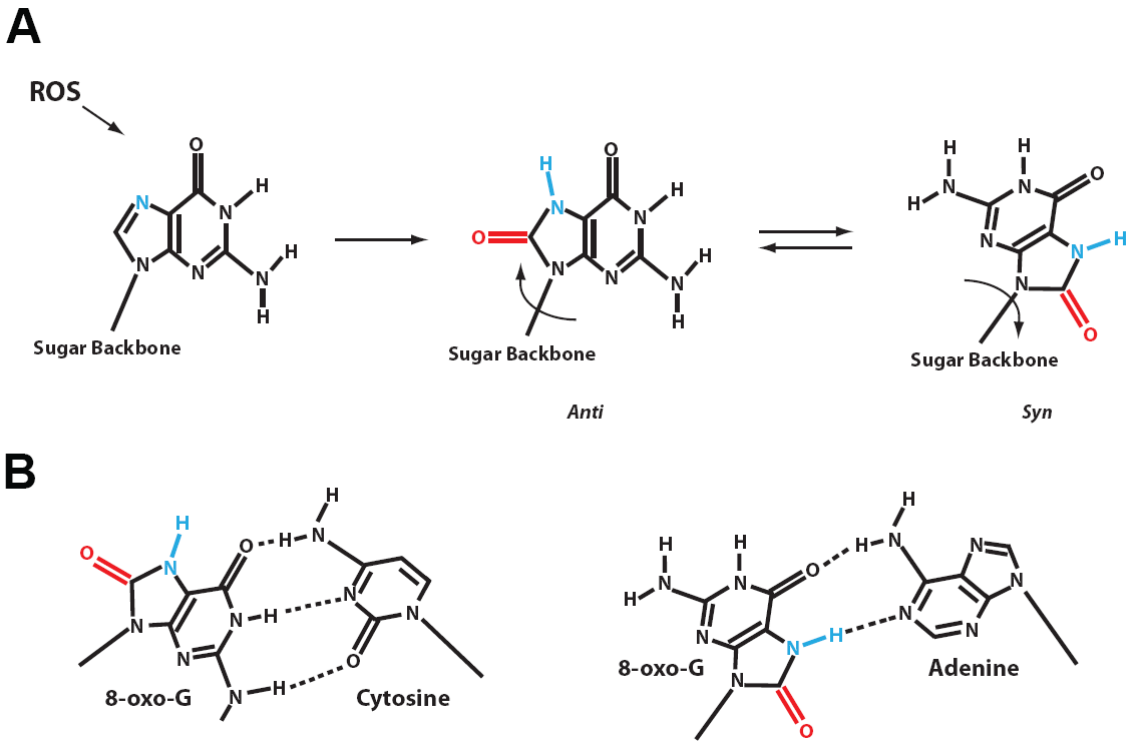

Figure 2.3 – The base flipping of guanine
(A) ROS attacks guanine by adding oxygen at carbon 8, which flips the base to create a *Syn* formation. (B) The *Syn* formation of oxidized guanine base pairs with cytosine (left) or adenine (right) after one round of DNA replication.

mutagenic potential of 8-oxodG, both prokaryotes and eukaryotes have come to rely on a group of DNA glycosylases for repair. In particular, the MutM, MutT, and MutY enzymes in bacteria and MTH1, OGG1, and MYH enzymes in human are mainly responsible for repairing 8-oxoG lesions in the BER pathway (125).

DNA glycosylase OGG1 is one of the most characterized enzymes in the BER pathway. In the mammalian system, it has been recognized to be the primary enzyme responsible for excising 8-oxodG lesions (125). The OGG1 protein was initially discovered in *Saccharomyces cerevisiae* and subsequent database search and cloning studies have lead to the identification of the human homolog. The sequence alignment between human and yeast OGG1 proteins revealed ~38% homology between the two. However, over ~60% homology was observed in segments including the highly conserved active site Helix-hairpin-Helix-Lysine/Glycine/Proline/Aspartic Acid motif and several unknown segments which suggest the structural importance in the enzyme's function (126,127). Interestingly, an analysis of the human cDNA sequence revealed an existence of two forms of mRNA, coding for two varieties of OGG1, namely α–hOGG1 and β–hOGG1. Comparison of these two proteins showed that they were identical in the first 316 amino acids and both have mitochondrial targeting signal (MTS) sequences at the amino terminal end (128). However, it was later shown that only α–hOGG1 has a nuclear localization signal (NLS) sequence at the carboxy-terminal ends while β–hOGG1 does not. This finding was later confirmed by immunofluroresence studies, where α–hOGG1 was almost exclusively detected in the nucleus while β–hOGG1 was found in the inner membrane of mitochondria (128,129). These studies suggest that the NLS

sequence overcomes the MTS sequence in α–hOGG1 making it primarily active in the nucleus and that β–hOGG1 may be responsible for the 8-oxoG repair activities in mammalian mitochondria (130).

The mRNA expression levels of human and mouse *OGG1* have revealed that the expression is ubiquitous, but it varies from tissues to tissue. In mice, low expression of *Ogg1* mRNA was detected while high expressions were observed in brain, testes, kidney, thymus, and intestine in humans (128,131,132). Sequence analysis revealed that the *OGG1* gene contains a classic housekeeping gene promoter that is consistent with the ubiquitous nature of its expression pattern. Tissue to tissue variation could be explained by having a possible negative regulator region upstream of promoter site. Furthermore, expression levels and enzyme activities of OGG1 protein in human fibroblast culture were not dependent on cell cycle (133).

The mammalian OGG1 have the typical Helix-hairpin-Helix-Lysine/Glycine/Proline/Aspartic Acid catalytic motif that is frequently found in DNA glycosylase with AP lyase activity (126). The substrate specificity for OGG1 was shown to be dependent on the base opposite to the 8-oxoG. For instance, the repair efficiency for removing the 8-oxoG which is base paired with cytosine was the highest while other bases were all significantly reduced (134). This is due to the conformational changes that allow the recognition of the 8-oxoG to cytosine base pair as the key in its catalytic mechanism. More specifically, hydrogen bonds made by Asparagine-149 and Aspartic acid-268 to cytosine and 8-oxoG, respectively, work like a locking mechanism. They both must be displaced to aid Lysine-249 to launch a nucleophilic attack at the carbon-1

glycosidic bond that connects 8-oxoG to the sugar backbone, promptly removing the lesion (Fig. 2.4). On the other hand, X-ray structure of protein/undamaged DNA complexes revealed that undamaged guanine was denied access into the active site pocket; thus allowing OGG1 to differentiate between 8-oxoG and undamaged bases (135,136). The significance of proper fit at the active site pocket was later strengthened when an opposing abasic site or SSBs towards the 3' of the active site pocket was found to greatly reduce OGG1 incision activity (137-139). In addition, characterization of OGG1 shows that it can excise fork substrates and increase the incision efficiencies by positioning the 8-oxodG up to 3 nucleotides away from the opening (139). OGG1 prefers to work in processive mode where the enzyme will move from substrate to adjacent substrate without disengaging from the DNA (140). In addition, a sequence-dependent study shows that OGG1's incision is affected by flanking sequences with preference to 5'-(C/G)me-FapyC-3' (141).

If the 8-oxoG-cytosine base pair does not get repaired and replication takes place after bypassing the lesion, then DNA glycosylase MYH will recognize the resulting 8-oxoG-adenine base pair and remove the adenine (142). This provides an opportunity for OGG1 to repair the 8-oxoG-cytosine base pair substrate after subsequent processing of the AP site, followed by one round of replication. These two repair proteins work cooperatively to ensure that the highly mutagenic 8-oxoG lesion is properly excised before mutations can harm the cells.

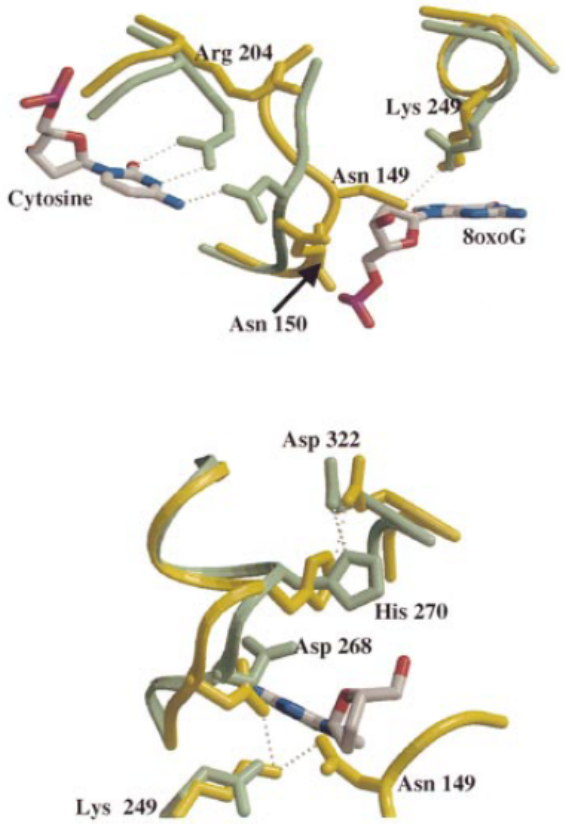

Figure 2.4 – The catalytic pocket of OGG1
(Top) Hydrogen bonds are made between Asparagine-149 and cytosine and Aspartic acid-268 and 8-oxoG to start the catalytic reaction. (Bottom) The Lysine-249 launches a nucleophilic attack at the carbon-1 glycosidic bond that connects 8-oxoG to the sugar backbone to remove the lesion. Image courtesy of Bjørås and Barrett, 2002.

The employment of the *Ogg1* knockout mice model has been instrumental in examining the consequences of 8-oxoG in the context of a whole organism. Interestingly, *Ogg1* knockout mice did not generate any obvious abnormal phenotypes. They were fertile, developed normally with comparable life span to wild type, and were mostly cancer free, except in one study with increased development of lung adenoma/carcinoma (143-145). The lack of predisposition to cancer in *Ogg1* knockout mice is consistent with the slight increase, only two to three fold, in the mutation frequency of embryonic stem cells derived from *Ogg1* knockout mice (144). However, it was found that 8-oxoG accumulated at an increased level in a tissue and age-dependent manner. More specifically, the accumulation of 8-oxoG in liver was considerably higher and was the only organ to show significant increase. Also, this accumulation was only observed in older mice (143,146).

The *OGG1* gene is not associated with any cancer or human disorders, some studies suggest that deficiency in *OGG1* could provide the initial step necessary in tipping the balance in the right direction for tumorigenesis. For instance, a number of tumors have guanine-to-thymine transversion mutations in *p53* gene, a tumor suppressor gene most commonly mutated in various cancers, which is accompanied by a loss of locus containing the *OGG1* gene (125). Although the *Ogg1* single knockout mice were not highly predisposed to cancer, *Myh* and *Ogg1* double knockout mice displayed increased incidence of lung and ovarian tumor formation. A subsequent study revealed that codon 12 of *K-ras,* an oncogene most commonly mutated in lung cancer, had a guanine-to-thymine transversion mutation (147). The double deficiency in *Myh* and *Ogg1*

had an additive effect by abolishing the main repair mechanism for oxidized guanines, thus making it highly susceptible to the hypermutator phenotype as described above. Together, these studies demonstrate the importance of OGG1 protein in providing one of the first lines of defense against oxidative DNA base damages as part of the BER pathway.

2.3 Fanconi Anemia Complementation Group C (FANCC) protein and its role in DNA repair

Fanconi Anemia (FA) is a rare genetic disorder transmitted in an autosomal recessive, or occasionally through X-linked means. The major complication associated with FA is progressive bone marrow (BM) failure and is one of the classical inherited BM failure syndromes (IBMFS). FA patients frequently exhibit increased predisposition to cancer and are often born with a variety of birth defects such as abnormal thumb or radii and short stature. Most FA patients do not make it beyond their young adulthood due to progressive BM failure or malignancy (148,149). Cells derived from FA patients are often characterized with chromosome abnormalities such as spontaneous chromosomal breakage and hypersensitivity to DNA interstrand cross-linking (ICL) agents such as cisplatin, psoralen/UV-A and mitomycin-C (MMC) (150). A measurement of chromosomal abnormality e.g. breaks after exposure to ICL agents is often used to diagnosis FA (151).

FA is a genetically heterogeneous disorder and there are currently 13 known complementation FA types (FANCA, B, C, D1, D2, E, F, G, I, J, L, M and N) that participate in the FA pathway (Fig. 2.5) (152). Eight of these proteins (FANCA, B, C, E,

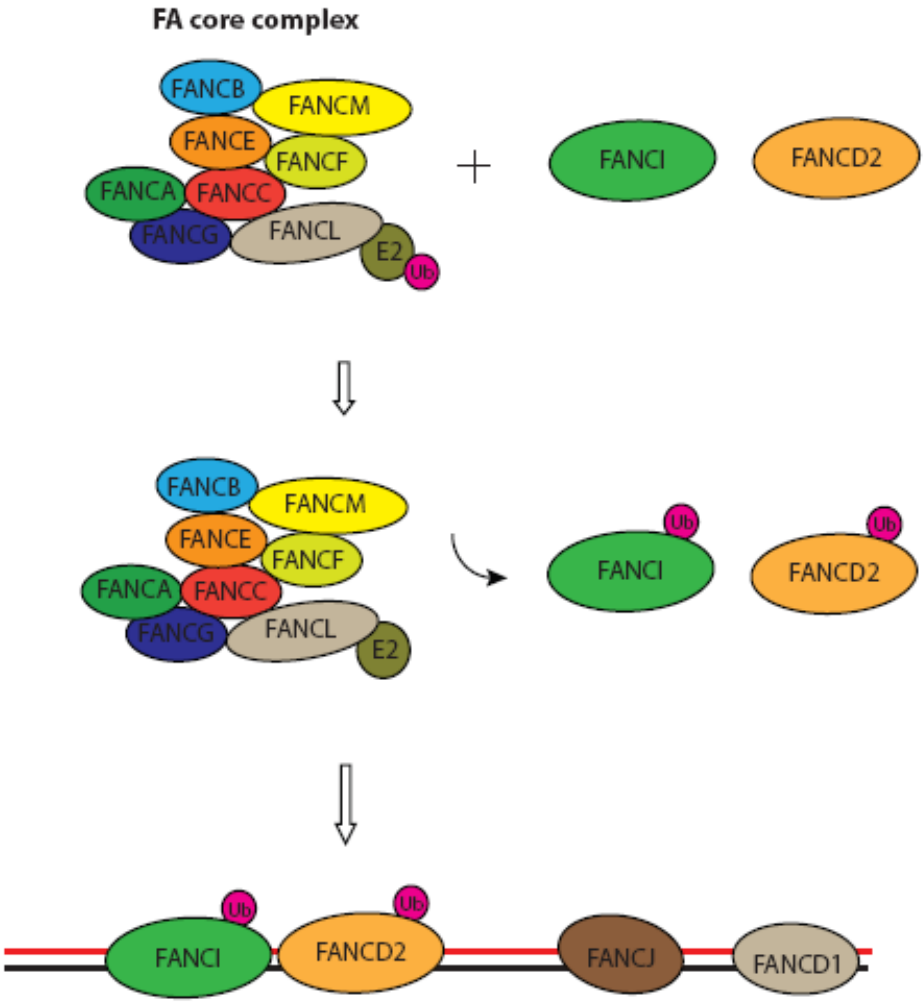

Figure 2.5 – An illustration of the FA pathway
There are 13 complementation types in the FA pathway. Eight of them form the FA core complex, which is required for monoubiquitination of FANCD2 and FANCI. FANCJ and FANCD1 works downstream of FA pathway.

F, G, L and M) form the FA core complex, and its assembly is mandatory for the monoubiquitination of FANCD2 and FANCI and their localization to chromatin. Abrogation in any of the FA core components disrupts the monoubiquitination of FANCD2 and FANCI, thus their ability to localize to chromatin (153). Some members of the FA core complex exist out in the cytoplasm and re-locate into the nucleus upon DNA damage, which is dependent on the nuclear localization signals of FANCA and FANCE. The mechanism that triggers the assembly of the FA core complex is still unclear. It is proposed that DNA damage caused by ICL agents such as MMC or ROS could activate the assembly. Alternatively, the FA core complex could be constitutively active during the S phase of the cell cycle since FA pathway is restricted and most active during that particular of the cell cycle (154). Once in the nucleus, the FA core complex associates with chromatin via FANCM and FAAP24 which are equipped with DNA-interacting domains. In addition, FANCM may play a vital part in moving the core complex along the DNA with its ATP-dependent DNA translocase activity (155). The localization of FANCD2 to DNA damage sites depends on the FANCL protein, which acts as an E3 ubiquitin-ligase and monoubiquitinates FANCD2 and FANCI with its ring-finger-type ubiquitin-ligase (PHD) motif. Evidence of this comes from a FANCD2 mutant, which did not localize to chromatin since it could not be monoubiquitinated (156).

The role of FANCD2 and FANCI after being recruited to a DNA damage site is still unclear. One line of evidence suggests that FANCD2 is involved in HR repair by recruiting BRCA2 to DNA damage sites (157). However, HR repair is only slightly affected in cells that are deficient in FA pathway, whereas HR repair is severely affected

in cells deficient in BRCA2 (158,159). Other studies suggest that FA pathway is involved in translesion synthesis during DNA repair by recruiting translesion polymerases to DNA damage site. For instance, translesion polymerase-deficient DT40 chicken cells showed hypersensitivity to ICL agents, and translesion polymerase REV1 and REV3 have been shown to participate to repair ICLs in the same pathway as FA proteins (160). This suggests that FANCD2 may have a similar function as a proliferating cell nuclear antigen protein during polymerase switching in response to DNA damage (160).

Traditionally, it has been widely accepted that FA cells are mainly sensitive to ICL agents. However, accumulating evidences suggest that FA cells are also sensitive to other endogenous stresses as well (150). For instance, hypersensitivity to oxidative damage inducing agents was observed in FA-deficient cells (161,162). Other DNA damage-inducing agents such as ultraviolet or ionizing radiation also have been shown to activate the FA pathway (163). FA patients seem to acquire typical FA phenotypes such as progressive BM failure and predisposition to malignancy even in the absence of environmental ICL-causing sources (150). Furthermore, commonly used ICL-inducing agents such as MMC can also cause other types of DNA damage and have been shown to predominantly induce alkylation of bases over ICLs (164,165). These data suggest that FA proteins may not respond exclusively to ICLs and may have a broader role in responding to endogenous DNA damage.

Accumulating evidence indicates that FA proteins may play a role in telomere maintenance, causing a number of studies linking disruption in telomere maintenance and IBMFS, including FA, to arise in recent years (7,166). For instance, an accelerated

telomere shortening has been observed in cultured primary FA fibroblasts when measured periodically during a long period of their lifespan (167). A similar result was obtained when telomere length was measured in FA patient's peripheral blood leukocytes (168). Whether this accelerated telomere shortening is a direct consequence of FA deficiency is still under debate since the telomere shortening occurred at similar rate between FA and non-FA-cells (95). Furthermore, FA proteins do not seem to have a direct role in telomere maintenance, as seen in cells with normal and functional telomeres, since they do not co-localize to telomeres in primary fibroblast and telomerase-positive cells. However, co-localization and deletion studies using various ALT cell lines suggest that FA proteins may play a role in telomere maintenance in ALT systems (169,170). It is plausible that the FA pathway may act as a general DNA damage response since ALT cells have an active DNA damage response and dysfunctional telomeres (4). (A more detailed description of dysfunctional telomeres and ALT can be found in chapter 1). However, FA protein's role in telomere length regulation and functions is still unclear.

FANCC is one of commonly mutated FA genes in FA patients (~10%) and is conserved among vertebrates. Its encoded protein, FANCC is 63kD in size and interacts with FANCE and FANCF in the FA core complex. Interestingly, FANCC protein does not contain any discernible motifs or domains that could connect it to one of many known DNA repair pathways (152,171). Historically, *FANCC* was the very first FA gene to be discovered. This was achieved via somatic cell hybridization study, where sensitivity to MMC was measured to identify different complementation groups. Briefly, the cells derived from complementation group C patients were transfected with various cDNA

expression libraries. The hypersensitivity to MMC was corrected when the library containing *FANCC* cDNA was transfected, therefore leading to identification of the gene responsible for the rescue (Fig. 2.6) (172).

Aside from participating in the FA pathway as the component of FA complex, FANCC protein has also been implicated in a HR-dependent DNA repair pathway. For instance, FANCC-deficient chicken DT40 cells had 2-fold increase in the rates of spontaneous sister-chromatid exchange (SCE) than its wild-type counterpart. The mechanism behind this event is partially dependent on Rad51 paralog XRCC3, an important player in HR, since *Fancc/Xrcc3* double mutant had decreased SCE levels, similar to that of *Xrcc3* single mutant (173). In addition, the SCE level in the *Fancc/Blm* double mutant was similar to *Blm* single mutant, which already had significantly increased SCE rates. This suggests that FANCC and BLM, a helicase implicated in bloom syndrome, may work together in the same pathway (173). Interestingly, the FA core complex, which includes FANCC, was purified as part of a multiprotein complex with BLM in HeLa cell extract. This complex, as revealed, is relatively large, about 600kD in size, and is properly termed BRAFT (BLM, replication protein A (RPA), FA, and topoisomerase IIIα) (174). However, an exact mechanism of how BRAFT complex participates in HR-dependent repair is still unclear.

Accumulating evidence suggests that FANCC may also play a role in oxidative DNA damage response. Mice deficient in both FANCC and SOD1, a Cu/Zn superoxide dismutase, showed that there was defective hematopoiesis due to oxidative induced stress (175). In addition, hypersensitivity to oxidative stress induced by H_2O_2 in FANCC-

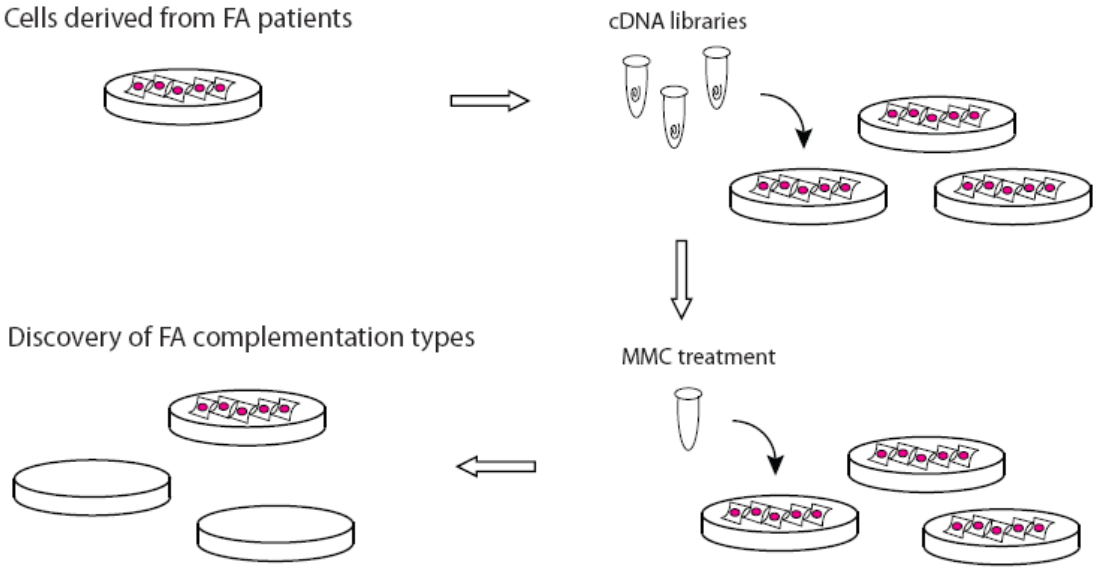

Figure 2.6 – The discovery of FA complementation group C
The somatic hybridization technique was utilized to identify the underlying gene. Briefly, various cDNA libraries are transfected into cells derived from FA patients; followed by mitomycin C (MMC) treatment. The underlying gene in the cDNA library complements the mutated gene in cells derived from FA patients; thus, surviving the MMC treatment.

deficient murine embryonic fiboblasts and BM hematopoietic progenitor cells was also observed. In this study, chemicals with an anti-oxidant property were able to increase the survival rates of FANCC deficient cells under oxidative stress conditions (161). The same group also showed that serine–threonine kinase apoptosis signal-regulating kinase 1 (ASK1), a major player in oxidant-induced apoptosis, was hyper-activated in FANCC-deficient cells under H_2O_2-induced oxidative stress conditions. Together, these data suggest that the redox states of these mice were altered and contributed to defective cell proliferation and enhanced apoptosis.

Since FANCC-deficient cells are hypersensitive to oxidative stress, it is plausible that FANCC protein plays a direct role in redox homeostasis. Several studies indicate that FANCC protein directly interacts with NADPH cytochrome P450 reductase and glutathione S-transferase P1-1, which are known to primarily function in redox homeostasis (176,177). Whether FANCC or these interactions have significant impact in cellular response to oxidative stress or repair is still unclear. Interestingly, several studies suggest that FA proteins may work in conjunction with the tumor suppressor protein p53 to regulate the oxidative DNA damage response. Mice deficient in *Fanca* demonstrated that hypersensitivity to H_2O_2-induced oxidative stress was correlated with overactivation of p53 (178), and cultured cells derived from FA patients showed altered p53 function under oxidative stress condition (179,180).

The mechanism behind the functional linkage between the FA proteins and oxidative stress induced p53 activation is still not clear, however it has been shown that p53 and FA protein functionally cooperate to regulate tumorigenesis in FA deficient cells.

The *Fancc* and *p53* double knockout mice displayed accelerated tumor development in hematopoietic or solid malignancies than in single p53 knockout mice, while no tumors were detected in *Fancc* single knockout mice. More importantly, this accelerated growth was associated with the appearance of tumor types that are found in patients with FA but not in *p53* single knockout mice (181). These data suggest that the increased malignancy observed in FA patients perhaps could be explained by the concerted effort between p53 and FA proteins in response to endogenous oxidative stress.

The FA is both a genetically and functionally complex disease. It has many complementation groups and all members of the FA pathway appear to be indispensible. One of its members, FANCC, is not only part of the FA core complex but surprisingly has functions outside of the FA pathway. Therefore, further studies to possibly find additional complementation groups as well as more in depth genetic and functional studies could provide a more detailed picture of the disease.

Chapter 3: FANCC Suppresses Short Telomere-initiated Telomere Sister Chromatid Exchange

The following chapter has been published as: David B. Rhee, Yisong Wang, Melissa Mizesko, Fang Zhou, Laura Haneline and Yie Liu, "FANCC suppresses short telomere-initiated telomere sister chromatid exchange", *Human Molecular Genetics.* 2010 March 1; 19(5): 879-887.

3.1 Introduction

Telomeres are specialized structures consisting of tandem repeats, TTAGGG in human and mouse, together with telomere associated proteins to form caps at the ends of linear chromosomes (2,182). Telomeres prevent the recognition of chromosome termini as broken DNA ends and are critical to maintaining genomic stability. Telomere dysfunction, resulting from loss of telomere repeats or loss of protection by telomere-associated proteins, can trigger DNA damage responses, cell apoptosis, cell proliferation defects, or genome instability. Telomere dysfunction has also been linked to bone marrow failure syndromes and tumor formation (3,183). Telomerase is essential in telomere length maintenance by replenishing telomere loss due to incomplete DNA replication (2). In mice, deficiency in either telomerase core component, telomerase RNA (*Terc*) or telomerase reverse transcriptase (*Tert*), leads to progressive telomere shortening (85-87,184), which is accompanied by cell proliferation defects and apoptosis in highly proliferating organs including the bone marrow (89,185,186). Furthermore, *Terc* or *Tert* heterozygous mice bred for increasing generations also exhibit progressive telomere

shortening and loss of tissue renewal capacity (184,187,188). In humans, mutations in the telomerase components are associated with accelerated telomere shortening and the development of bone marrow failure syndromes, such as dyskeratosis congenita, acquired aplastic anemia, and idiopathic pulmonary fibrosis (7). Previous reports show that peripheral blood cells derived from FA patients have shorter telomeres compared to age-matched healthy donors (168,189-192), but it is unclear if telomere attrition in hematopoietic cells from FA patients contributes to the pathogenesis of bone marrow failure in FA.

Telomere shortening is considered a biological clock counting down cellular replicative senescence (57). Cells may overcome this barrier and become immortalized by maintaining telomere length through activation of telomerase and homologous recombination (HR)-mediated pathways (52,57). In human and murine telomerase deficient cells, short telomeres can initiate HR between telomere sister chromatids, or telomere sister chromatid exchange (T-SCE), by which telomere length is maintained (50,68,69,193,194). Furthermore, short telomeres are also capable of initiating telomere recombination in the presence of telomerase (195). Although it is not entirely clear what molecules regulate telomere recombination, a loss of function in the pathways controlling telomere length maintenance, telomere capping, or telomere chromatin can affect telomere recombination. For example, inactivation of Werner (Wrn) protein promotes T-SCEs in spontaneously immortalized telomerase-null mouse embryonic fibroblasts (196). Alterations in telomere capping or epigenetic modifications due to disruption of murine telomere capping proteins (e.g. Pot1 or Trf2 in combination with Ku70) or histone

methyltransferases (e.g. Suv4-20h or Suv39h) can also contribute to elevation of T-SCEs (197-200).

Fanconi anemia is an autosomal recessive disorder characterized by cancer susceptibility, bone marrow failure, and cellular sensitivity to DNA inter-strand crosslinking agents. To date, 13 FA proteins (FANCA, B, C, D1, D2, E, F, G, I, J, L, M, N) have been identified. Increasing evidence demonstrates that FA proteins play an important role in genome integrity via DNA replication-dependent repair (152,171). Several FA proteins form the FA nuclear core complex, which is required for the monoubiquitination of FANCD2 and FANCI and the localization of FA proteins to chromatin, possibly at the sites of DNA repair. FANCD2 and FANCI function as signal transducers and DNA-processing molecules in a DNA damage response network consisting of ATR, BRCA1, and a RecQ helicase, BLM. Abrogation in any of FA core components disrupts the monoubiquitination of FANCD2 and FANCI. FA proteins may respond to endogenous DNA damage, such as DNA inter-strand crosslinks or oxidative DNA damage (150). Whether the FA pathway can respond to dysfunctional telomeres is yet to be determined.

FANCC is one of the most commonly mutated genes in FA patients and is conserved among vertebrates (201). Its encoded protein, FANCC is 63kDa in size with no discernable motifs or domains (152,171). FANCC is a member of the FA core complex where it interacts with FANCE and FANCF, and it also associates with the Bloom syndrome protein complex in a supercomplex called BRAFT (152,171,174). In addition to participating in monoubiquitination of FANCD2 and FANCI as part of the

core complex, FANCC is also involved in HR pathways (158,173,202). These observations, together with prior reports showing telomere shortening in FA patients, led us to investigate if FANCC regulates telomere length and telomere recombination *in vivo.* In this study, we employed *Fancc* deficient mouse models in the strain background with long (C57BL/6 strain) or short telomeres (telomerase reverse transcriptase mutant strain after successive breedings) and wild type recipient mice that had undergone serial transplantations with *Fancc*$^{-/-}$ bone marrow cells. Using these genetically modified murine models, we demonstrate that Fancc plays a role in stress-induced telomere attrition and short telomere-initiated recombination in primary murine hematopoietic cells.

3.2 Results

Fancc deficiency does not compromise telomeres in a mouse strain with intrinsically long telomeres

FA patients were reported to harbor short telomeres (168,189-192). To investigate if FANCC plays a direct role in telomere length maintenance *in vivo*, we examined telomere length of wild type and *Fancc*$^{-/-}$ mice in the C57BL/6 genetic background, known to have several-fold longer telomeres than humans (203). Hematopoietic cells were isolated from 2-4 month old mice. The mean and median telomere signal intensity as well as the distribution of individual telomere signal intensities were similar between wild-type and *Fancc*$^{-/-}$ mouse bone marrow cells by Q-FISH analysis (Figure 3.1). In addition, the average telomere signal intensity was comparable between wild type and

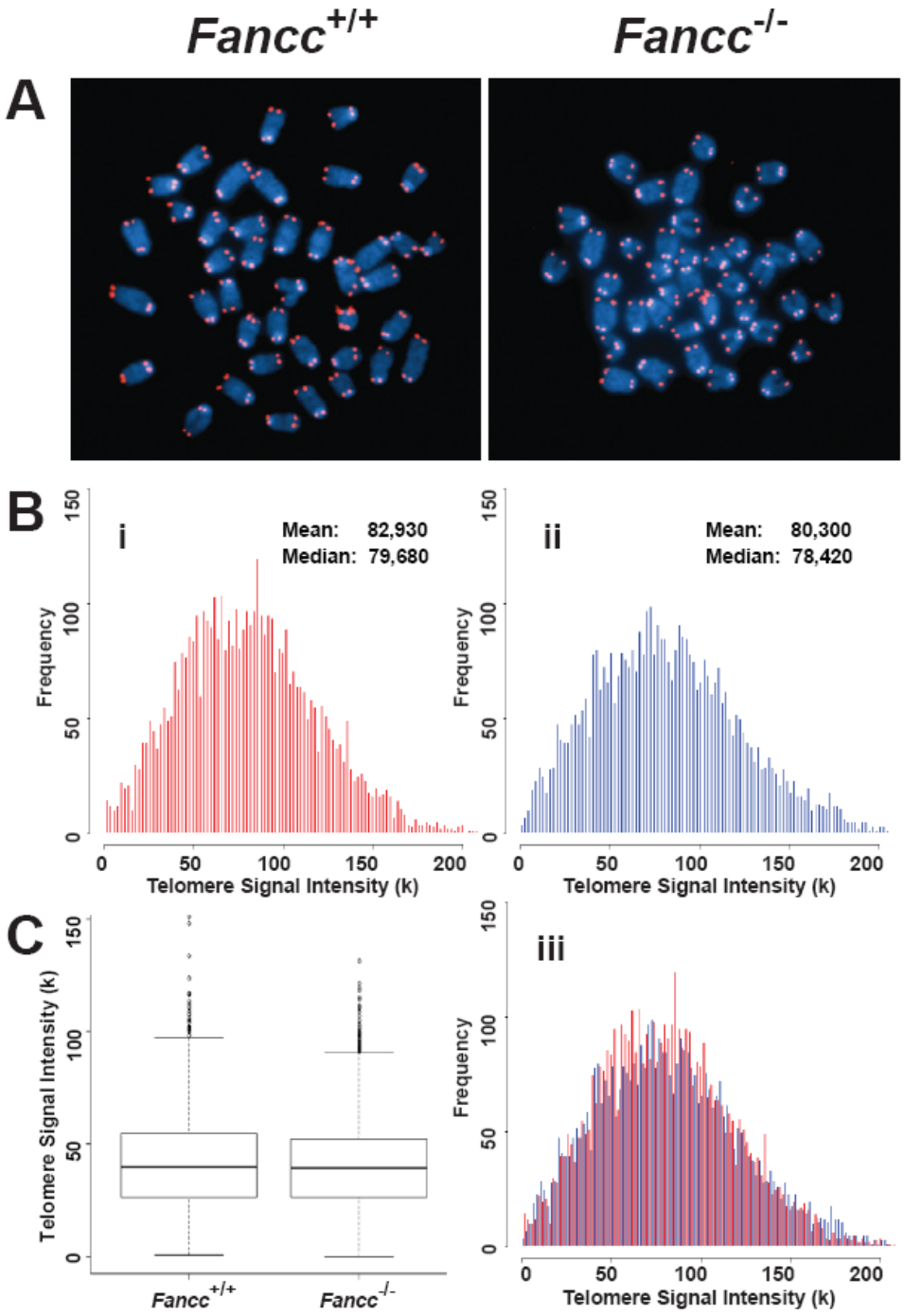

Figure 3.1 – Telomere lengths are comparable between wild type and *Fancc*$^{-/-}$ bone marrow cells derived from C57BL/6 mice.

Q-FISH analysis of bone marrow cells derived from wild type and *Fancc*$^{-/-}$ mice (n=6). (A) Representative metaphase spreads of wild type (Bi) and *Fancc*$^{-/-}$ (Bii) bone marrow cells showing DAPI staining (blue) and telomere fluorescence signals (red). There was no significant difference in the mean telomere signal intensities and distribution of telomere signal intensities between two genotypes in overlapping histogram (Biii) and box-plot (C).

Fancc$^{-/-}$ bone marrow, spleen, and thymus cells via Flow-FISH measurements (Figure 3.2). No significant differences in telomerase activity and the expression of the telomerase core components, *Tert* and *Terc* were observed between wild type and *Fancc*$^{-/-}$ mouse bone marrow cells (Figure 3.3).

Accumulating evidence suggest that telomere integrity depends not only on telomere length, but also on the proper capping of chromosome ends by telomere associated proteins and telomere special structures (3,183,204). Therefore, telomeres with normal length do not necessarily reflect that they are functionally capped. To explore if FANCC plays a direct role in telomeric end-capping *in vivo*, we examined *Fancc*$^{-/-}$ bone marrow cells for evidence of telomeric end-capping defects, i.e. chromosome end-to-end fusion and telomere signal free end (SFE). *Fancc*$^{-/-}$ bone marrow cells did not exhibit chromosome end-to-end fusions and SFEs (Figure 3.1 and Table 3.1). Furthermore, *Fancc*$^{-/-}$ bone marrow cells did not display spontaneous chromosomal abnormalities, e.g. chromosome breakages and fragments (Table 3.1). Together, these results suggest that FANCC does not play a direct role in regulating telomere length, telomerase activity, and telomeric end-capping, when telomeres are long and functional.

Inactivation of Fancc accelerates telomere attrition in serially transplanted bone marrow cells

In both humans and mice, telomere dysfunction leads to cell proliferation defects and apoptosis in highly proliferating organs, especially in the bone marrow (7,89,185,186). *Fancc*$^{-/-}$ mice do not have obvious bone marrow abnormalities (205).

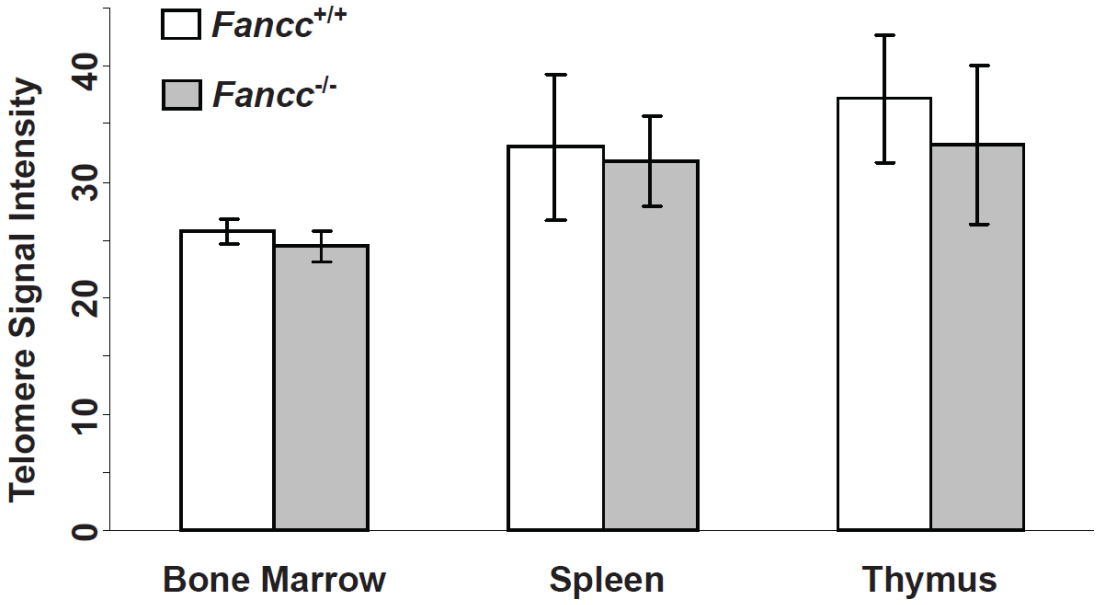

Figure 3.2 – Average telomere lengths in wild type and *Fancc*$^{-/-}$ hematopoietic cells derived from C57BL/6 mice.
Flow-FISH analysis of average telomere signal intensity of bone marrow cells, splenocytes, and thymocytes derived from wild type and *Fancc*$^{-/-}$ mice. Error bars represent the standard error from different mice of each genotype (n=5).

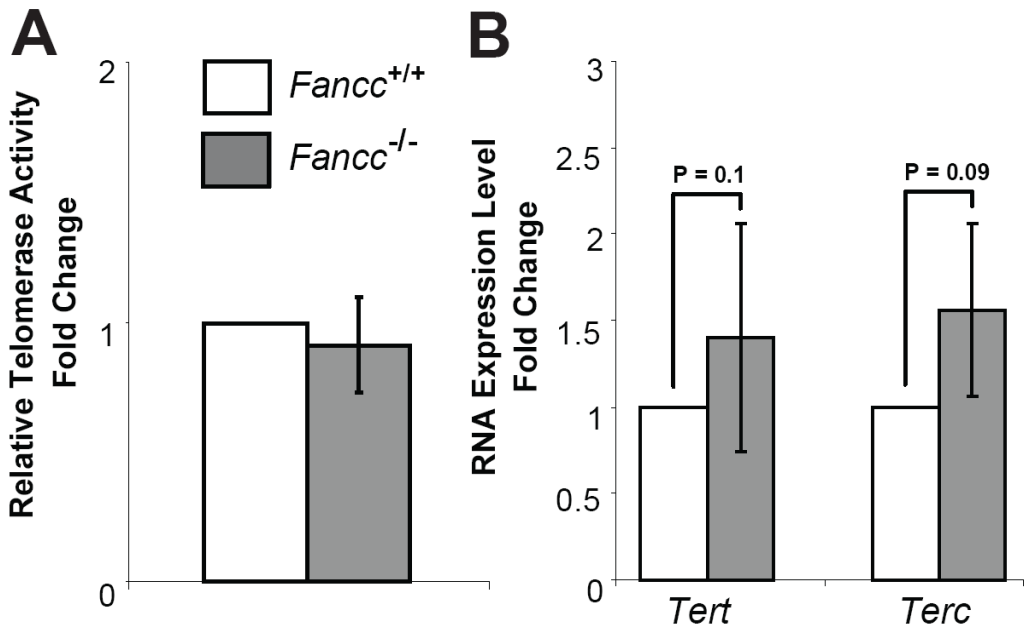

Figure 3.3 – Telomerase activity and *Tert* and *Terc* RNA level in wild type and *Fancc*$^{-/-}$ mouse bone marrow cells derived from C57BL/6 mice.
qT-PCR analysis indicates a comparable telomerase activity (A), and *Tert* and *Terc* RNA level (B) in wild type and *Fancc*$^{-/-}$ mouse bone marrow cells (n=6). Error bars represent the standard error obtained from different mice of each genotype. *P*-values are not significant between wild type and *Fancc*$^{-/-}$ mouse bone marrow cells.

Table 3.1 – Frequencies of chromosomal and telomeric abnormalities in bone marrow cells derived from wild type and *Fancc*$^{-/-}$ mice in C57BL/6 genetic background and G2 *Tert*$^{-/-}$ *Fancc*$^{+/+}$ and *Tert*$^{-/-}$ *Fancc*$^{-/-}$ mice

Cell Types	Aneuploidy[a]	Chr. fragments & breaks[b]	SFEs[b]
Wild type	7.9% ± 1.8%	0%	0%
Fancc$^{-/-}$	16% ± 4.3%	0%	0%
p-value	0.1842	NA	NA
G2 *Tert*$^{-/-}$*Fancc*$^{+/+}$	21.6% ± 1.7%	0.42% ± 0.21%	4.33% ± 1.22%
G2 *Tert*$^{-/-}$*Fancc*$^{-/-}$	7.2% ± 4.9%	0.63% ± 0.29%	0.73% ± 0.32%
p-value	0.07328	0.3948	0.0024

[a] % of abnormal cells. [b] % of abnormal events per chromosome. SFE: telomere signal free end. The data were obtained from wild type and *Fancc*$^{-/-}$ mice (n=6) as well as G2 *Tert*$^{-/-}$*Fancc*$^{+/+}$ and G2 *Tert*$^{-/-}$*Fancc*$^{-/-}$ mice (n=6), and more than 50 mouse bone marrow cells from each mouse were scored. *P*-values were calculated by comparing wild type with *Fancc*$^{-/-}$, or G2 *Tert* $^{+/-}$ *Fancc*$^{+/+}$ with *Tert* $^{+/-}$ *Fancc*$^{-/-}$ bone marrow cells.

Thus, it is not surprising that the mutant mice do not have any detectable telomere defects. On the other hand, *Fancc*$^{-/-}$ bone marrow cells display decreased hematopoietic stem cell repopulating ability after primary and secondary transplantations (206,207). It is unclear if telomere length is altered in *Fancc*$^{-/-}$ hematopoietic cells during serial bone marrow transplantation and consequently contributes to the decreased repopulating ability of these cells. Utilizing Q-FISH analysis, we examined telomere length of wild type and *Fancc*$^{-/-}$ bone marrow cells, which had previously undergone serial transplantation in lethally-irradiated secondary recipient mice. Wild type bone marrow cells from secondary transplant recipients had a decrease in mean and median telomere signal intensity compared to wild type bone marrow cells from untransplanted mice (mean telomere signal intensity was 34,780 and 82,930, after and before transplantation, respectively) (Figures 3.1 and 3.4). Interestingly, *Fancc*$^{-/-}$ bone marrow cells from secondary transplant recipients had an additional reduction in telomere signal intensity compared to transplanted wild type cells (Figure 3.4). The appearance of chromosome ends with greatly reduced or no detectable telomere signals was increased in *Fancc*$^{-/-}$ hematopoietic cells from secondary transplant recipients (Table 3.2). To investigate whether altered telomerase activity during serial transplantation accelerated telomere attrition in *Fancc*$^{-/-}$ bone marrow cells, we next examined telomerase activity. Deletion of *Fancc* had no effect on telomerase activity in serially transplanted bone marrow cells (Figure 3.5). Furthermore, spontaneous chromosomal abnormalities, including aneuploidy and chromosome breakages, were not significantly different between wild type and *Fancc*$^{-/-}$ hematopoietic cells (Table 3.2). Collectively, these data indicate that

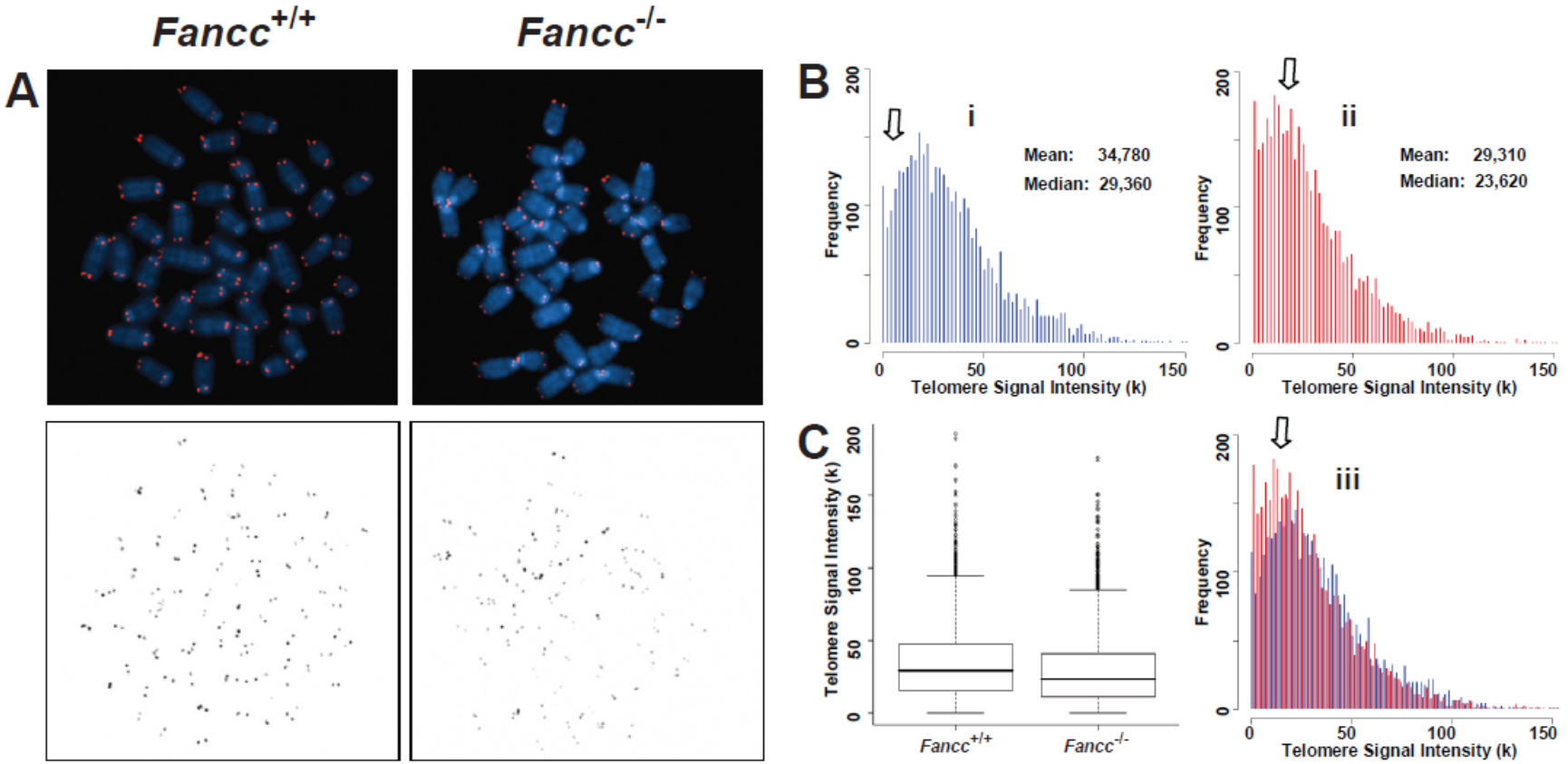

Figure 3.4 – Accelerated telomere attrition is observed in *Fancc*$^{-/-}$ bone marrow cells after two serial bone marrow transplantations.
Q-FISH analysis of wild type and *Fancc*$^{-/-}$ bone marrow cells after two serial bone marrow transplantation (n=4). (A) Representative metaphase spreads of wild type and *Fancc*$^{-/-}$ bone marrow cells showing DAPI staining (upper panel: blue) and telomere fluorescence signals (upper panel: red; lower panel: black). There was a decrease in telomere signal intensities in *Fancc*$^{-/-}$ cells (Bii) in comparison to wild type cells (Bi), shown here as shift of the dynamic range in overlapping histogram (Biii) and box-plot (C).

Table 3.2 – Frequencies of chromosomal abnormalities in wild type and *Fancc*$^{-/-}$ bone marrow cells after two series of transplantations

Cell types	Aneuploidy [a]	Fragments & breaks/chromosomes[b]	SFEs[b]
Wild type	17% ± 6%	0.77% ± 0.32%	2.7% ± 1%
Fancc$^{-/-}$	20.7% ± 4%	0.48% ± 0.27%	4.2% ± 0.8%
p-value	0.7034	0.3619	0.03123

[a] % of abnormal cells. [b] % of abnormal events per chromosome. The data were obtained from wild type and *Fancc*$^{-/-}$ mice (n=4), and more than 50 mouse bone marrow cells from each mouse were scored.

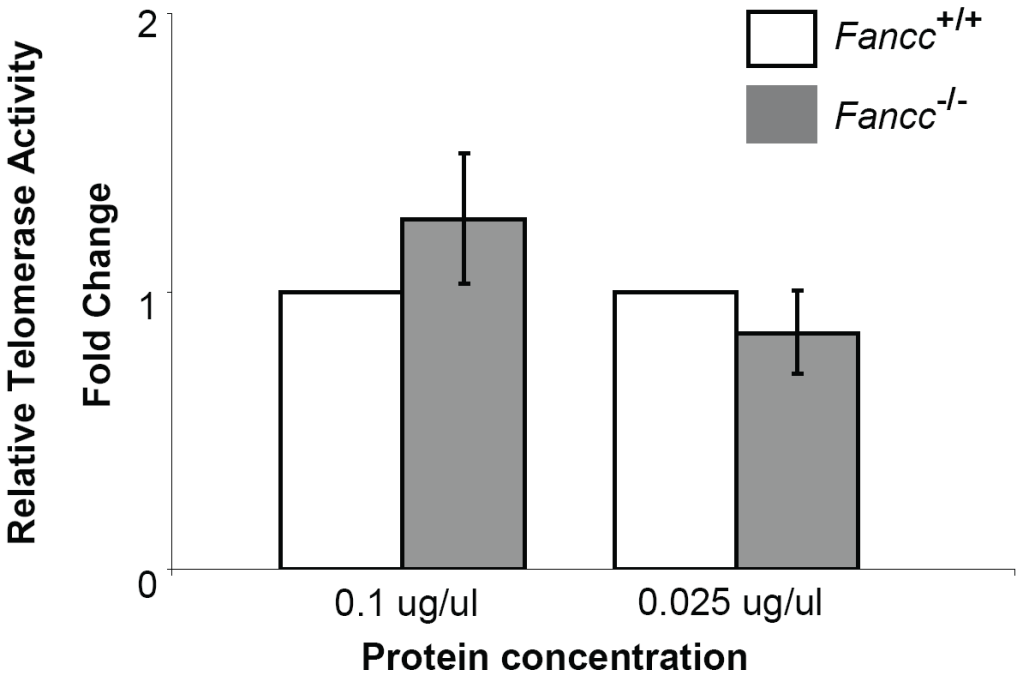

Figure 3.5 – Telomerase activity in wild type and *Fancc*$^{-/-}$ bone marrow cells after two serial bone marrow transplantations.
qT-PCR analysis indicates a comparable telomerase activity in serially transplanted wild type and *Fancc*$^{-/-}$ mouse bone marrow cells (n=4). Error bars represent the standard error from different mice of each genotype.

Fancc deficiency accelerates telomere attrition during the hematologic stress of serial bone marrow transplantation.

Fancc deficiency promotes short telomere-initiated telomere sister chromatid exchange in late generation *Tert* mutant mice

Although these data suggest that FANCC does not directly control long telomeres, it is unclear if FANCC regulates short telomeres. A body of evidence suggests that short telomeres can initiate recombinogenic events, including T-SCEs (50,68,69,193-195), even in the presence of telomerase (195). However, the molecular mechanism of short telomere-initiated telomere recombination is not well known. Given that FANCC is involved in HR pathways, we questioned whether FANCC may be involved in HR to resolve endogenous DNA damage, such as critically shortened telomeres. To test this hypothesis, we introduced $Fancc^{+/-}$ into $Tert^{+/-}$ mice (Figure 3.6). After successive breeding (Figure 3.6), bone marrow cells from $Fancc^{+/+}$ and $Fancc^{-/-}$ (HG5 in $Tert^{+/-}$ background and G2 in $Tert^{-/-}$ background) exhibited decrease in overall telomere length and increases in the appearance of chromosome ends with greatly reduced, or non-existent, telomere signals as detected by telomere restriction fragment and Q-FISH analysis (Figures 3.7 and 3.8, Table 3.1). These mutant mice with short telomeres allowed us to investigate the impact of *Fancc* deficiency on short telomere-initiated T-SCEs in the presence or absence of telomerase.

We examined the frequencies of T-SCEs in HG1 and HG5 $Tert^{+/-}$ $Fancc^{+/+}$ and $Tert^{+/-}$ $Fancc^{-/-}$ bone marrow cells via CO-FISH analysis. In HG1 mice with long

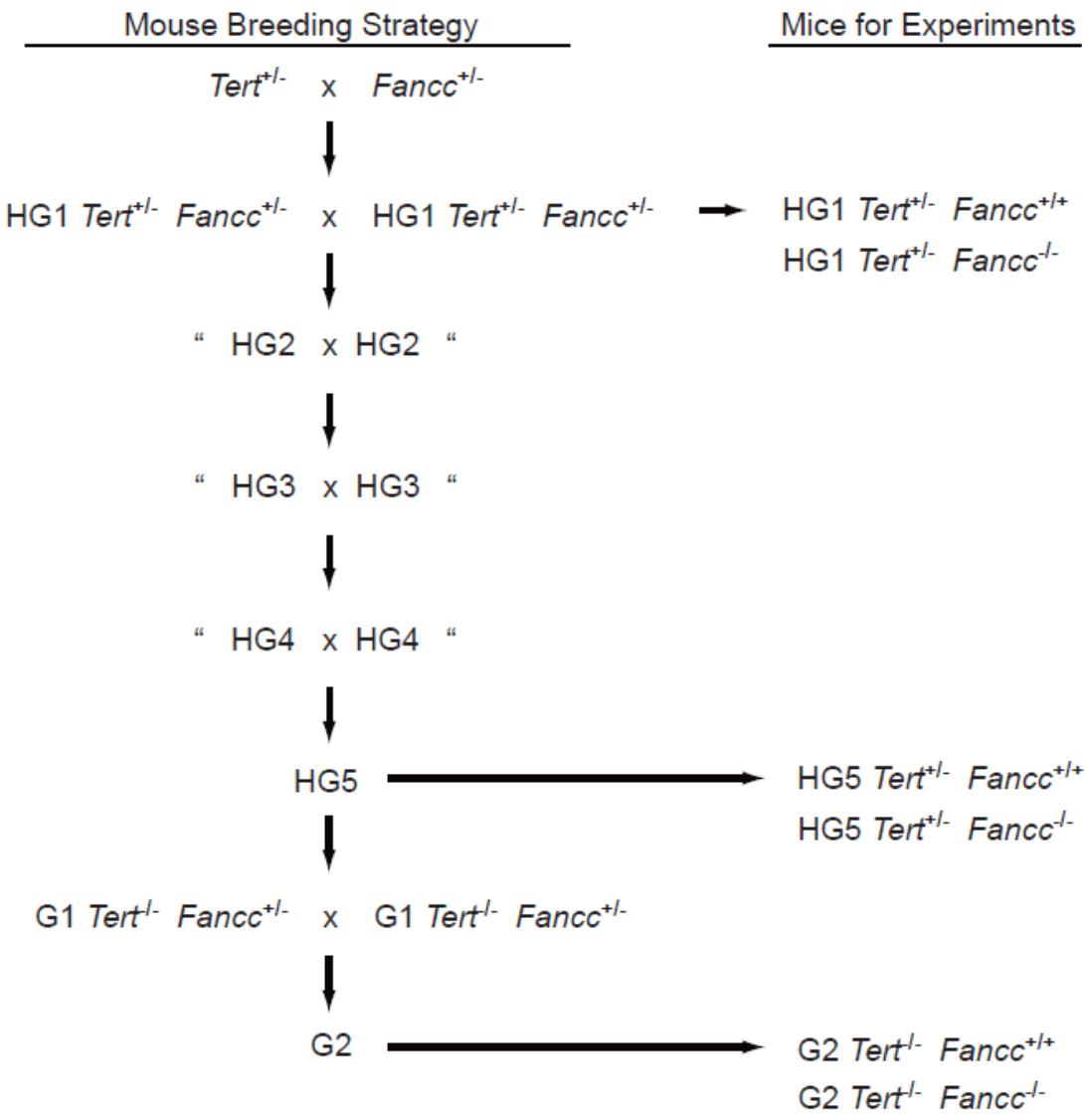

Figure 3.6 – A schematic representation of mouse breeding strategy for different generation Tert mutant mice.

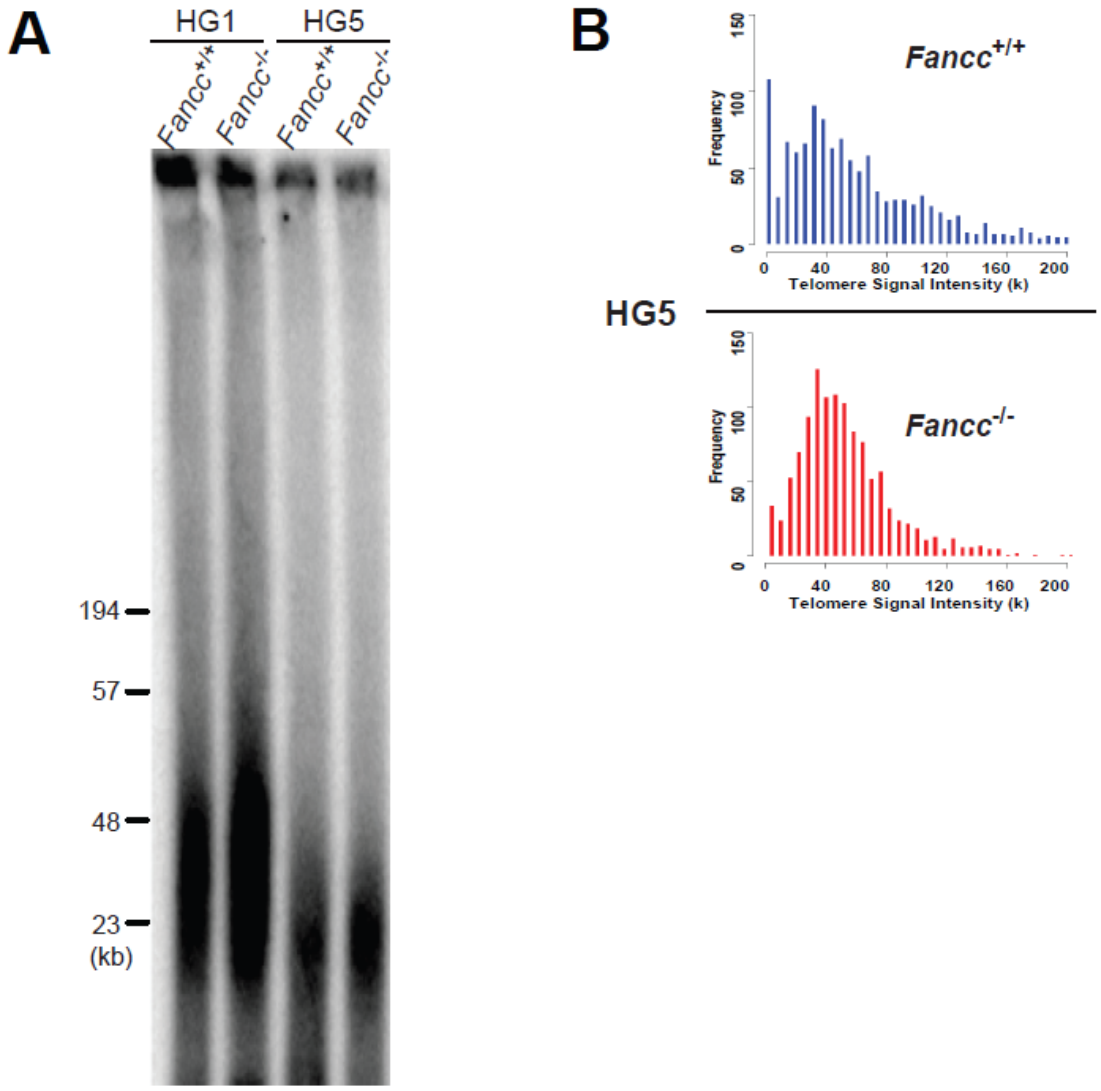

Figure 3.7 – A significant reduction in overall telomere length was evident in HG5 mutant mice. (A) Telomere restriction fragment analysis of mouse bone marrow cells derived from HG1 and HG5 Fancc+/+ and Fancc-/- mice. Genomic DNA was resolved by pulsed-field gel electrophoresis and hybridized with a radioactively labeled (AATCCC)4 probe. A significant decrease in telomere length was detected in HG5 mice in comparison to HG1 mice. (B) Q-FISH analysis of bone marrow cells derived from HG5 Tert+/- Fancc+/+ and Tert+/- Fancc-/-.

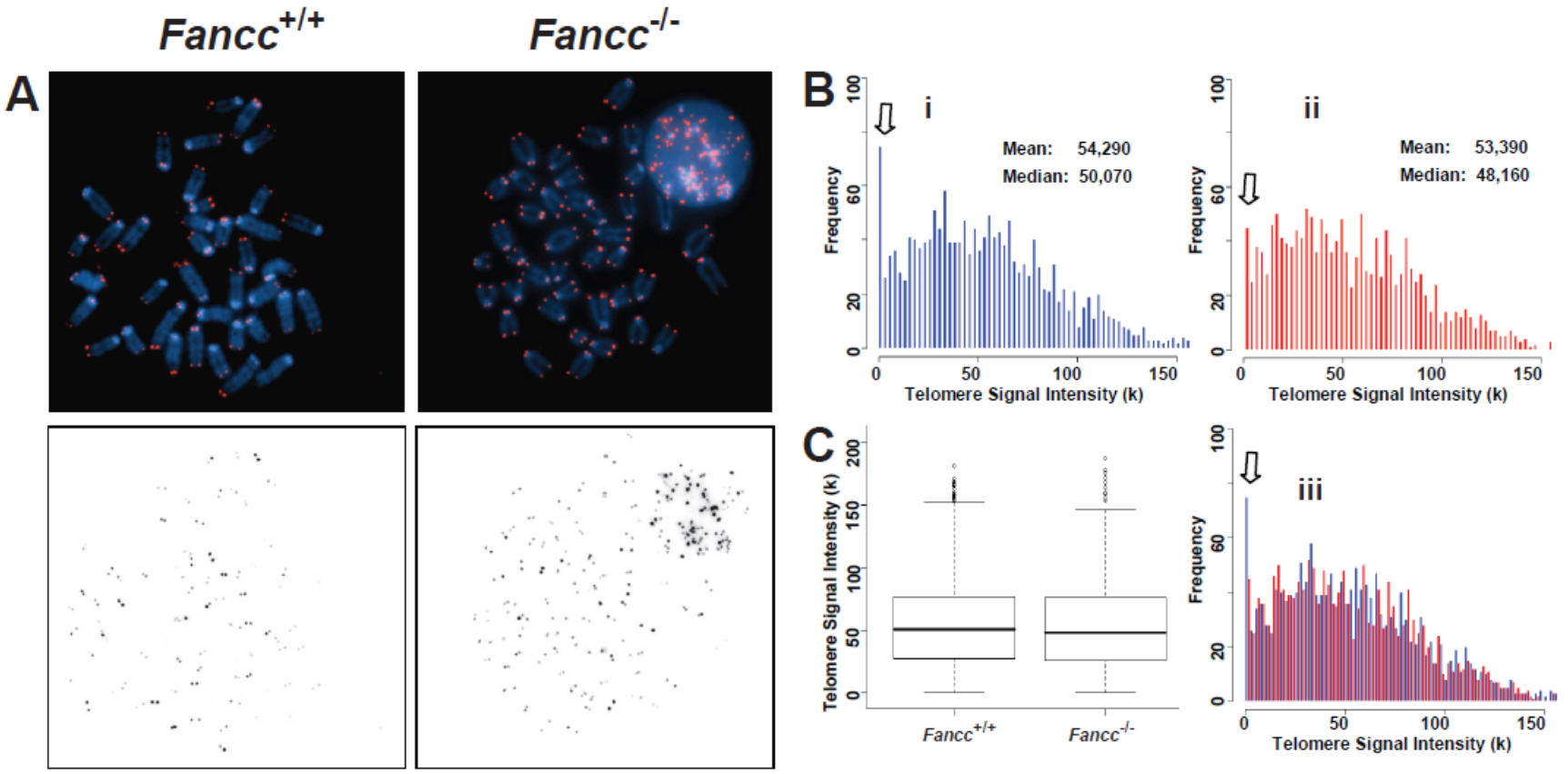

Figure 3.8 – Critically short telomeres are detectable in G2 *Tert*$^{-/-}$ *Fancc*$^{+/+}$ and *Tert*$^{-/-}$ *Fancc*$^{-/-}$ mutant mice.
Q-FISH analysis of bone marrow cells derived from G2 *Tert*$^{-/-}$ *Fancc*$^{+/+}$ and *Tert*$^{-/-}$ *Fancc*$^{-/-}$ mice (n=6). Representative metaphase spreads of G2 *Tert*$^{-/-}$ *Fancc*$^{+/+}$ and *Tert*$^{-/-}$ *Fancc*$^{-/-}$ mouse bone marrow cells showing DAPI staining (upper panel: blue) and telomere fluorescence signals (upper panel: red; lower panel: black). SFEs are detectable in G2 *Tert*$^{-/-}$ *Fancc*$^{+/+}$ and *Tert*$^{-/-}$ *Fancc*$^{-/-}$ mice (see arrows).

telomeres (Figure 3.7), T-SCEs were nearly undetectable in both *Tert*$^{+/-}$ *Fancc*$^{+/+}$ and *Tert*$^{+/-}$ *Fancc*$^{-/-}$ mice (Figure 3.9). In HG5 mice with short telomeres (Figure 3.7), higher frequencies of T-SCEs were observed in *Tert*$^{+/-}$ *Fancc*$^{-/-}$, compared to *Tert*$^{+/-}$ *Fancc*$^{+/+}$ (average 5.5% T-SCEs/chromosome in *Tert*$^{+/-}$ *Fancc*$^{-/-}$ and 3.5% T-SCEs/chromosome in *Tert*$^{+/-}$*Fancc*$^{+/+}$) (Figure 3.9). T-SCEs further increased in G2 *Tert*$^{-/-}$ *Fancc*$^{+/+}$ and *Tert*$^{-/-}$ *Fancc*$^{-/-}$ bone marrow cells harboring critically short telomeres (see SFEs in Figure 3.8 and Table 3.1), and the latter displayed more T-SCE events (average 24% T-SCEs/chromosome in *Tert*$^{-/-}$ *Fancc*$^{-/-}$ and 13% T-SCEs/chromosome in *Tert*$^{-/-}$ *Fancc*$^{+/+}$) (Figure 3.9). Thus, deletion of *Fancc* leads to elevated T-SCEs in late generation telomerase mutant mice with short telomeres. These observations suggest that short telomeres in late generation telomerase mutant mice become prone to T-SCEs and that inactivation of Fancc promotes T-SCEs.

Inactivation of FANCC in chicken DT40 cells results in elevated genome SCEs (173). We hypothesized that inactivation of Fancc in mice would cause spontaneous genome SCEs that in turn contribute to T-SCE events. We examined the frequencies of genome SCEs in HG5 *Tert*$^{-/-}$ *Fancc*$^{+/+}$ and *Tert*$^{-/-}$ *Fancc*$^{-/-}$ mouse bone marrow cells, and our data showed that the frequencies of genome SCEs in these mice were comparable (average 12% SCEs/chromosome in *Tert*$^{-/-}$ *Fancc*$^{+/+}$ and 10.7% SCEs/chromosome in *Tert*$^{-/-}$ *Fancc*$^{-/-}$) (Figure 3.10). Thus, deletion of *Fancc* does not affect the rate of spontaneous genome SCEs in primary hematopoietic cells derived from late generation *Tert* mutant mice.

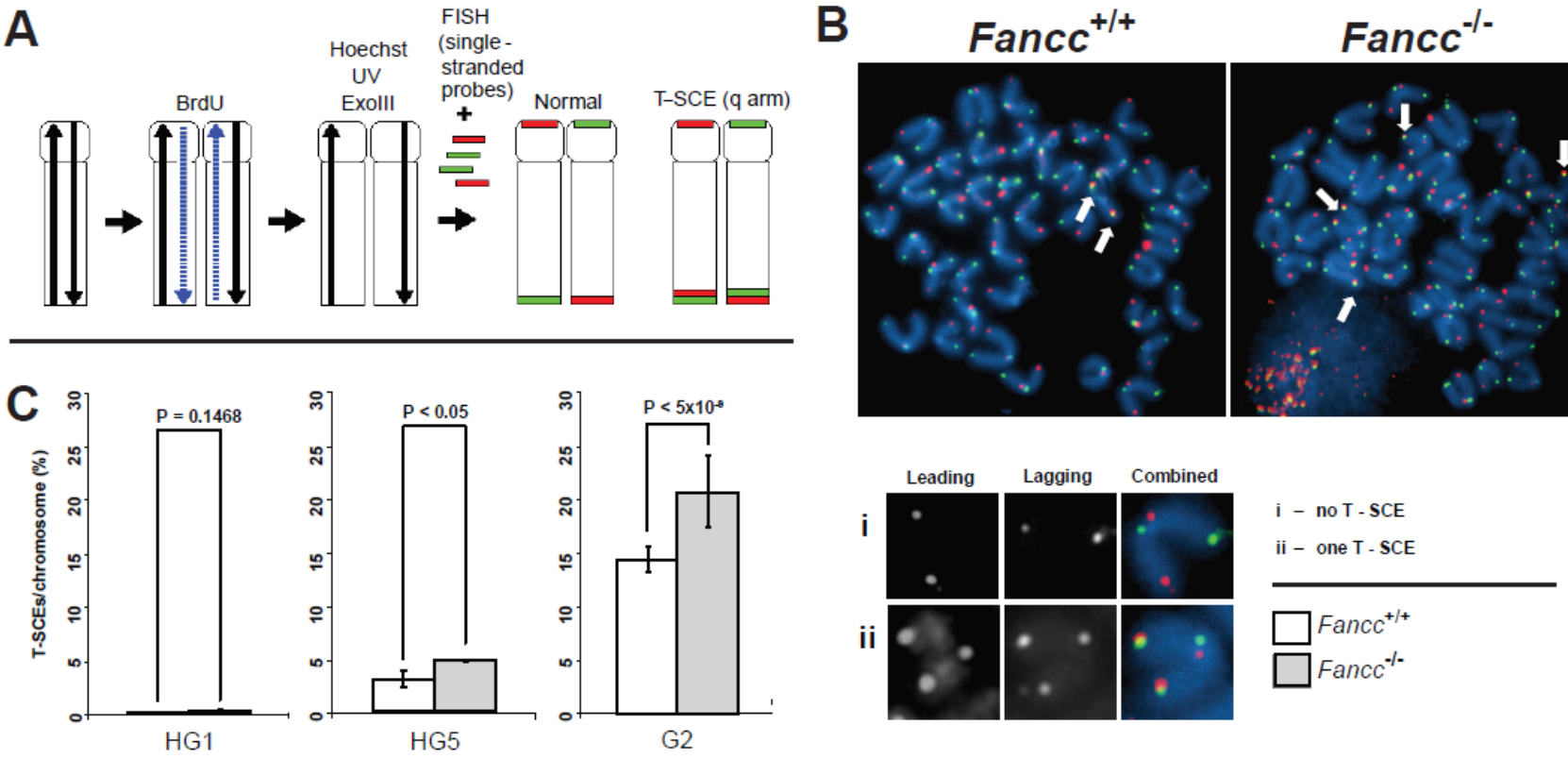

Figure 3.9 – *Fancc* deletion increases the frequencies of telomere sister chromatid exchange in late generation *Tert* mutant mice.
CO-FISH analysis of mouse bone marrow cells with indicated genotypes. (A) A schematic representation of CO-FISH procedure. In brief, newly synthesized strands are removed, leaving parental strands to be detected by fluorescent-labeled telomeric C-rich or G-rich probes. A chromosome with more than two telomere signals is considered to be positive for T-SCE. (B) Representative metaphase spreads of G2 *Tert*$^{-/-}$ *Fancc*$^{+/+}$ and *Tert*$^{-/-}$ *Fancc*$^{-/-}$ mouse bone marrow cells showing DAPI staining (blue), leading strand telomere fluorescence signals (red) and lagging strand telomere fluorescence signals (green). Arrows indicate T-SCEs. (C) The frequencies of T-SCEs in HG1, HG5, and G2 *Fancc*$^{+/+}$ and *Fancc*$^{-/-}$ mice. Error bars represent standard errors from different mice of each genotype (n=3).

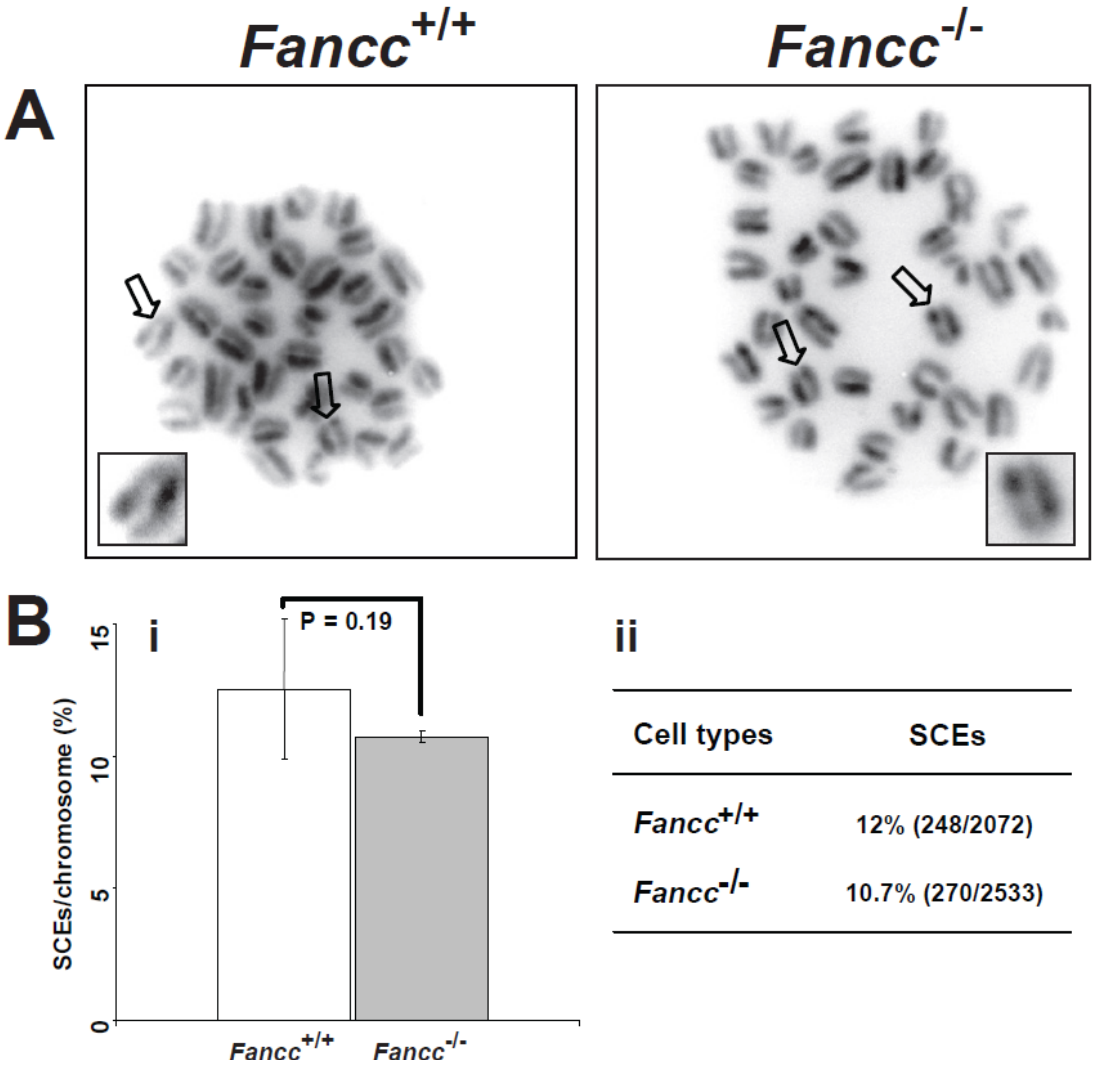

Figure 3.10 – The frequencies of genome SCEs are comparable between HG5 *Tert*$^{+/-}$ *Fancc*$^{+/+}$ and *Tert*$^{+/-}$ *Fancc*$^{-/-}$ mouse bone marrow cells.
(A) Representative metaphase spreads of bone marrow cells with indicated genotypes, showing genome SCE events. (B) (i) The incidences of genome SCEs are comparable between *Tert*$^{-/-}$ *Fancc*$^{+/+}$ and *Tert*$^{-/-}$ *Fancc*$^{-/-}$ bone marrow cells (n=4). Arrows indicate genome SCE events. (ii) The frequencies are derived from the number of SCE events divided by total number of chromosomes (%).

3.3 Discussion

In this study, we examined the role of FANCC in telomere length regulation and telomere recombination *in vivo*. Although deletion of *Fancc* did not directly affect telomere length or end-capping in a strain with long telomeres, it led to an increase in the incidence of T-SCEs in late generation telomerase mutant mice with short telomeres. These genetic data support the notion that FANCC does not directly regulate long telomeres, but does regulate short telomere-initiated telomere recombination. Thus, ablation of FANCC function may promote telomere recombination. To our knowledge, this is the first study to demonstrate a molecular event that regulates short telomere initiated-telomere recombination in non-transformed murine tissues.

Fancc$^{-/-}$ mice did not show telomere attrition or telomere defects in the C57BL/6 genetic background that has exceedingly longer telomeres than humans. A similar observation was reported in a mouse model deficient in *Fancg* (95). Interestingly, in an experimental system that dramatically increases the hematopoietic stem and progenitor cell turnover (i.e. serial bone marrow transplantation); *Fancc*$^{-/-}$ bone marrow cells showed elevated telomere shortening compared to wild type bone marrow cells, even though telomerase activity was comparable in these cell types. Since *Fancc*$^{-/-}$ hematopoietic stem and progenitor cells exhibit increased cycling compared to wild type cells (208,209), it is possible that higher turnover of *Fancc*$^{-/-}$ bone marrow cells may accelerate telomere shortening, which may, in turn, contribute to decreased *Fancc*$^{-/-}$ hematopoietic stem cell repopulation ability (206). Thus, telomere shortening may be an indirect consequence of *Fancc* deficiency.

Late generation *Tert*$^{-/-}$ mice displayed short telomeres and increased T-SCE events. When *Fancc* was deleted, the incidence of T-SCEs was exacerbated. These observations suggest that inactivation of FANCC promotes short telomere-initiated T-SCEs. It is possible that Fancc inhibits short telomere-initiated telomere recombination in primary murine hematopoietic cells, but inactivation of Fancc leads to loss of this suppressive mechanism. The exact mechanism of how FANCC suppresses telomere recombination is unclear. FANCC does not directly bind to DNA (176), and it may thus regulate proteins or pathways that are involved in telomere recombination. As a component of the FA core complex, FANCC regulates the monoubiquitination of FANCD2. A previous report demonstrates that the modified FANCD2 localizes to telomeres in an immortalized cell line that maintains telomeres through HR based mechanisms; however, depletion of FANCD2 causes increased short telomeres and decreased T-SCEs in this line (170). These telomere phenotypes are in contrast to the observations in HG5 *Tert*$^{+/-}$ *Fancc*$^{-/-}$ and G2 *Tert*$^{-/-}$ *Fancc*$^{-/-}$ mice. A possible explanation for these apparent inconsistencies could be that FA proteins may not only serve as checkpoint proteins that prevent primary cells from the engagement of illegitimate telomere recombination, but also regulate the maintenance of telomere recombination to keep the shortest telomeres intact in immortalized cells. Alternatively, these discrepant findings may be because the former study employed an immortalized cell line that had already escaped checkpoints for the illegitimate telomere recombination, while our studies utilized primary hematopoietic cells with intact checkpoints for illegitimate telomere recombination. FANCC also associates with the Bloom syndrome protein complex (174). It has been shown that the

frequencies of spontaneous SCEs in *fancc* and *blm* double mutant chicken DT40 cells are similar to those in *blm* single mutant (173). These studies suggest a functional linkage between FANCC and BLM in a common pathway to suppress sister chromatid exchange. Deletion of *Fancc* leads to reduced levels of Blm in mice (Suhasini AN and Brosh RM, personal communication). Decreased Blm levels may thus serve a role in promoting telomere recombination in *Fancc* and *Tert* double mutant mice. Although ablation of another member of RecQ helicase proteins, Wrn also results in elevated T-SCEs in late generation telomerase null mice (196), the *Wrn* and telomerase double null cells display elevated incidence of critically short telomeres (196). In contrast, *Fancc* deficiency reduces the incidence of critically short telomeres in late generation telomerase null mice (Table 3.1). These observations do not support the involvement of Wrn in Fancc-regulated telomere recombination in mice. However, deletion of *fancc* in chicken DT40 cells can lead to elevated spontaneous SCEs that depends upon a key HR protein, the RAD51 paralog, XRCC3 (173). In addition, ablation of murine telomere capping proteins (e.g. Pot1 or Trf2 in combination with Ku70) and histone methyltransferases (e.g. Suv4-20h or Suv39h) can cause elevated T-SCEs (197-200). It is unknown if FANCC regulates XRCC3, telomere binding proteins, or histone methyltransferases in telomere recombination.

FA patients without functional FA proteins are predisposed to bone marrow failure and malignancies (152,171). FANCC may therefore control cell viability and immortalization of primary cells, including bone marrow cells, by safeguarding genome stability. Telomere dysfunction triggers cell apoptosis and genomic instability

preferentially in highly proliferating organs, e.g. bone marrow. In rare events, cells may overcome this barrier and become immortalized by activating the pathway involved in maintaining telomere length (52). Increasing evidence suggests that short telomeres initiate telomere recombination likely due to a dysfunction in the highly regulated mechanisms controlling homologous recombination. We have shown that inactivation of FANCC facilitates short telomere-initiated telomere recombination. In addition, *Fancc* deficiency can accelerate telomere shortening during high hematopoietic cell turnover. It is possible that FANCC may function to control cell viability and immortalization of primary cells by influencing telomere attrition and telomere recombination.

3.4 Materials and Methods

Mice

Fancc and *Tert* knockout mice ($Fancc^{-/-}$ and $Tert^{-/-}$) in C57BL/6 genetic background were produced as described previously (87,184,205,206). Figure 3.6 illustrated mouse breeding strategy. In brief, *Tert* and *Fancc* heterozygous mice ($Tert^{+/-}$ $Fancc^{+/-}$) were generated by interbreeding $Tert^{+/-}$ and $Fancc^{+/-}$ mice and were named as heterozygous generation 1 (HG1) mice. HG1 mice from separate mating events were mated to obtain HG2 mice, which were crossed again until generation 5 (HG5). $Tert^{-/-}$ $Fancc^{+/-}$ mice were generated from HG5 $Tert^{+/-}Fancc^{+/-}$ breeders and were named as generation 1 (G1) mice. G1 mice from separate mating events were mated to obtain G2. All animal experiments were carried out according to the "Guide for the Care and Use of Laboratory Animals" (National Academy Press, USA, 1996) and were approved by the NIA IACUC.

Serial mouse bone marrow transplantation

Bone marrow was flushed from tibias and femurs of experimental mice and low-density mononuclear cells were prepared by density centrifugation (ficoll-hypaque density 1.119, Sigma, St. Louis, MO). Primary and secondary transplants were conducted as described previously with slight modification (206,207). Briefly, low-density mononuclear bone marrow cells ($2x10^6$ cells) were resuspended in 200 μl IMDM supplemented with 20% fetal bovine serum (FBS, Biowhittaker, Walkersville, MD). Cells were transplanted into congenic lethally-irradiated B6.SJL-PtrcaPep3b/BoyJ recipient mice obtained from the Stem Cell Transplant Mouse Core in the Indiana University Cancer Center. Bone marrow from primary recipients was harvested 12 months after transplantation and prepared for secondary transplantation. Secondary transplants were conducted exactly the same as primary transplants. Four months after secondary transplantation, bone marrow was harvested for telomere studies.

Telomere length measurements

Flow-FISH: the average telomere fluorescence in splenocytes, thymocytes, and bone marrow cells was scored for each mouse and the data were pooled from the indicated number of mice in each genotype and measured according to previously published protocol with minor modifications (210). A telomere specific FITC conjugated $(CCCTAA)_3$ PNA probe (0.3 μg/ml, Panagene) was used.

Q-FISH: Mice were injected with 100 µl of 0.5% colchicine intraperitoneally for approximately 30 minutes before being scarified. Bone marrow cells were then collected by flushing 1ml of PBS from femurs. Collected bone marrow cells were immediately incubated in 0.075M KCl for 15 minutes in 37^{o}C, followed by fixation in ice-cold (3:1) methanol and glacial acetic acid. Metaphase spreads were then hybridized with a Cy3–labeled PNA $(CCCTAA)_3$ probe (0.3 µg/ml, Panagene) and counterstained with 4,6 diamidino-2-phenylindole as previously described (211). Images were captured using Cytovision™ software (Applied Imaging Corp.) on a fluorescence microscope (Axio2; Carl Zeiss, Germany), followed by quantification of telomere fluorescence signals using the TFL-Telo software (a kind gift from P. Lansdorp, Vancouver, BC). For histograms and box-plots, data from different mice of each genotype were pooled and scored and R statistical package (http://www.braju.com/R/) along with R.utils package and Biobase package (http://www.bioconductor.org/) was used. The frequencies of telomeres within a given range of telomere signal intensities were plotted against the telomere signal intensity using arbitrary units. Metaphases from different mice of each genotype were scored for chromosomal and telomeric abnormalities (i.e. frequencies of cells with > or < 40 chromosomes, frequencies of chromosomal fragmentations and breakages, and frequencies of chromosome ends with no detectable telomere signals) as previously described (193,212).

Telomere restriction fragment analysis: The analysis was carried out as described by Hemann *et al*. (213). Approximately 1 X 10^6 mouse bone marrow cells were embedded in agarose plugs. DNA was digested with *DnpII* (BioLabs) and

electrophoresed through 1% w/v pulsed field grade agarose (Bio-Rad) in 1 X Tris-acetate-EDTA buffer. Electrophoresis was carried out in a CHEF DR-III pulsed-field apparatus (Bio-Rad) at 14°C with 3 volt/cm and a switch time of 10 sec for 48 h. The gel was denatured, dried, probed with P^{32}-labeled $(AATCCC)_4$ probe, and visualized by autoradiography.

Measurement of telomere sister chromatid exchange (T-SCE) and genome sister chromatid exchange (SCE)

Chromosome orientation FISH (CO-FISH) was used to measure the frequency of T-SCE (50). The measurement for genome SCEs was carried out as described previously (193). Briefly, bone marrow cells were flushed from femurs and tibias and cultured with Iscove's modified Dulbecco's medium (IBCO-BRL, Gaithersburg, MD) supplemented with 20% fetal calf serum (Hyclone, Logan, UT) in the presence of interleukin 6 (200 U/mL) and stem cell factor (100 ng/mL; Peprotech Rocky Hill, NJ) (206). Bone marrow cells were subcultured in medium containing a 3:1 ratio of BrdU/BrdC (Sigma) at a final concentration of 1 x 10^{-5} M and collected around 12 or 24 hours for detecting T-SCE or SCE, respectively. Colcemid (0.1 μg/ml) was added 2 hours before harvest. Metaphase spreads were then stained with Hoechst 33258, exposed to UV light, and digested with exonuclease III to remove newly synthesized DNA strands. Hybridization and wash conditions were identical to those described for telomere FISH (211). A chromosome with more than two telomeric DNA signals by FITC-labeled $(CCCTAA)_3$ or Cy-3-labeled $(TTAGGG)_3$ PNA probes (0.3 μg/ml, Panagene) was scored as T-SCE positive.

A SCE was scored each time a color switch between dark or light sister chromatids occurred. The frequencies of T-SCEs and SCEs were obtained from different mice of each genotype.

Analysis of telomerase activity and *Tert* and *Terc* level

Telomerase activity was measured by using Biomax Telomerase detection kit (Biomax Inc., MD, USA) according to the manufacturer's recommendations. Briefly, freshly isolated bone marrow cells were lysed, and the cell extracts were then added to a pre-mix for quantitative telomerase activity in a real-time PCR reaction. For detecting *Tert* and *Terc* level, total RNA was extracted from mouse bone marrow using RNeasy kit (Qiagene) and then reverse-transcribed with random hexamers by the SuperScript III first-strand synthesis system for RT-PCR (Invitrogen Life Technologies). The PCR reaction included cDNA reaction, 2x Sybr master mix (Biorad), and a set of primers for mouse *Tert, Terc,* or *Beta-Actin* (Table 3.3). The levels of *Tert* and *Terc* were normalized to that of *Beta-Actin*. MyiQ Single-Color Real-Time PCR Detection System (Bio-Rad, CA, USA) was used to conduct the reaction where each sample was done in triplicates and performed according to the manufacturer's instructions. *Tert* deficient mouse bone marrow cell extracts or cDNA were used as control. Relative telomerase activity was expressed as log of C_T value. Relative *Tert* and *Terc* RNA levels were normalized to *Beta-Actin* and expressed using the comparative C_T method according to the manufacturer's instructions.

Table 3.3 – Summary of primer sequences for qT-PCR analysis

Primer	Sequence
Tert Forward	5'-TGGTGGAGGTTGTTGCCAA-3'
Tert Reverse	5'-CCACTGCATACTGGCGGATAC-3'
Terc Forward	5'-GTGGTGGCCATTTTTTGTCTAAC-3'
Terc Forward	5'-TGCTCTAGAATGAACGGTGGAA-3'
Beta-Actin Forward	GACCTCTATGCCAACACAGTGCTG
Beta-Actin Reverse	CACCGATCCACACAGAGTACTTGC

Chapter 4: Characterization of Oxidative Guanine Damage and Repair in Mammalian Telomeres

The following chapter has been published as: Zhilong Wang, David B. Rhee, Jian Lu, Christina Bohr, Birija S. Patro, Nadja C. de Souza-Pinto, and Yie Liu, "Characterization of oxidative guanine damage and repair in mammalian telomeres*", PLoS Genetics.* 2010 May 13; 6(5): e1000951.

DBR contributed figures 4.1, 4.5, 4.6, 4.8, 4.13, and 4.14 of this chapter.

4.1 Introduction

Telomeres are chromosome end nucleoprotein structures that are composed of telomere associated proteins and TTAGGG repeats in mammals (2). Telomeres cap chromosome ends and prevent them from being recognized as broken DNA. Dysfunctional telomeres, emanating from loss of telomere repeats and/or loss of protection by telomere-associated proteins, are recognized by many DNA damage response proteins, including γH2AX, 53BP1, and ATM that form telomere dysfunction-induced foci (TIF) and induce cellular senescence or apoptosis (3,183).

Telomere length homoeostasis is maintained through interplay among telomerase extension, telomere recombination, telomere replication, and telomere capping (2). Telomerase, a ribonucleoprotein complex, replenishes replication dependent-telomere repeat loss and is essential in telomere length maintenance (2). Telomere associated proteins also play a key role in telomere length regulation and capping. Mammalian telomeres are coated by a telomere protein complex, referred as shelterin. Shelterin includes telomere binding proteins TRF1, TRF2, and POT1 (3) that negatively control

telomere length in cis by limiting the access of telomerase to the ends of individual telomeres (36,53,214,215). Reduced telomere-bound TRF1 promotes telomere lengthening in human cells (214,215), but telomeres that are severely or completely stripped off the protective telomere protein complex result in telomere uncapping and evoke ATM or ATR dependent DNA damage response, nucleolytic degradation and undesirable recombination (28,29,31,197,198,216-218). Efficient telomere replication also requires the telomere associated proteins, e.g. TRF1 and WRN (219-222).

Oxidative stress has been proposed to be a major cause of telomere shortening in cultured cells (101). For instance, normoxia, hyperoxia (40% oxygen), and mitochondrial dysfunction-induced reactive oxygen species (ROS) accelerate telomere shortening and severely reduce proliferative lifespan of human somatic cells *in vitro*; while these phenotypes are delayed when cells are grown in hypoxia or in the presence of antioxidants (101). Interestingly, human cells with long telomeres show increased sensitivity to hydrogen peroxide, but not to etoposide and bleomycin, supporting the notion that telomeres are particularly vulnerable to oxidative damage (102). These studies suggest that oxidative stress causes telomere shortening or damage; however it is unclear which types of oxidative DNA damage arise in telomeres and how they compromise telomere length and integrity. Previous studies have demonstrated that oxidative stress causes single strand breaks (SSBs) in telomeric DNA (105). Thus, telomere shortening could arise from SSBs. Oxidative stress has also been shown to induce oxidative base damage in telomeric oligonucleotides *in vitro* (106,108,223), and 8-oxoG at double-stranded telomeric nucleotides attenuates binding by TRF1 and TRF2 (112). It is unclear

if oxidative base damage has any impact on telomere length and integrity in mammalian cells.

Oxidative DNA damage, resulting from ROS, increases with age and can accumulate as a variety of oxidative modifications in purines and pyrimidines (115,224). Oxidized bases may lead to mutagenesis, block DNA replication, or alter the affinity of DNA binding proteins, which can, in turn, attenuate cell viability or promote tumorigenesis (119,225,226). BER is the primary DNA repair pathway for the repair of non-bulky damaged bases, and the initial step in BER is base removal by a DNA glycosylase. Several DNA glycosylases with distinct, but overlapping substrate specificities have been characterized, and OGG1 primarily excises 8-oxoG and FapyG paired with cytosine in duplex DNA (119,226). OGG1 is well conserved from bacterial to mammals, implying its significant functional importance in maintaining genome integrity (115,224). If 8-oxoG is unrepaired, it becomes highly mutagenic, because it can pair with adenine and lead to GC to TA transversions after two rounds of replication (227-229). The removal of adenine opposite 8-oxoG is via the adenine-specific mismatch DNA glycosylase, MYH (230). Mice lacking these repair genes exhibit an increased spontaneous mutation rate and a marked increase in tumor predisposition (144,147,230,231). In addition, *Ogg1* and *Myh* deficient murine cells are sensitive to oxidative stress (232-234). These studies are consistent with the idea that oxidative base lesions contribute to genome instability, neoplastic transformation, and cell death.

Ogg1 deficiency causes an increase in 8-oxoG and FapyG lesions in the mouse genome (144,225,235). This genetic model therefore allows us to study whether these

unique oxidative guanine lesions can affect telomere integrity. Here, we present evidence that deletion of the mouse *Ogg1* gene attenuates telomere integrity via multiple ways. Thus, interfering with telomere integrity may be one of the mechanism(s) by which oxidative base damage leads to genome instability.

4.2 Materials and Methods

Mice and primary mouse cells

The generation of *Ogg1* null mice was described elsewhere (144). *Ogg1*$^{-/-}$ mice were further backcrossed into C57BL/6 background. Wild type and *Ogg1*$^{-/-}$ mice were derived from heterozygous (*Ogg1*$^{+/-}$) breeders. Primary MEFs were isolated from 13.5 day embryos of *Ogg1*$^{+/-}$ female bred with *Ogg1*$^{+/-}$ male and cultured in Dulbecco's Modified Eagle Medium containing 10% fetal bovine serum. Splenocytes were prepared from mouse spleens, cultured in RPMI 1640 with 10% FBS and 0.1% 2-mercaptoethanol, and stimulated with 50 μg/ml *Escherichia coli* LPS serotype O111:B4 (Sigma-Aldrich) and 50 ng/ml mouse IL-4 (R&D Systems). Bone marrow cells were flushed from femurs and tibias and cultured with Iscove's modified Dulbecco's medium (IBCO-BRL) supplemented with 20% fetal calf serum (Hyclone) in the presence of interleukin 6 (200 U/mL; Peprotech) and stem cell factor (100 ng/mL; Peprotech). To decrease or enhance oxidative stress, mouse cells were cultured in 3% oxygen (SANYO O_2/CO_2 incubator, MCO-18M) or 20% oxygen or in the presence of paraquat. All animal experiments were carried out according to the "Guide for the Care and Use of Laboratory Animals"

(National Academy Press, USA, 1996), and were approved by the Institutional Animal Care and Use Committee of National Institute on Aging.

Telomere quantitative fluorescence in situ hybridization

The telomere fluorescence in cell populations of spleen, bone marrow, and primary MEFs was measured by Flow cytometry and FISH (Flow-FISH) according to previously published protocol (210). A telomere specific FITC conjugated $(CCCTAA)_3$ PNA probe (0.3 μg/ml, Panagene) was used.

Quantitative FISH (Q-FISH) was performed as previously described (194,211,212). Metaphase spreads were prepared from freshly isolated or subcultured mouse bone marrow cells, activated splenocytes, and primary MEFs. Briefly, mice were injected with 100 μl of 0.5% colchicine intraperitoneally for approximately 30 minutes before being sacrificed. Bone marrow cells were then collected by flushing 1ml of PBS through femurs and tibias. Cultured mouse cells were incubated with 0.1 μg/ml colcemid for 2-6 hr at 37°C to allow mitotic cells to accumulate. Metaphase spreads were obtained by incubating colchicine- or colcemid- treated mouse cells in 0.075 M KCl for 15 minutes in 37°C, followed by fixing cells in ice-cold 3:1 methanol and glacial acetic acid and dropping the fixed cells onto slides. Metaphase spreads were hybridized with Cy3-labeled $(CCCTAA)_3$ (0.3 μg/ml, Panagene), washed, and then counterstained with 4,6 diamidino-2-phenylindole (DAPI). For the detection of telomere signal intensity in G and C strands, metaphase spreads were initially hybridized with FITC-labeled $(CCCTAA)_3$ PNA probes (0.3 μg/ml, Panagene). The free-$(CCCTAA)_3$ probe were washed off the

slides, and then hybridized with TAMRA-labeled $(TTAGGG)_3$ (0.3 μg/ml, Panagene). Images were captured using Cytovision™ software (Applied Imaging) on a fluorescence microscope (Axio2; Carl Zeiss); followed by quantification of telomere fluorescence signals using the TFL-Telo software (a kind gift from Dr. Peter Lansdorp). For histograms and box-plots, data from different mice of each genotype were scored and R statistical package (http://www.r-project.org/) along with R.utils package and Biobase package (http://www.bioconductor.org/) were used. The frequencies of telomeres within a given range of telomere signal intensities were plotted against the telomere signal intensity using arbitrary units. Metaphases from different mice of each genotype were scored for chromosomal and telomeric abnormalities as previously described (194,212).

Telomerase activity

Telomerase activity was measured by Biomax Telomerase Detection Kit (Biomax) according to the manufacturer's recommendations. Briefly, mouse cell extracts were added to a pre-mix for quantitative telomerase activity in a real-time PCR reaction. MyiQ Single-Color Real-Time PCR Detection System (Bio-Rad) was used to perform the reactions, where each sample was done in triplicates and performed according to the manufacturer's instructions. HeLa cell extracts were used as positive control. *Tert* knockout mouse cell extracts and RNase-treated HeLa cell extracts were used as negative controls. Relative telomerase activity was expressed as log of C_T value.

Measurement of telomere sister chromatid exchanges (T-SCEs)

CO-FISH was used to measure T-SCEs and telomere lagging or leading strand loss (50,219). Briefly, mice were injected with 3:1 ratio of BrdU/BrdC (Sigma) at a final concentration of 1 x 10^{-5} M intraperitoneally for approximately 20 hours, and subsequently with 100 μl of 0.5% colchicine for approximately 30 minutes before being sacrificed. Bone marrow cells were then collected by flushing 1ml of PBS through femurs and tibias. MEFs were cultured in medium containing a 3:1 ratio of BrdU/BrdC (Sigma) at a final concentration of 1 x 10^{-5} M for 24 hours, and colcemid (0.1 μg/ml) was added 4 hours before harvest. Metaphase spreads were prepared from mouse bone marrow cells or MEFs, stained with Hoechst 33258, exposed to UV light, and digested with exonuclease III to remove newly synthesized DNA strands. Hybridization and wash conditions were identical to those described for Q-FISH. FITC-labeled $(CCCTAA)_3$ and TAMRA-labeled $(TTAGGG)_3$ PNA probes were used for the detection of lagging and leading strand, respectively. A chromosome with more than two telomeric DNA signals by both FITC-labeled $(CCCTAA)_3$ and TAMRA-labeled $(TTAGGG)_3$ PNA probes was scored as T-SCE positive. A chromosome with loss of one or two telomeric DNA signals by either FITC-labeled $(CCCTAA)_3$ or TAMRA-labeled $(TTAGGG)_3$ PNA probes was scored for telomere lagging or leading strand loss.

Indirect immunofluorescence and telomere FISH (TEL-FISH)

TEL-FISH was performed as described previously (212) with minor modifications. Briefly, cells were fixed in 1:1 methanol:acetone (Sigma) at –20°C for 10 minutes, permeabilized with 0.5% NP-40, and blocked in 1% Bovine serum albumin

(BSA) (IgG-free, Sigma). Cells were first immunostained with a rabbit anti-γH2AX antibody (16193, Upstate Biotechnology), a rabbit anti-53BP1 antibody (BN 100-304, Novus Biologicals), or a mouse anti-XRCC1 antibody (X0629, Sigma) overnight at 4°C followed by Alexa 488-labeled secondary antibody (1:500; Molecular Probes) for one hour at 37°C. Slides were washed with PBS for 15 minutes, fixed in 2% paraformaldehyde at room temperature for 10 minutes, dehydrated through ethanol series, and air-dried briefly. Slides were then hybridized to a TRAMA-labeled $(CCCTAA)_3$ PNA probe (Panagene), then counterstained with DAPI. Z-stack images were captured and deconvoluted using Axiovision 4.6.3 software on a fluorescence microscope (Axiovert 200M; Carl Zeiss).

Detection of oxidative base lesions in telomeres

Identification of oxidative base lesions in telomeres was performed as previously described (236) with modifications. In brief, DNA was isolated from mouse liver or primary MEFs by salting out. 4 μg of DNA was treated with *HinfI* and *RsaI* restriction enzyme at 37°C overnight. The reaction was heated at 65°C for 15 minutes and then divided into two equal portions; one was treated with 8 units of *E. coli* formamidopyrimidine-DNA glycosylase (Fpg) (New England Biolabs) and another was treated with a mock buffer at 37°C for 30 minutes. Fpg was inactivated by heating at 60°C for 15 minutes. Genomic single-stranded DNA fragments were separated on 1% alkaline agarose gel according to their sizes, treated with UV light, then transferred to a nylon membrane. Single-stranded telomere DNA fragments were detected by ^{32}P-labeled

$(CCCTAA)_4$ probe and visualized by autoradiography. ImageQuant software was applied in quantifying DNA cleavage in mock and Fpg-treated samples. A grid object was created as a single column with multiple rows and was placed over the lane corresponding to the molecular size markers. The density measurement was conducted in each row in which each marker was recorded. The mean length (ML) was calculated as a center of mass and expressed in kb: $ML=\Sigma (MWi \times ODi)/ \Sigma (ODi)$, in which MWi is the length of the telomeric DNA at each row and ODi is the densitometer output at each row. The frequencies of Fpg-sensitive lesions in a sample were calculated based on ML values in Fpg- and mock-treated samples: lesions = (ML untreated /ML treated) -1, in which ML is expressed in kb. Fold-changes in each sample were further normalized with respect to the number of Fpg-sensitive lesions in a control.

4.3 Results

Ogg1 deficient mouse tissues and primary MEFs under low oxygen tension display telomere lengthening

Ablation of OGG1 function in *S. cerevisiae* can cause telomere elongation (13,237). Since OGG1 is conserved from *S. cerevisiae* to mice, we investigated the impact of *Ogg1* deficiency on telomere length in mice. Mouse bone marrow cells were freshly isolated from 1-3 month old mice and analyzed by Q-FISH. Compared to the wild type, $Ogg1^{-/-}$ mouse bone marrow displayed higher mean and median telomere signal intensities (Figure 4.1). Similar results were obtained from bone marrow cells from 12 month old mice (Figure 4.2). This observation was further confirmed by Flow-FISH,

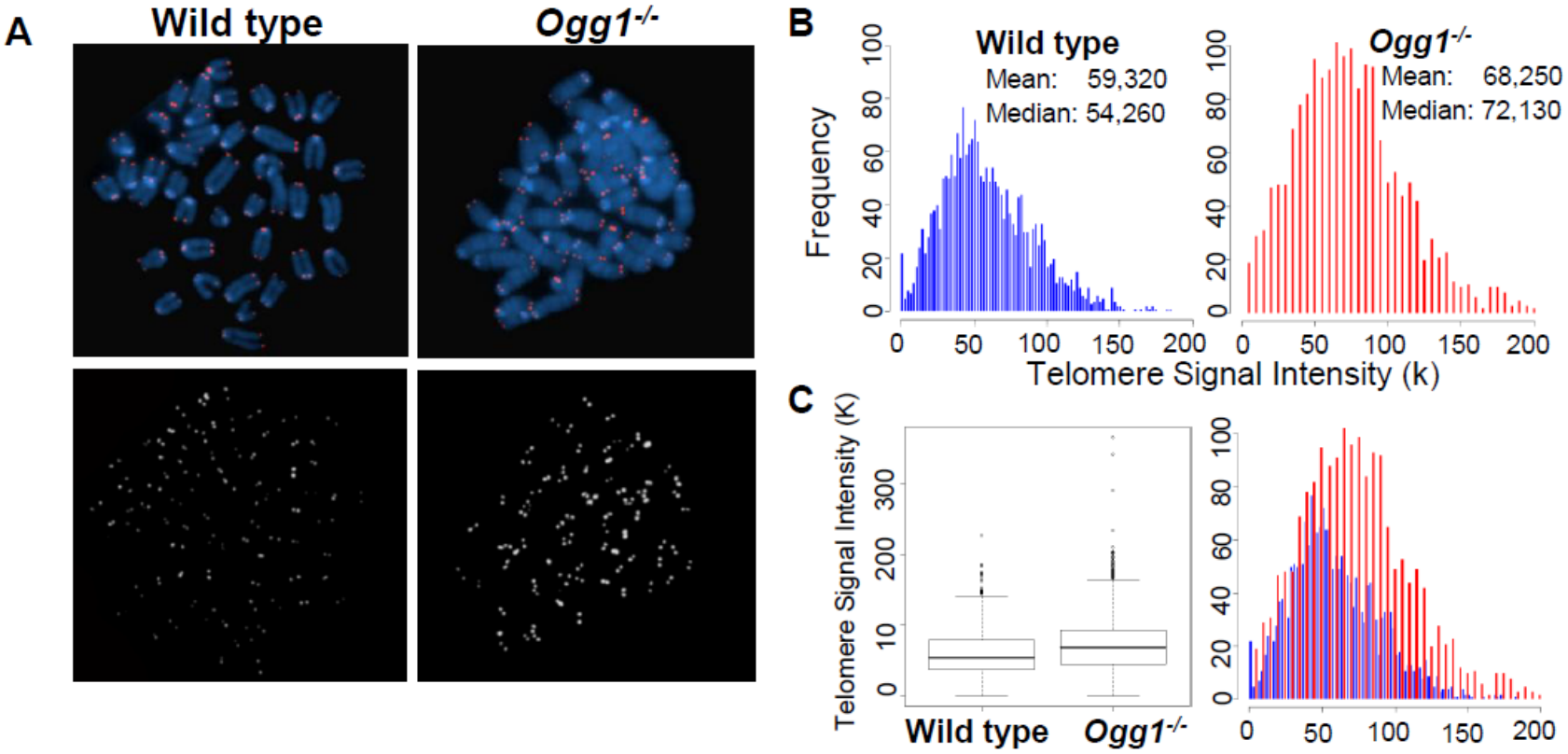

Figure 4.1 – Telomere length in hematopoietic cells freshly isolated from wild type and *Ogg1*$^{-/-}$ mice.
Q-FISH analysis of metaphase spreads of the mouse bone marrow cells from wild type and *Ogg1*$^{-/-}$ mice (n=6). (A) Representative metaphase spreads of wild type and *Ogg1*$^{-/-}$ mouse bone marrow cells showing DAPI staining (blue, upper panel) and telomere fluorescence signals (red, upper panel; white, lower panel). Representative quantitative measurement and dynamic range of telomeric DNA signal intensity at individual chromosome ends in a wild type and an *Ogg1*$^{-/-}$ mouse are shown as histogram (B) and box-plot (C). An increase in telomere signal intensity was repeatedly observed in *Ogg1*$^{-/-}$ mice, compared to age-matched wild type mice (1.5-, 1.3-, 1.2-fold increase in three pairs of mice, respectively).

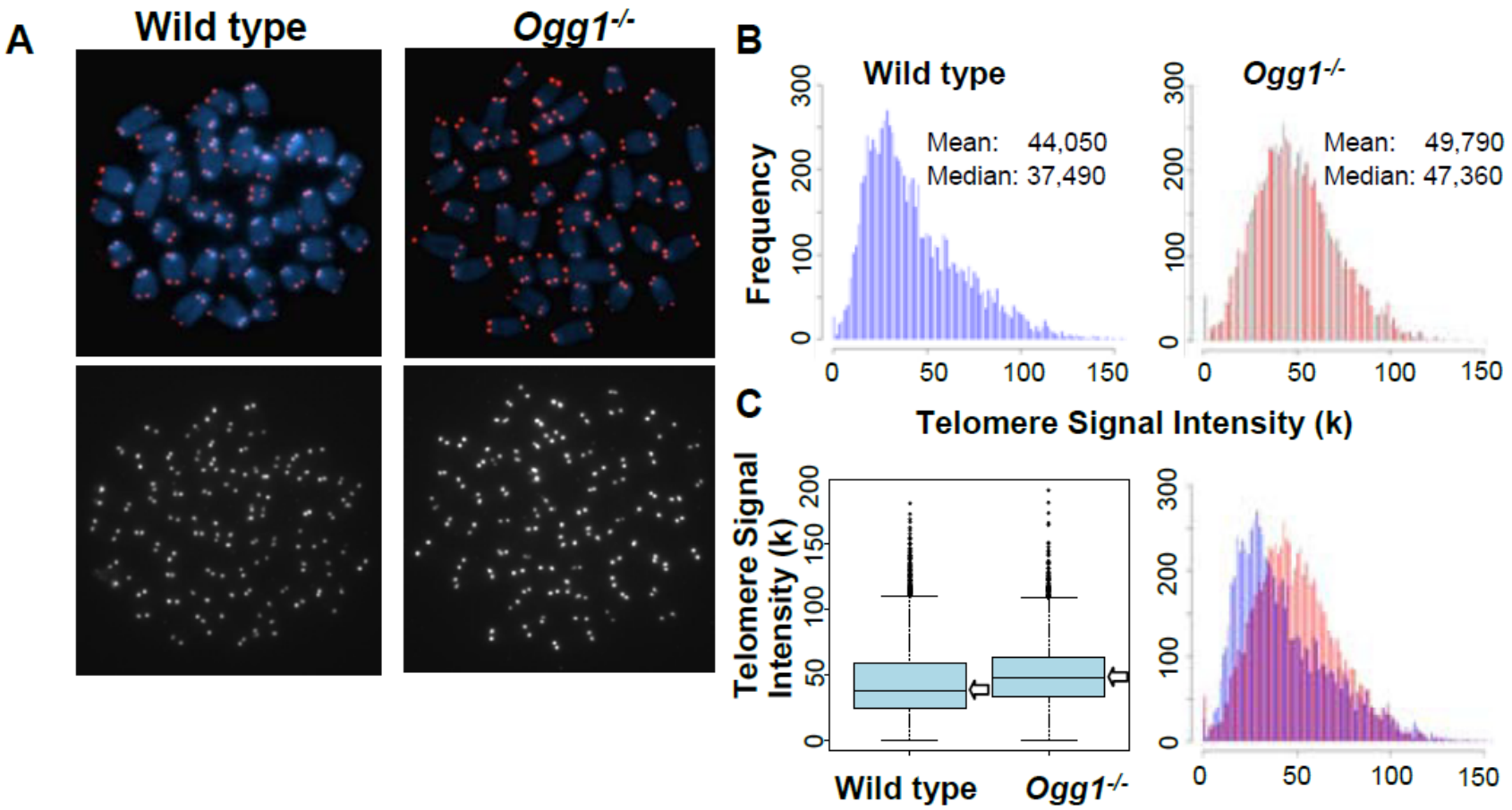

Figure 4.2 – Q-FISH analysis of mouse bone marrow cells from 12-month-old wild type and *Ogg1*$^{-/-}$ mice.
(A) Representative metaphase spreads of wild type and *Ogg1*$^{-/-}$ mouse bone marrow cells showing DAPI staining (blue, upper panel) and telomere fluorescence signals (red, upper panel; white, lower panel). Quantitative measurement and dynamic range of telomeric DNA signal intensity at individual chromosome ends are shown as histogram (B) and box-plot (C). An increase in telomere signal intensity was observed in *Ogg1*$^{-/-}$ mice. *This figure is provided by Zhilong Wang.

showing that telomere signal intensity was moderately increased in *Ogg1*$^{-/-}$ mouse bone marrow cells from young and old animals (Figure 4.3A). Freshly isolated splenocytes from >3 month old *Ogg1*$^{-/-}$ mice also displayed higher telomere signal intensity than those of age-matched wild type mice (Figure 4.3A). Additionally, we examined telomere length in wild type and *Ogg1*$^{-/-}$ primary MEFs cultivated in 3% O_2 that mimics the *in vivo* oxygen level in mice. Telomere signal intensity was moderately increased in *Ogg1*$^{-/-}$ primary MEFs as shown by Flow-FISH (Figure 4.3B) and, to a lesser extent, by Q-FISH (Figure 4.4).

Next, we examined if deletion of *Ogg1* could affect telomere capping *in vivo*. Freshly isolated mouse bone marrow cells and primary MEFs cultivated in 3% O_2 were examined for the frequencies of chromosome end-to-end fusions and telomere signal free ends (SFEs). *Ogg1*$^{-/-}$ mouse cells did not show any chromosome end-to-end fusions. The incidence of SFEs was low and not significantly different between wild type and *Ogg1*$^{-/-}$ mouse cells. Furthermore, *Ogg1*$^{-/-}$ mouse cells did not display spontaneous chromosomal abnormalities, e.g. chromosome breaks or fragments (Table 4.1). These data suggest that ablation of OGG1 function does not lead to telomere uncapping and chromosomal instability, but moderate telomere lengthening in mouse tissues and primary cells that are subjected to low levels of oxidative stress.

High oxidative stress increases telomere attrition in *Ogg1* deficient mouse cells

To determine if high oxidative stress has the same or different impact on telomere length, primary wild type and *Ogg1*$^{-/-}$ MEFs were cultivated in 20% O_2 or in the presence

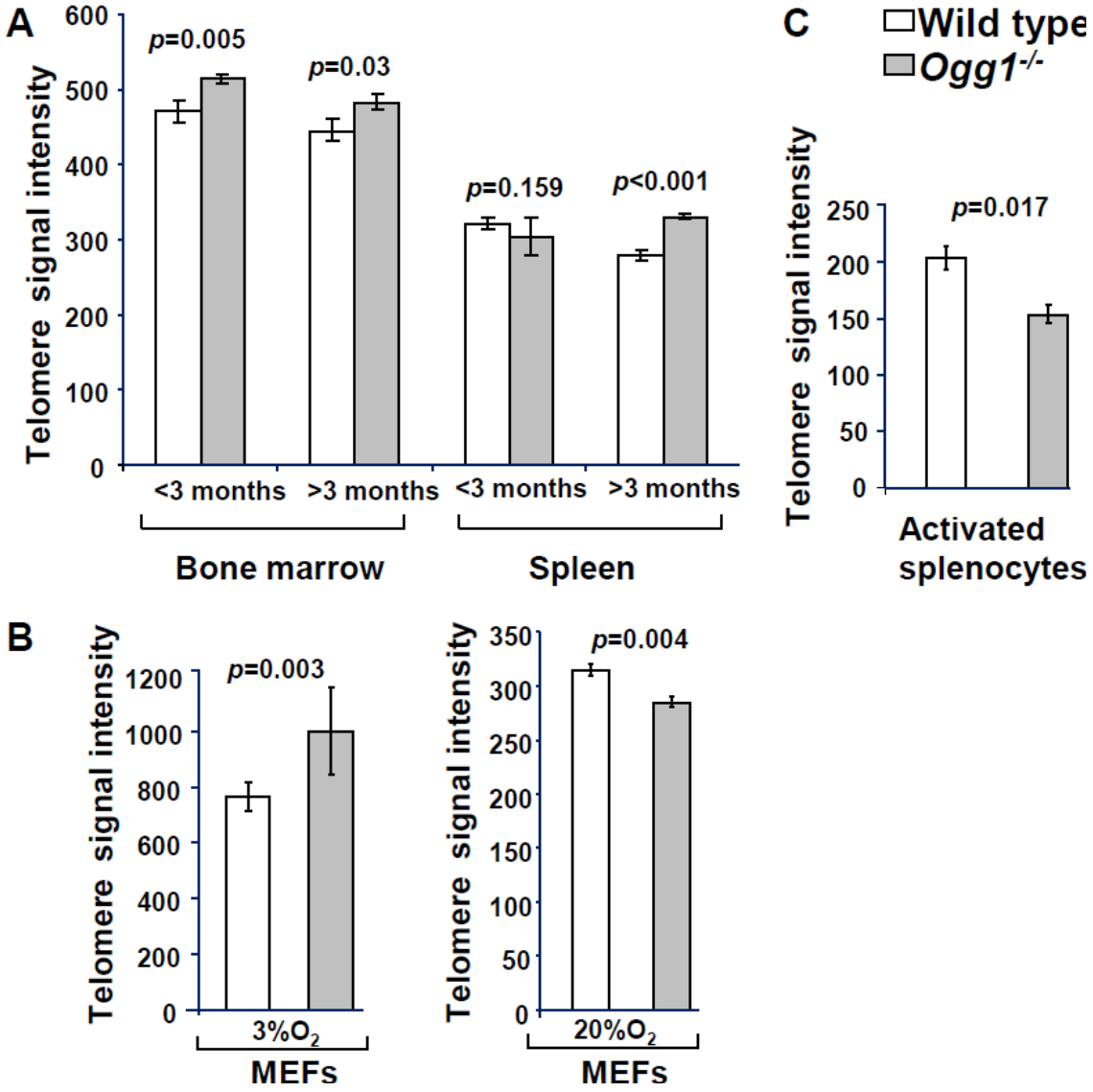

Figure 4.3 – Average telomere length in wild type and *Ogg1*$^{-/-}$ mouse tissues and primary MEFs. Flow-FISH analysis of telomere signal intensity in freshly isolated bone marrow and spleen from wild type and *Ogg1*$^{-/-}$ mice (n=15) at different age (A), wild type and *Ogg1*$^{-/-}$ primary MEFs cultivated in 3% and 20% oxygen for 6 passages (B), and wild type and *Ogg1*$^{-/-}$ splenocytes cultivated in 20% oxygen for 3 days (C). Telomere signal intensity was altered in *Ogg1*$^{-/-}$ mouse tissues and cells, compared to the wild type control.*This figure is provided by Zhilong Wang.

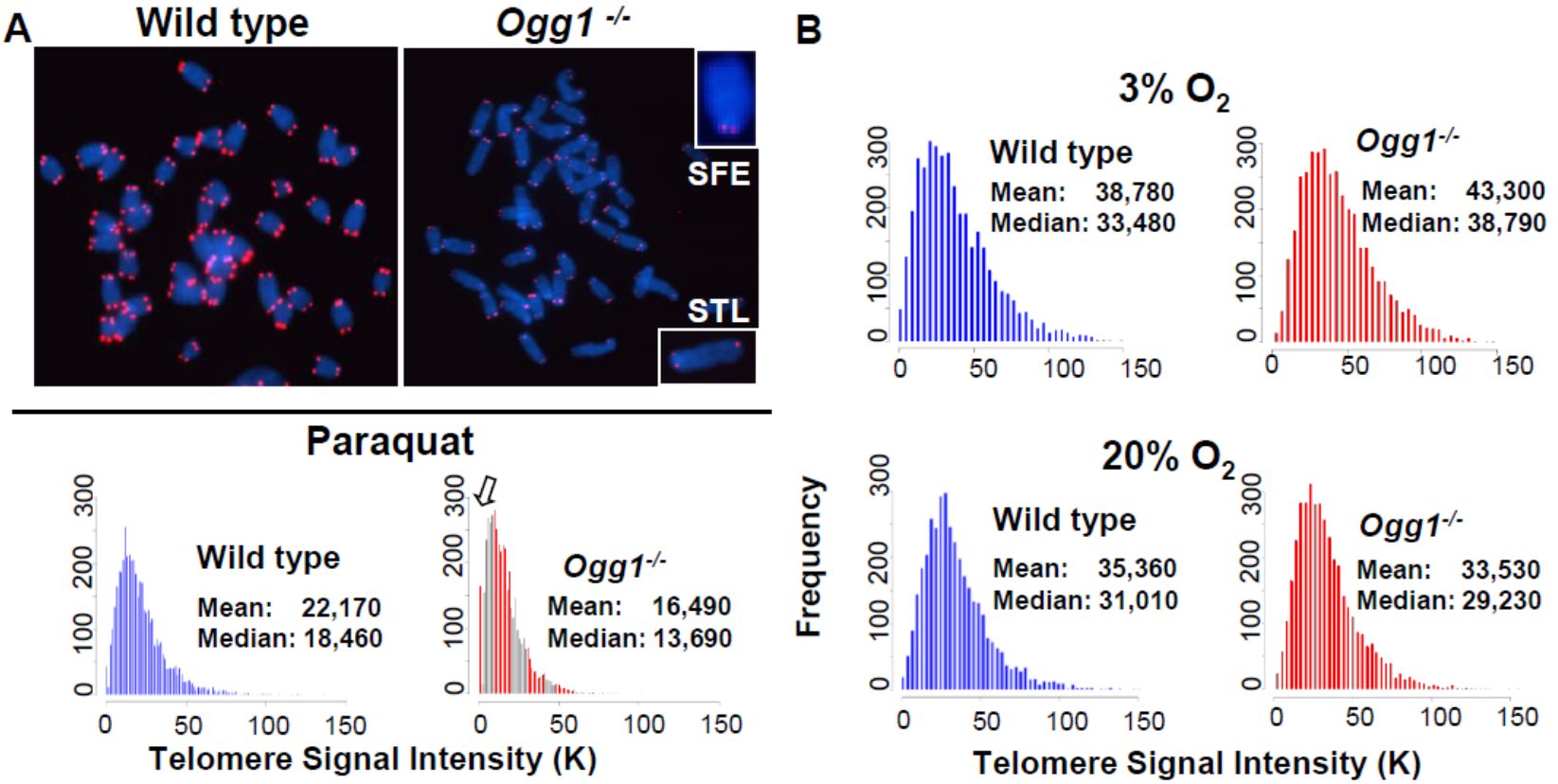

Figure 4.4 – Telomere length in primary MEFs cultivated in low or high oxidative environment.
Q-FISH analysis of metaphase spreads of wild type and *Ogg1*$^{-/-}$ primary MEFs cultivated in 3% O_2, 20% O_2, or 3% O_2 in the presence of 0.5 μM paraquat for 6 passages. (A) Representative metaphase spreads of wild type and *Ogg1*$^{-/-}$ primary MEFs cultivated in 20% O_2. Loss of telomere signals at chromosomes or chromatids were more frequently observed in *Ogg1*$^{-/-}$ MEFs (see enlarged chromosomes in boxes). (B) Representative histogram of dynamic range of telomeric DNA signal intensity at individual chromosome ends in a wild type and an *Ogg1*$^{-/-}$ primary MEF line. In comparison to wild type MEFs, slight increase in telomere signal intensity was repeatedly detected in *Ogg1*$^{-/-}$ MEFs in 3% O_2 (approximately 1.1- fold increase in three pairs of MEF lines); and decreased telomere signal intensity and increased SFEs (see arrow) were repeatedly observed in *Ogg1*$^{-/-}$ MEFs cultivated with 20% O_2 (2-, 1.7-, and 1.4-fold decrease in three pairs of MEF lines, respectively) and 0.5 μM paraquat (1.8-, 1.3-, and 1.2- fold decrease in three pairs of MEF lines, respectively). *This figure is provided by Zhilong Wang.

Table 4.1 – Frequencies of chromosomal and telomeric abnormalities in wild type and *Ogg1*$^{-/-}$ bone marrow cells and primary MEFs

Cell types	Chr. Fragment & Breaks	End-to-end fusion	SFEs
Bone marrow			
Wild type	0% (0/1919)	0% (0/1919)	0.4% (7/1919)
Ogg1$^{-/-}$	0% (0/1980)	0% (0/1980)	0.7% (14/1980)
Primary MEFs (3% O_2)			
Wild type	0% (0/1087)	0% (0/1087)	3.2% (35/1087)
Ogg1$^{-/-}$	0% (0/1140)	0% (0/1140)	4.1% (47/1140)
Primary MEFs (20% O2)			
Wild type	0.1% (1/846)	0% (0/846)	4.5% (38/846)
Ogg1$^{-/-}$	0.7% (7/946)	0.11% (1/946)	8.4% (79/946)*
Primary MEFs (0.5 μM paraquat)			
Wild type	0.1% (1/993)	0.1% (1/993)	4.1% (41/993)
Ogg1$^{-/-}$	0% (0/983)	0.2% (2/983)	18.6% (183/983)*

*Number of abnormal events/total chromosomes. SFEs: telomere signal free ends. The data were obtained from metaphase spreads and Q-FISH analysis of different mice (n=6) or MEF lineages of each genotype (n=6). * *p*-value between wild type and *Ogg1*$^{-/-}$ yielded a statistical difference in indicated categories.
^This table is provided by Zhilong Wang.

of 0.5 μM of paraquat (an oxidant). After six passages, they were evaluated for telomere length by Q-FISH and Flow-FISH. Surprisingly, under these conditions *Ogg1*$^{-/-}$ MEFs showed reduced telomere signal intensity, in comparison to wild type MEFs (Figures 4.3B and 4.4). In addition to overall reduction in telomere signal intensity, *Ogg1*$^{-/-}$ MEFs had increased number of chromosomes and chromatids without detectable telomere signals (referred to SFEs and sister telomere loss, STL, respectively) (Figure 4.4 and Table 4.1). Notably, wild type MEFs also showed reduced telomere signal intensity after prolonged exposure to 20% O_2 and 0.5 μM paraquat, in comparison to 3% O_2. Nevertheless, they had less degree of telomere loss than *Ogg1*$^{-/-}$ MEFs (Figure 4.4). Similarly, subcultured *Ogg1*$^{-/-}$ mouse splenocytes and bone marrow cells showed reduced telomere signal intensity than wild type splenocytes, after being exposed to 20% O_2 for the period of three days or to 200 μM paraquat for 16 hours, respectively (Figures 4.3C, 4.5 and 4.6). Collectively, these results suggest that high oxidative stress increases telomere attrition in *Ogg1*$^{-/-}$ mouse cells.

Telomere recombination is altered in *Ogg1* deficient mice

8-oxoG in telomeric DNA attenuates binding by telomere binding proteins (112), which may consequently evoke undesirable telomere recombination (29,197). On the other hand, *Ogg1* deficiency may hamper telomere recombination (238). We thus examined the frequencies of telomere sister chromatid exchange (T-SCE) in wild type and *Ogg1*$^{-/-}$ mouse cells using CO-FISH (Figure 4.7A and 4.7B, and (50)). Freshly isolated *Ogg1*$^{-/-}$ bone marrow cells showed moderately increased T-SCEs (1.12 ± 0.25%

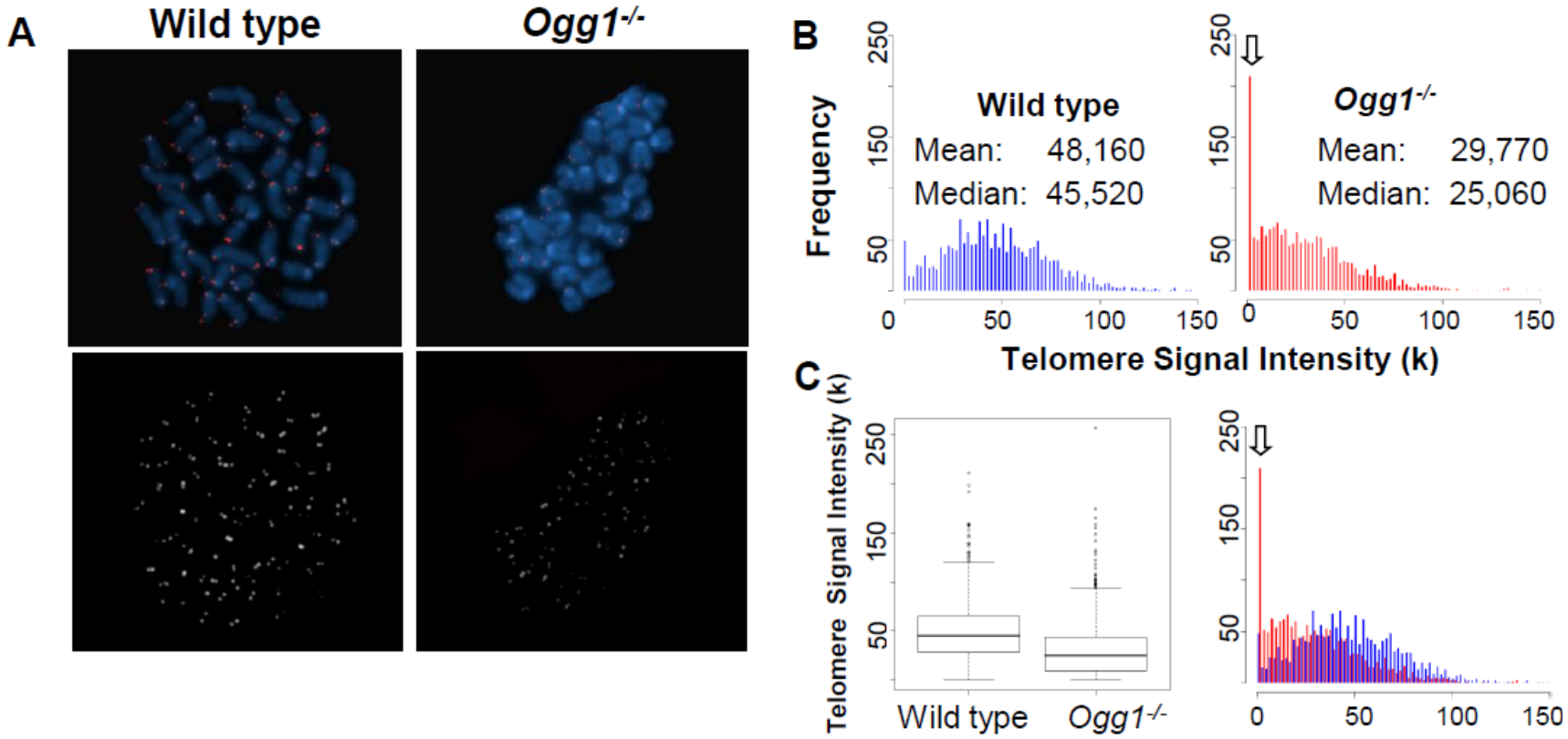

Figure 4.5 – Q-FISH analysis of telomere length in activated mouse splenocytes cultivated in 20% O_2.
(A) Representative metaphase spreads of wild type and *Ogg1*$^{-/-}$ mouse splenocytes. Quantitative measurement and dynamic range of telomeric DNA signal intensity at individual chromosome ends are shown as histogram (B) and box-plot (C). A decrease in telomere signal intensity was observed in mouse *Ogg1*$^{-/-}$ splenocytes. Arrows: chromosome ends without detectable telomere signals.

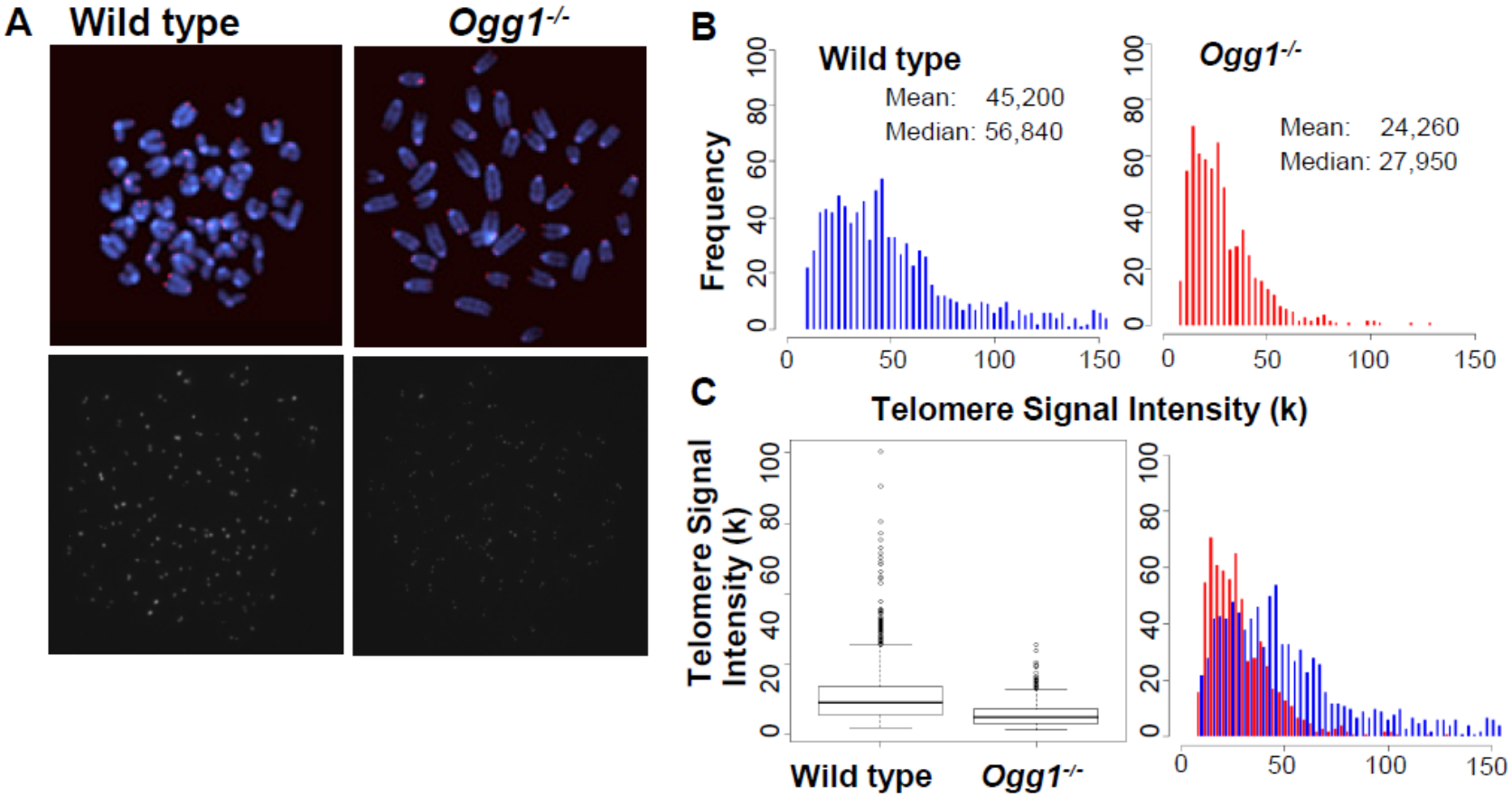

Figure 4.6 – Q-FISH analysis of telomere length in mouse bone marrow cells subcultured with paraquat.
(A) Representative metaphase spreads of wild type and *Ogg1*$^{-/-}$ mouse bone marrow cells. Quantitative measurement and dynamic range of telomeric DNA signal intensity at individual chromosome ends are shown as histogram (B) and box-plot (C). A decrease in telomere signal intensity was observed in mouse *Ogg1*$^{-/-}$ bone marrow cells.

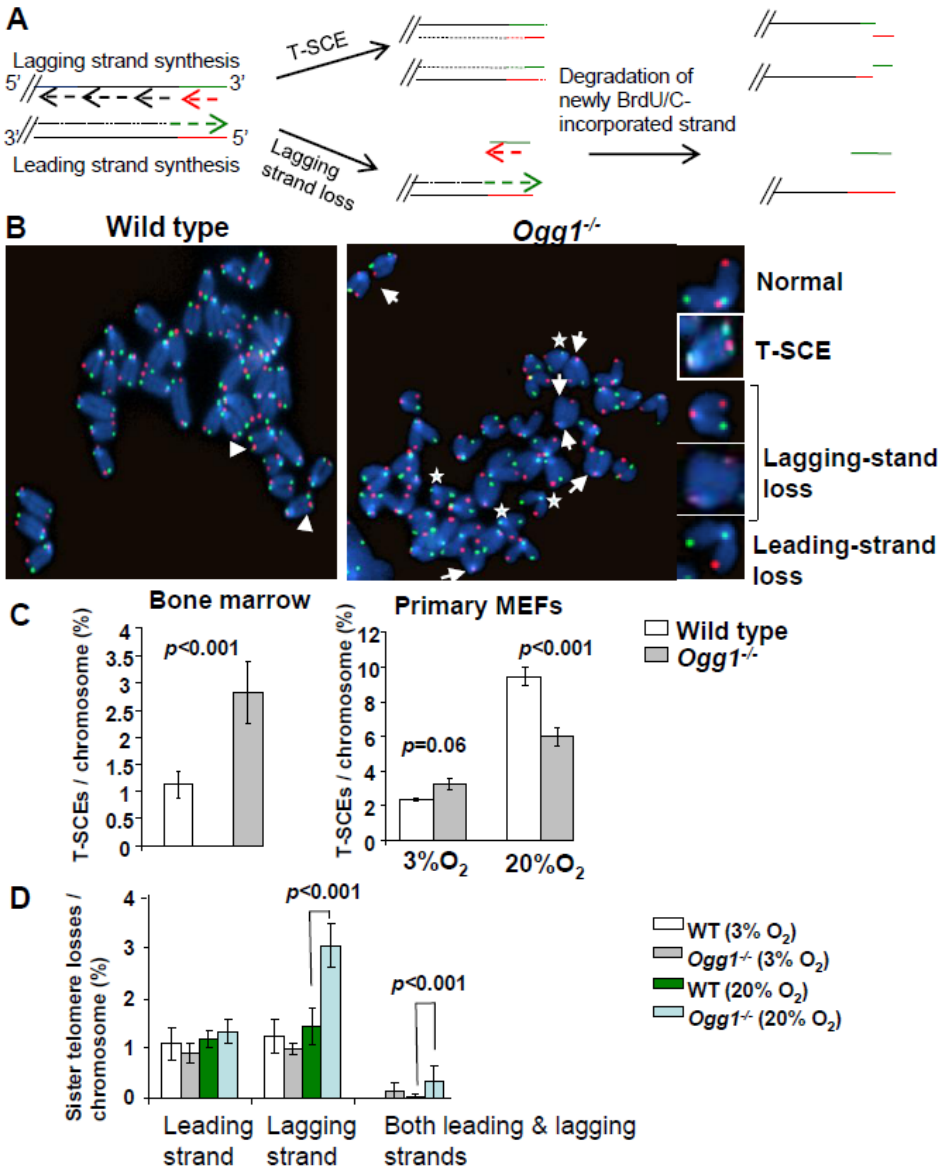

Figure 4.7 – T-SCEs and telomere lagging or leading strand loss in wild type and *Ogg1*$^{-/-}$ mouse cells. (A) A schematic presentation of CO-FISH. In brief, newly synthesized strands are removed, leaving parental strands to be detected by TRAMA-labeled $(TTAGGG)_3$ PNA probe (red color) and FITC-labeled telomere $(CCCTAA)_3$ PNA probe (green color). In an event of T-SCE, an end shows telomere signals in both green and red. In the event of collapse in telomere lagging strand synthesis, an end displays loss or reduction in telomere signal intensity in lagging strand. (B) Representative metaphase spreads of wild type and *Ogg1*$^{-/-}$ primary MEFs showing DAPI staining (blue), leading strand telomere fluorescence signals (red) and lagging strand telomere fluorescence signals (green). Arrow head: T-SCEs. Arrow: telomere lagging strand loss. *: telomere leading strand loss. (C) The frequencies of T-SCEs in freshly isolated wild type and *Ogg1*$^{-/-}$ mouse bone marrow cells (left panel) and primary MEFs cultured in 3% O_2 or 20% O_2 (right panel). (D) The frequencies of telomeric loss in either telomere lagging or leading strand or both strands within a chromosome in wild type and *Ogg1*$^{-/-}$ primary MEFs cultured in 3% O_2 or 20% O_2. When cultivated in 20% O_2, *Ogg1*$^{-/-}$ MEFs showed significant increase in lagging strand loss, compared to wild type MEFs. *This figure is provided by Zhilong Wang.

and 2.82 ± 0.57% T-SCEs/chromosome in wild type and *Ogg1*$^{-/-}$, respectively, $p<0.001$) (Figure 4.7C). In 3% O_2 primary *Ogg1*$^{-/-}$ MEFs displayed slight yet insignificant increase in T-SCE events (2.35 ± 0.08% and 3.28 ± 0.35% T-SCEs/chromosome in wild type and *Ogg1*$^{-/-}$ respectively, $p=0.06$) (Figure 4.7C). In 20% O_2 primary *Ogg1*$^{-/-}$ MEFs, however, had fewer T-SCEs than the wild type (5.98 ± 0.52 % and 9.43 ± 0.51% T-SCEs/chromosome in *Ogg1*$^{-/-}$ and wild type, respectively, $p<0.001$) (Figure 4.7C). These results suggest that deletion of *Ogg1* may induce or inhibit telomere recombination, possibly depending on the level of oxidative stress.

Telomerase activity is not altered in *Ogg1* deficient mice

Telomerase plays a key role in telomere elongation (2). Telomere lengthening in *ogg1*-deleted *S. cerevisiae* is dependent on telomerase (13). We therefore examined if telomerase activity was altered in *Ogg1*$^{-/-}$ mice. No detectable differences in telomerase activity were observed between wild type and *Ogg1*$^{-/-}$ mouse bone marrow cells by qT-PCR TRAP assay (Figure 4.8). Telomere lengthening is therefore unlikely through enhanced telomerase activity in *Ogg1*$^{-/-}$ mice; however, we cannot exclude the possibility that there is an increased accessibility of telomerase to telomeres in *Ogg1*$^{-/-}$ mice.

High oxidative stress enhances telomeric DNA strand breaks in *Ogg1* deficient primary MEFs

Previous studies suggest that oxidative stress-induced SSBs could result in telomere shortening (105). In addition, oxidative base damage in the vicinity of DNA

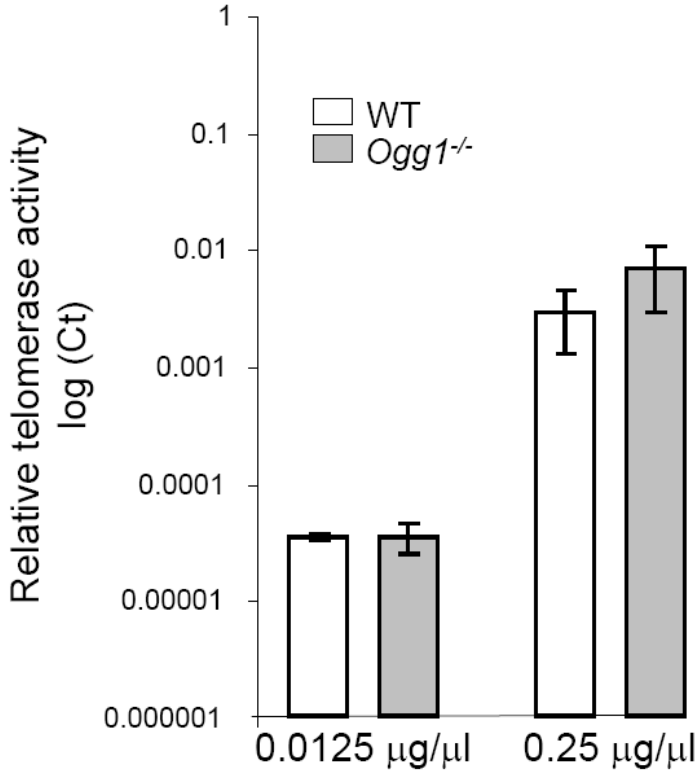

Figure 4.8 – Telomerase activity in wild type and *Ogg1*$^{-/-}$ mouse bone marrow cells.
qT-PCR analysis was performed on bone marrow cell lysate at indicated concentration. The Ct value was converted into log value. A comparable telomerase activity was detected in wild type and *Ogg1*$^{-/-}$ mouse bone marrow cells.

breaks can impose hindrance for resolving DNA ends (139,238-240). Under high oxygen tension, *Ogg1*$^{-/-}$ mouse cells displayed telomere attrition (Figures 4.3 and 4.4). It is unclear if oxidative stress-induced DNA strand breaks can accumulate in telomeres due to unrepaired oxidative base lesions and contribute to telomere attrition in *Ogg1*$^{-/-}$ mouse cells. We thus examined the frequencies of genomic and telomeric DNA strand breaks in wild type and *Ogg1*$^{-/-}$ primary MEFs cultivated in 20% O_2. γH2AX and XRCC1 are known to form foci at the sites of double strand breaks (DSBs) and SSBs, respectively (241,242), and formation of γH2AX and XRCC1 foci were therefore used as markers for DSBs and SSBs in the genome and telomeres.

γH2AX foci were detected in late passage wild type and *Ogg1*$^{-/-}$ MEFs by indirect immunofluorescence. A greater fraction of *Ogg1*$^{-/-}$ MEFs showed > 3 γH2AX foci compared to the wild type (approximately 12% wild type and 38% *Ogg1*$^{-/-}$ MEFs, respectively) (Figure 4.9A). γH2AX foci were detected in telomeres in both wild type and *Ogg1*$^{-/-}$ MEFs by TEL-FISH, and the latter had approximately 2-fold more telomeric γH2AX foci (Figure 4.9B and 4.9C). To further clarify telomeric γH2AX foci, we examined the formation of 53BP1 foci in telomeres by TEL-FISH (43). The 53BP1 foci were also detected in telomeric DNA in *Ogg1*$^{-/-}$ MEFs (Figure 4.10). Similarly, XRCC1 foci were found in the genome in both wild type and *Ogg1*$^{-/-}$ MEFs (Figure 4.9D), and *Ogg1*$^{-/-}$ MEFs had higher occurrence of telomeric XRCC1 foci (Figure 4.9E and 4.9H). This phenotype was further enhanced when MEFs were treated with 10 μM hydrogen peroxide for 24 hours (Figure 4.9F and 4.9G). Under low oxygen tension (i.e. 3% O_2), the frequencies of γH2AX and XRCC1 foci were low, and no detectable difference was

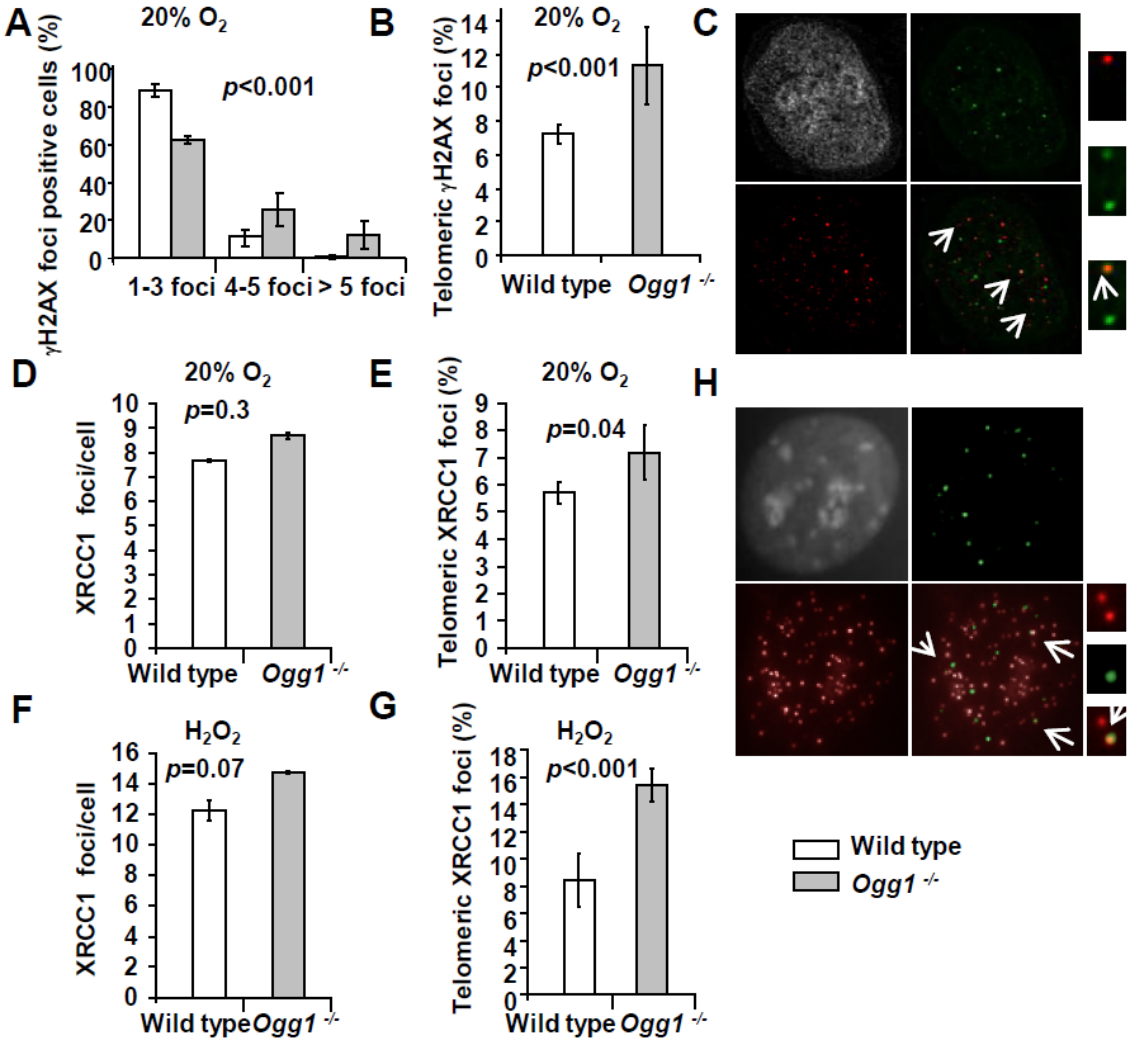

Figure 4.9 – DNA damage foci in wild type and *Ogg1*$^{-/-}$ primary MEFs cultivated in high oxidative environment.

(A-C) γH2AX in late passage primary MEFs cultivated in 20% O_2. A: Percentage of γH2AX positive cells was divided into subgroups according to the number of foci in a cell. B: Percentage of γH2AX foci in telomeres. C: A representative *Ogg1*$^{-/-}$ primary MEF, showing DAPI staining (grey), γH2AX foci (green), and telomere fluorescence signals (red). Colocalization of γH2AX staining with telomere signal was illustrated in enlarged images at far right. (D-H) Genomic or telomeric XRCC1 foci in primary MEFs. D and E: MEFs cultivated in 20% O_2. F and G: MEFs exposed to 10 μM H_2O_2 for 24 hours. Average genomic XRCC1 foci /cell (D or F) and percentage of XRCC1 foci in telomeres (E or G) were indicated. H: A representative *Ogg1*$^{-/-}$ primary MEF cultivated in 20% O_2, showing DAPI staining (grey), XRCC1 foci (green), and telomere fluorescence signals (red). Colocalization of XRCC1 signals with telomere signals was illustrated in enlarged images at far right.*This figure is provided by Zhilong Wang.

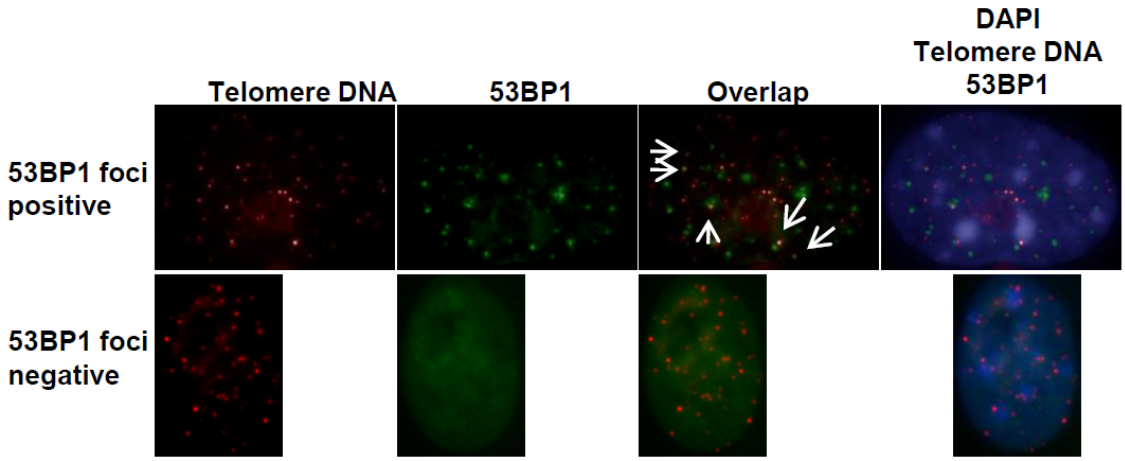

Figure 4.10 – 53BP1 foci are detected in telomeres in *Ogg1*$^{-/-}$ MEFs.
Upper panel: a representative *Ogg1*$^{-/-}$ late passage primary MEF, showing DAPI staining (blue), 53BP1 foci (green), and telomere fluorescence signals (red). Arrows: colocalization of 53BP1 staining with telomere signal. Lower panel: a primary MEF negative for 53BP1 foci.
*This figure is provided by Zhilong Wang.

observed between wild type and *Ogg1*$^{-/-}$ MEFs (data not shown). Collectively, these results support the notion that oxidative stress can increase DSBs and SSBs in the genome and telomeres when *Ogg1* is deleted.

High oxygen tension leads to preferential telomere strand loss in *Ogg1* deficient primary MEFs

CO-FISH has been applied to detect defects in telomere lagging and leading strand loss, and it is proposed that such loss is caused by defects in lagging or leading strand synthesis (Figure 4.7A and 4.7B, and (243,244)). Because oxidative stress can increase DNA strand breaks in *Ogg1*$^{-/-}$ MEFs, it is possible that these DNA strand breaks may block telomere DNA replication and contribute to telomere attrition in *Ogg1*$^{-/-}$ MEFs. We therefore examined the frequencies of telomere lagging and leading strand loss in wild type and *Ogg1*$^{-/-}$ primary MEFs by CO-FISH. No significant difference in leading and/or lagging strand loss was detected between wild type and *Ogg1*$^{-/-}$ MEFs under low oxygen tension (3% O_2); however, under high oxygen tension (20% O_2), more telomere loss was found in the lagging strand in *Ogg1*$^{-/-}$ MEFs (1.80 ± 0.37% and 3.50 ± 0.44% lagging strand losses/chromosome in wild type and *Ogg1*$^{-/-}$ MEFs, respectively, $p<0.001$) (Figures 4.7D and 4.11). These results indicate that oxidative stress-induced oxidative DNA lesions (possibly DNA strand breaks with adjacent oxidized guanines) may preferentially affect lagging strand DNA synthesis in telomeres in *Ogg1*$^{-/-}$ MEFs.

Aside from telomere lagging or leading strand synthesis defect, other factors (e.g. DNA strand breaks and nucleolytic degradation in a telomere strand) may also contribute

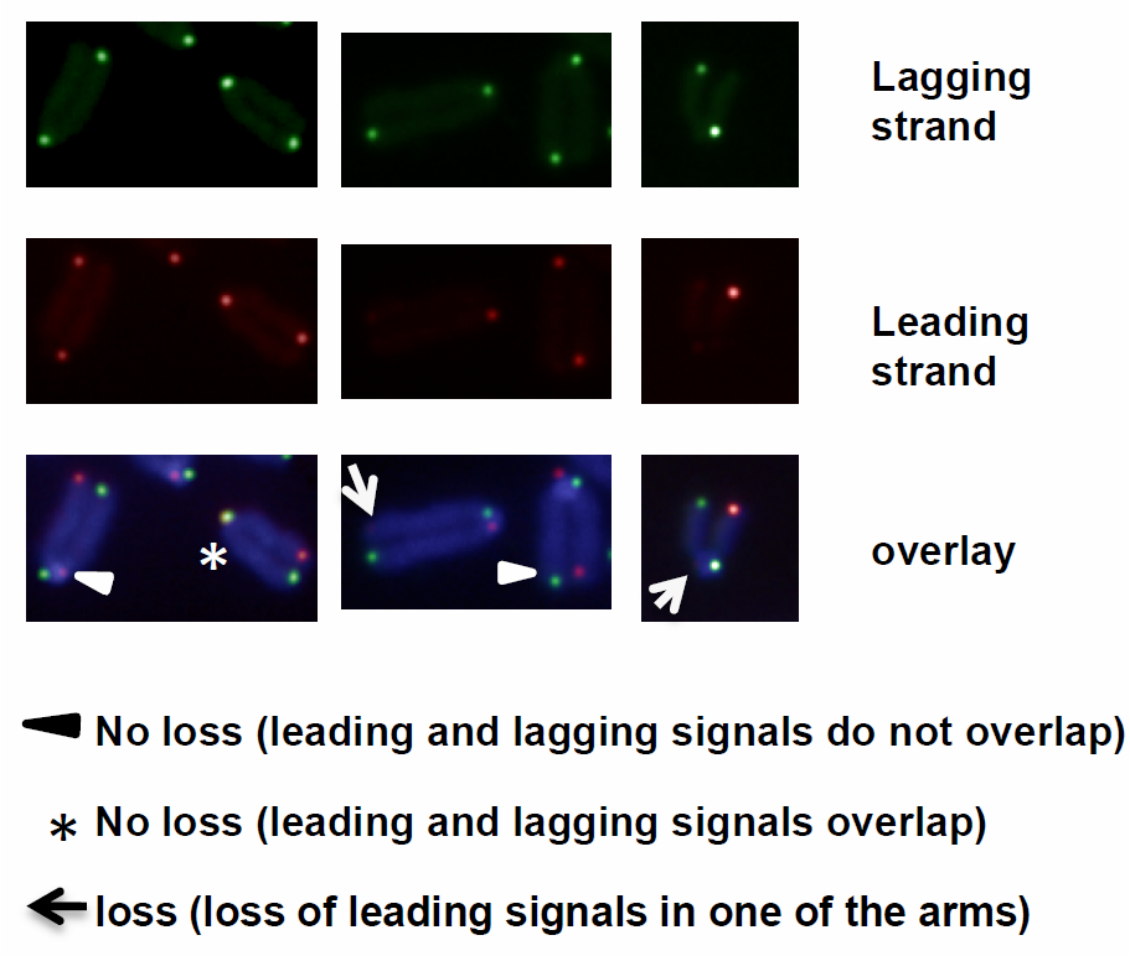

Figure 4.11 – CO-FISH analysis of primary *Ogg1*$^{-/-}$ MEFs.
Individual images represent leading-strand (red) and lagging-strand (green) telomere fluorescence signals. Chromosomes without telomere loss had two telomere fluorescence signals in each image. Merged images were shown at the bottom. *This figure is provided by Zhilong Wang.

to the loss of telomeric repeats in a telomere strand. To distinguish these possibilities, we employed a two-color telomere-FISH that detects telomere signals in G and C strands of a chromatid (Figure 4.12A and 4.12B). In 20% O_2, loss of telomere signals in both G and C strands of a chromatid (or loss of a chromatid) was detected in wild type and *Ogg1*$^{-/-}$ MEFs, with higher frequencies in the latter (1.57 ± 0.47% and 3.32 ± 0.11% telomere chromatid losses/chromosome in wild type and *Ogg1*$^{-/-}$ MEFs, respectively, $p<0.001$) (Figure 4.12B and 4.12C). However, loss of telomere signal intensity in one of the telomere strands, either G or C strand was also evident in wild type and *Ogg1*$^{-/-}$ MEFs (Figure 4.12B and 4.12C), but G-strand loss appeared to be more prominent and was approximately 2-fold higher in *Ogg1*$^{-/-}$ MEFs (Figure 4.12C). Thus, telomere loss occurred in either one strand or both strands of a chromatid in *Ogg1*$^{-/-}$ MEFs. These results suggest that besides telomere replication defects, DNA breakage/degradation-mediated strand loss may have occurred in telomeres in *Ogg1*$^{-/-}$ MEFs. Because only the G-rich strand of telomeric DNA can harbor oxidized guanines, this may explain why oxidative DNA damage induces telomere attrition with strand bias.

Deletion of mouse *Ogg1* is associated with increased oxidative guanine lesions in telomeres *in vivo*

Guanine has a lower oxidation potential compared to other bases, and triple guanines, composed of the mammalian telomere repeats, have an even lower oxidation potential (245,246). Consistently, it has been found that triple guanines in telomere repeats are prone to oxidative damage *in vitro* (106-108,223). To determine the level of

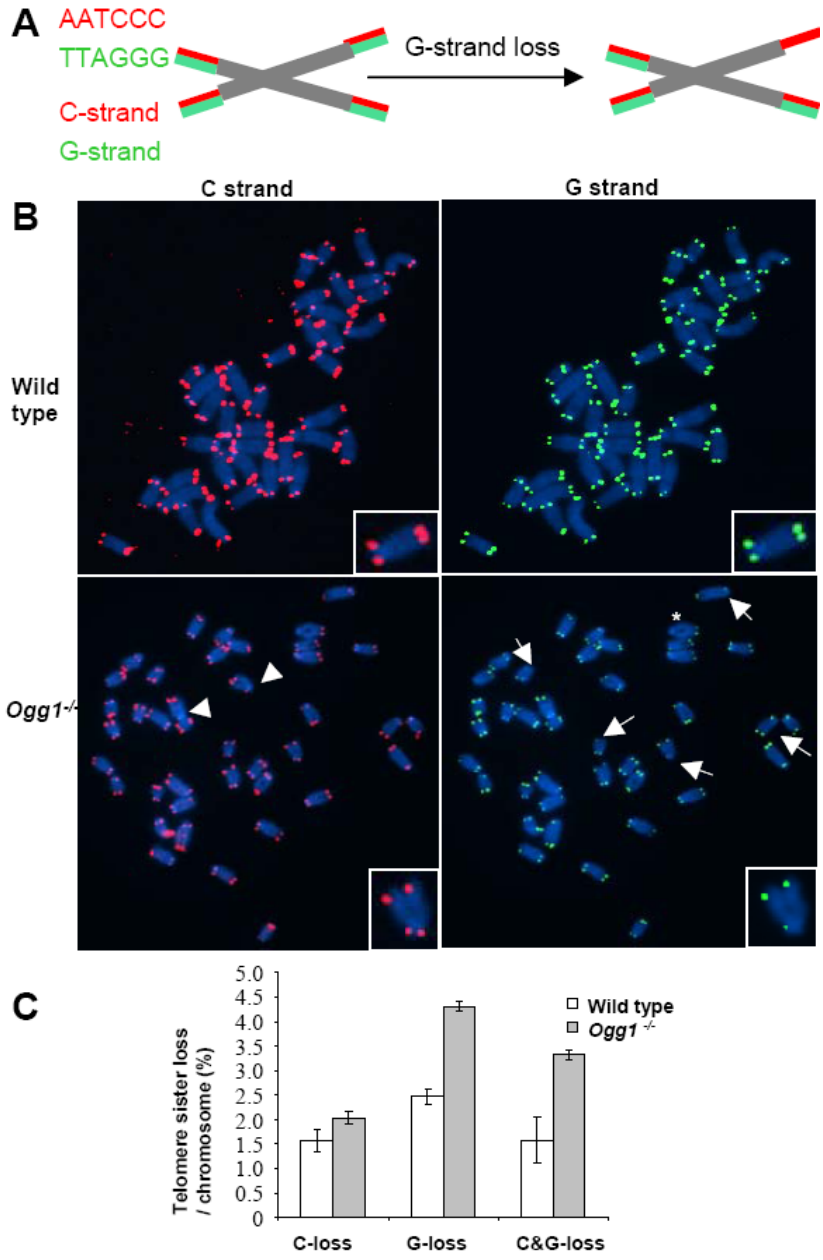

Figure 4.12 – Preferential telomere loss in G strands in primary *Ogg1*$^{-/-}$ MEFs cultivated in 20% oxygen.
(A) A schematic presentation of a two-color Q-FISH measurement of telomere signals on G- and C-strands by TRAMA-labeled $(TTAGGG)_3$ PNA probe (red color) and FITC-labeled telomere $(CCCTAA)_3$ PNA probe (green color). (B) Representative metaphase spreads of wild type and *Ogg1*$^{-/-}$ primary MEFs, showing DAPI staining (blue), C-strand (red), and G- strand (green) telomere fluorescence signals. (C) Percentage of telomere losses / chromosome in MEFs. Arrows: chromosomes with loss or reduced telomere signal intensity in G-strand. Arrowheads: chromosomes with loss or reduced telomere signal intensity in C-strand. *: chromosomes with loss of telomere signals in both G- and C-strands in a chromatid. ^This figure is provided by Zhilong Wang.

guanine oxidation in telomeres *in vivo*, genomic DNAs from wild-type and *Ogg1* deficient mouse liver and primary MEFs were digested with restriction enzymes and then examined for their sensitivity to *E. coli* Fapy DNA glycosylase (Fpg). Fpg excises oxidized guanines, resulting in abasic sites that are further processed by the lyase activity of Fpg to create SSBs (115,224). The extent of increased smaller single stranded telomeric DNA fragments is proportional to the amount of Fpg-sensitive lesions present within the telomeric DNA and can be extrapolated to estimate the number of lesions (Figures 4.13A and 4.14, and (236)).

To validate the method, genomic DNA was treated *in vitro* with increasing concentration of hydrogen peroxide (H_2O_2) plus Cu^{2+}. Higher doses of H_2O_2 treatment caused detectable increase of Fpg-sensitive lesions (Figure 4.13B), demonstrating that the method is feasible in estimating Fpg-sensitive lesions in telomeres. Next, we measured Fpg-sensitive lesions in telomeres in mouse livers derived from wild type and *Ogg1*$^{-/-}$ mice. The level of telomeric Fpg-sensitive lesions was not significantly changed in the hepatocytes from 2- and 8-month old wild type mice; however, telomeric Fpg-sensitive lesions were elevated in the hepatocytes from 8-month old *Ogg1*$^{-/-}$ mice (Figure 4.13C). We also measured oxidative guanine lesions in primary MEFs during prolonged culture under low and high oxygen tensions (3% O_2 and 20% O_2). Higher levels of Fpg-sensitive lesions were observed in primary MEFs under high oxygen tension, and *Ogg1*$^{-/-}$ MEFs harbored more lesions than wild type MEFs (Figure 4.13C). Collectively, these results indicate that ablation of OGG1 function can increase oxidative guanine lesions in

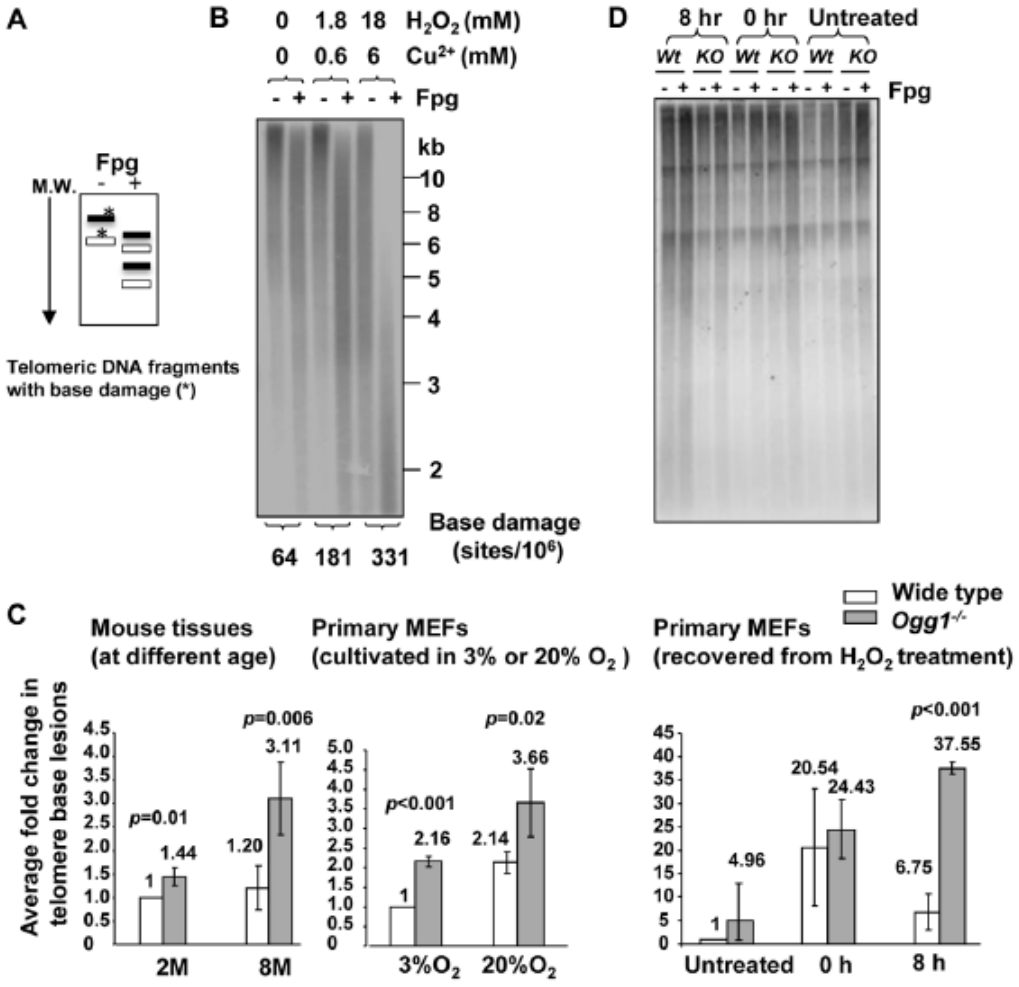

Figure 4.13 – Increased level of Fpg-sensitive DNA lesions in telomeres in *Ogg1* deficient mouse tissues and cells.

(A) Schematics of telomere guanine damage detection. A telomere DNA fragment with guanine lesions is converted into smaller fragments due to Fpg's treatment. M.W: molecular marker from high (top) to low (bottom) molecular weight. (B) Validation of the method. Mouse genomic DNA was treated *in vitro* with increasing concentration of hydrogen peroxide (H_2O_2) plus Cu^{2+}, followed by restriction enzyme and Fpg treatment. Telomeric DNA fragments with (+) or without (-) Fpg treatment were detected by Southern blot analysis using a radio-labeled telomere probe. Higher doses of H_2O_2 treatment caused Fpg-dependent increase of shorter telomere DNA fragments and more detectable Fpg-sensitive sites in the telomeric DNA. (C) Detection of telomeric base lesions in wild type and *Ogg1*$^{-/-}$ mouse tissues and primary MEFs. DNA was extracted from wild type and *Ogg1*$^{-/-}$ liver tissues from 2 and 8 month old mice (left panel), late passage primary MEFs cultured in 3% and 20% O_2 (middle panel), or early passage primary MEFs collected at 0 hour and 8 hours after exposure to 500 μM H_2O_2 treatment for 60 minutes (right penal). In each experiment, fold changes in telomere base lesions in a testing sample were derived by normalizing the number of Fpg-sensitive lesions in the testing sample to that in a wild-type control. The control value was set to 1. The fold change represented average value from at least three independent experiments. M: month. H: hours. (D) Representative image of primary MEFs recovered from H_2O_2 treatment. 8 hours after exposure to H_2O_2, *Ogg1*$^{-/-}$ MEFs still showed smaller telomere DNA fragments after Fpg treatment, while wild type MEFs displayed similar distribution of telomere DNA fragments with or without Fpg treatment.

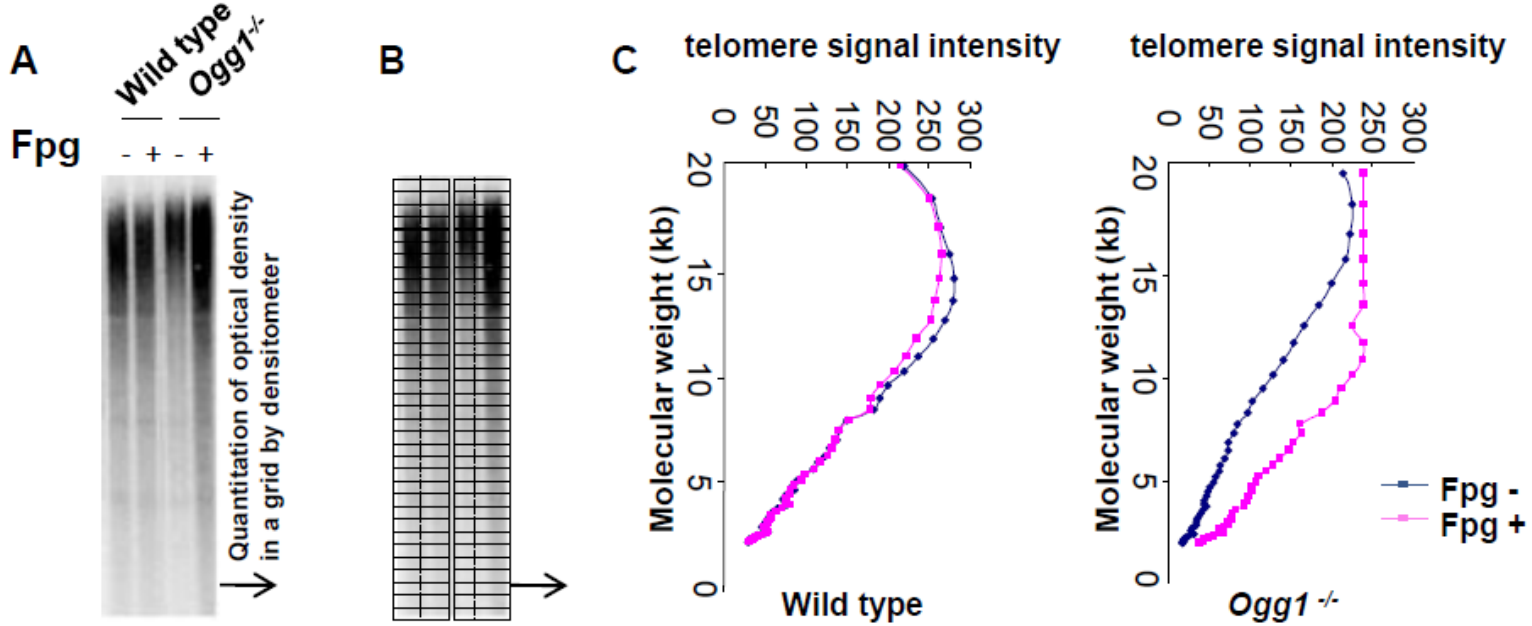

Figure 4.14 – Schematics of telomerase base lesion calculation.
(A) Gel profiles of wild type and *Ogg1*$^{-/-}$ mouse cells with or without Fpg treatment. (B) The density in each data point was measured by densitometer and ImageQuant software and collected into a grid. (C) The histogram illustrates a density profile of a grid and the corresponding molecular size at each data point. The mean length (ML) was calculated as a center of mass, and the frequencies of Fpg-sensitive lesions in a sample were based on ML values, as described in Methods.

telomeres in mouse tissues with aging or in primary MEFs during prolonged culture or under oxidative stress conditions.

To further verify if OGG1 participates in oxidative guanine repair in telomeres *in vivo*, early passage wild type and *Ogg1*$^{-/-}$ primary MEFs were exposed to 500 μM hydrogen peroxide for 60 minutes and then allowed to recover for 8 hours. Immediately after hydrogen peroxide treatment (0 hour), high levels of Fpg-sensitive lesions were detected in wild type and *Ogg1*$^{-/-}$ MEFs, compared to untreated MEFs. Eight hours after removal of hydrogen peroxide, Fpg-sensitive lesions were significantly reduced in wild type MEFs; in contrast they remained at a higher level in *Ogg1*$^{-/-}$ MEFs (Figure 4.13C and 4.13D). Thus, *Ogg1*$^{-/-}$ MEFs were inefficient in the repair of hydrogen peroxide-induced Fpg-sensitive lesions in telomeres, while wild type MEFs repaired these lesions with high efficiency. These results demonstrate that OGG1 is involved in the repair of oxidative guanine lesions in telomeres *in vivo*.

4.4 Discussion

BER is the primary DNA repair pathway for the repair of oxidative base lesions. Here, we studied the impact of *Ogg1* deficiency on telomeres in mammalian cells. We found that ablation of OGG1 function resulted in increased oxidative guanine lesions in telomeres in mice with aging or in primary MEFs during prolonged culture or cultivated in a high oxidative environment. In addition, lack of *Ogg1* led to telomere length alteration that was dependent on the level of oxidative stress. Furthermore, deletion of *Ogg1* caused altered recombination, increased DNA strand breaks, and preferential strand

loss in telomeres. Our data support that oxidative guanine lesions affect telomere integrity and that the OGG1-initiated BER pathway plays an important role in telomere base damage repair and telomere maintenance in mammals.

Ogg1 deficient mouse cells showed moderate telomere lengthening under low oxygen tension (e.g. in tissues or 3% O_2); however, they displayed accelerated telomere shortening under high oxygen tension (20% O_2) or with paraquat treatment. This observation suggests that the level and types of oxidative DNA damage in telomeres may affect the outcome of telomere length. Several possibilities may contribute to the telomere length alteration in *Ogg1* deficient mouse cells.

8-oxoG can directly disrupt telomeric DNA binding by TRF1 and TRF2 (112), and unrepaired 8-oxoG can lead to GC to TA transversions (228). The affinity of telomere binding proteins to telomeric DNA is sequence-specific and can be altered by mutations in telomeric DNA (247). Thus, both base lesions and base lesion-induced mutations may affect the association of telomere binding proteins to telomeres. Opresko et al have previously shown that the level of 8-oxoG in telomeres adversely affects binding by telomere binding proteins (112). Thus, the number of oxidative base lesions and mutations may determine the severity of telomere binding protein depletion in telomeres. It is known that reduced binding or severe loss of telomere binding proteins in telomeres can lead to different telomere phenotypes; the former causes telomere lengthening and the latter results in telomere uncapping (3). Thus, when few base lesions affect telomeric DNA repeats, they may moderately reduce telomere binding proteins in telomeres, which could liberate the negative regulation of telomere binding proteins on

telomerase and consequently increase telomerase-dependent telomere repeat additions. Our studies in *S. cerevisiae* support this notion, in which telomere lengthening in *ogg1*-deleted *S. cerevisiae* is dependent on telomerase-mediated telomere elongation (13). On the other hand, once oxidized bases accumulate to a certain level in telomeres, they may severely deplete telomere binding proteins in telomeres and result in telomere uncapping. Uncapped telomeres can become targets for nucleolytic degradation and hence cause telomere shortening.

When exposed to 20% O_2 or hydrogen peroxide, *Ogg1* deficient mouse cells showed increased incidences of SSBs and DSBs in telomeres, evident by XRCC1 and γH2AX foci formation in telomeres. These DNA strand breaks can represent an obstacle for DNA replication. Furthermore, base lesions in the vicinity of DNA strand breaks can somehow accelerate end resection, possibly by stimulating an endonuclease activity close to the breaks (248). As a result, these DNA defects may ultimately lead to telomere shortening in *Ogg1* deficient mouse cells. However, fewer DNA strand breaks may also arise in *Ogg1* deficient mouse tissues and partially inhibit DNA replication, which could consequently enhance telomerase pathway and induce telomere elongation (249,250). DNA strand breaks in *Ogg1* deficient mouse cells may arise in telomeres by several means. High oxygen tension has been shown to cause detectable levels of SSBs in telomeres, especially in the G-strand (105). Since the presence of oxidative guanine damage in the vicinity of DNA breakages may impose a hindrance to the resolution of DNA ends (139,238-240), they may possibly inhibit repair of DNA strand breaks in telomeres. If adenine is incorporated opposite unrepaired 8-oxoG, removal of adenine by

the MYH DNA glycosylase and subsequent abasic site processing can lead to SSBs in the C-strand (233). SSBs may also be indicative of increased partial repair products of back-up DNA glycosylase activity, e.g. Neil1 (251).

Previous reports demonstrate that telomere lagging strand loss can be detected in WRN and FEN1 mutant cells via CO-FISH, which may reflect lagging strand telomere synthesis defects (243,244). Because oxidative guanine lesions are located at G-strand in telomeres, they may preferentially inhibit repair of SSBs in this strand. As a result, lagging strand telomere synthesis may be affected. Indeed, *Ogg1* deficient MEFs showed an increase in telomere lagging strand loss by CO-FISH analysis. This result suggests that oxidative guanine damage and/or its negative effect on the repair of telomere strand breaks may perturb lagging strand DNA synthesis in telomeres. Telomere lagging strand loss may also result from SSBs in G-strand along with loss of distal telomeres or nucleolytic degradation. In fact, the two-color Q-FISH showed that telomeric G-strand loss can occur alone without a loss of its complementary C-strand in *Ogg1*$^{-/-}$ MEFs, supporting the latter possibility.

Besides changes in telomere length, the incidence of T-SCEs either increased or decreased in *Ogg1* deficient mouse cells, which was reversely associated with the level of oxidative stress. Several possibilities may account for the altered telomere recombination in *Ogg1* deficient mouse cells. First, variable levels of oxidative base damage may have different impact on recombination activity. For example, recombination rates are substantially increased in BER deficient yeast cells harboring low levels of oxidative DNA damage in the genome, and it has been postulated that a moderately damaged

genome could promote illegitimate recombination that serves as a compensatory response in order to tolerate oxidative DNA damage (252). However, high density of oxidative base lesions can inhibit RAD52 annealing activity and thus result in reduced recombination resolution (238). Second, OGG1 can inhibit RAD52 strand annealing and exchange activity (238), and removal of OGG1 would therefore relieve this inhibition and activate the recombination pathway. Third, oxidized guanines may affect telomere recombination by disrupting shelterin's association to telomeres. Previous studies demonstrate that telomere binding proteins prevent telomeres from becoming substrates for HR, and deletion of telomere binding proteins invokes T-SCE events (197,198). Because oxidative base lesions in telomeric DNA can attenuate binding by telomere binding proteins (112), it is possible that reduced binding of telomere binding proteins to telomeres may promote telomere recombination. Finally, increased telomere sister chromatid exchanges may associate with recombination repair of stalled or broken replication forks that might occur at the sites of oxidative bases and/or DNA strand breaks in telomeres.

We found that oxidative guanine lesions in telomeres were elevated in older animals or in primary MEFs cultivated under oxidative stress conditions. Thus, oxidative damage on guanine bases can increase in telomeres in aging or by environmental oxidative stress. The level of Fpg-sensitive lesions in telomeres was increased in *Ogg1*$^{-/-}$ mouse liver and primary MEFs, in comparison to their wild type counterparts. These results indicate that OGG1 is involved in repairing oxidative guanine lesions in telomeres

in vivo. This view was further supported by the evidence that *Ogg1*$^{-/-}$ MEFs were defective in the repair of hydrogen peroxide-induced Fpg-sensitive lesions in telomeres.

Oxidative stress-induced SSBs can cause telomere shortening in mammalian cells (101). Here, we report that another form of oxidative DNA damage, oxidative base lesions can induce either telomere lengthening or shortening, depending on the level of oxidative stress. In a given organism, telomere length is maintained via a balance between telomere elongation and shortening (2). It is possible that moderate oxidative base damage may favor the pathways for telomere lengthening (e.g. telomerase), while extensive oxidative base damage may attenuate telomere capping, telomere recombination, telomere replication, and the resolution of DNA strand breaks and ultimately result in telomere attrition (Figure 4.15). Telomere shortening has been linked to human aging and cancer development. Perhaps extensive base damage occurs in individuals with the conditions, such as defective BER and increased ROS levels (for example, chronic inflammation), which may consequently lead to accelerated telomere attrition, thus contributing to premature aging and cancer formation.

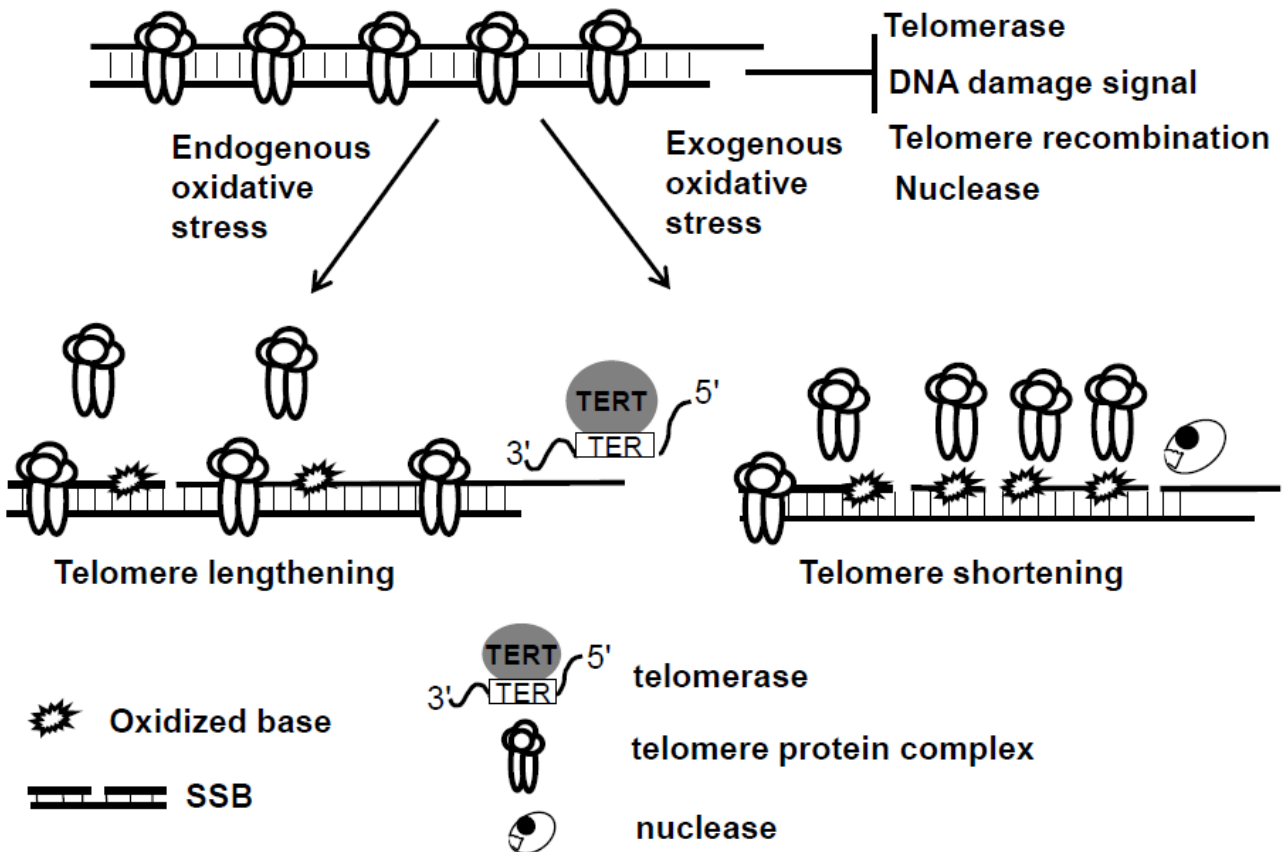

Figure 4.15 – The levels and types of oxidative DNA damage may determine telomere length alteration.
Telomeres are normally capped by telomere protein complex which limit the access of telomerase to telomeres and prevent telomeres from evoking DNA damage response and becoming the subject of nucleolytic degradation and recombination. Under low oxidative condition, base damage is low and affects fewer telomeric DNA repeats, which may moderately reduce telomere protein complex in telomeres, thus causing increased telomerase-mediated telomere lengthening. High oxidative stress can, however, not only increase base damage but also induce DNA strand breaks, and the former may severely deplete telomere protein complex in telomeres and impose a hindrance to the resolution of DNA breaks. As a result, it may lead to telomere uncapping, increased telomere strand breaks, and nucleolytic degradation, hence causing telomere shortening.

Chapter 5: Investigating Factors that Influence Telomeric Oxidative Guanine Damage and Repair by 8-oxoguanine Glycoyslase

The following chapter has been slightly modified and submitted to DNA Repair: David B. Rhee, Avik Ghosh, Jian Lu, Vilhelm A. Bohr and Yie Liu, "Investigating factors that influence telomeric oxidative guanine damage and repair by 8-oxoguanine glycosylase", July 2010.

5.1 Introduction

All eukaryotic linear chromosomes consist of nucleoprotein complexes called telomeres. Telomeres are composed of extended tracts of short G-rich tandem repeat sequences, 5'-TTAGGG-3', and a short terminal single-stranded 3'-overhang in humans and mice. Functional telomeres prevent chromosome termini from being recognized as broken DNA ends. On the other hand, dysfunctional telomeres, as a consequence of loss of telomere repeats or loss of protection by telomere-associated proteins, can trigger a DNA damage response and subsequently lead to genomic instability, cell proliferation defects, and cell death (4).

Telomere length homoeostasis is maintained through interplay between telomerase extension, telomere replication, and telomere capping (53). Telomerase, a ribonucleoprotein complex, is essential in telomere length maintenance since it can anchor to the 3'-overhang and extend telomeric DNA repeats (2). All functional telomeres are coated with telomere-specific binding proteins (*e.g.*, TRF1 and TRF2) and

their associated proteins, collectively known as the shelterin protein complex (253). With the aid of shelterin proteins, telomeres normally exist in a loop structure (also known as T-loop) with the 3'-single-stranded overhang invading the telomeric double-stranded DNA (22). Disruption of the T-loop and exposure of the 3'-overhang destabilizes the telomere since the "capped" telomere normally inhibits undesirable recombination and DNA damage response (3,183). Evidence indicates that shelterin proteins also regulate telomerase extension and efficient telomere replication (53,221,222,254).

Genomic DNA is continuously exposed to DNA damaging agents through both endogenous (*e.g.*, reactive oxygen species, ROS, as by-products of normal metabolism) and exogenous (*e.g.*, physical and chemical agents such as γ- or UVA-irradiation) means. ROS can generate oxidative DNA lesions including oxidized bases and single-strand-breaks (SSBs) (255). 7, 8-dihydro-8-oxogaunine (8-oxodG) is one of the most abundant and widely studied oxidative base lesions. If unrepaired, it is mutagenic and detrimental to cells since it results in guanine-to-thymine transversion mutations (256). The primary repair pathway responsible for removing such oxidative lesions is the base excision repair (BER) pathway. Briefly, 8-oxoguanine DNA Glycosylase (OGG1) initiates the BER pathway by removing the damaged guanine base, followed by incision, repair synthesis, and ligation by various members in the BER pathway to complete the repair process (115,257,258). OGG1 glycosylase activity on 8-oxodG modified substrates has been extensively studied. For instance, OGG1 can remove 8-oxodG opposite of cytosine efficiently (259) and prefers to work in a processive mode where OGG1 move from one substrate to adjacent substrate without disengaging from the DNA (140). OGG1's

incision is affected by flanking sequences with preference for 5'-(C/G)me-FapyC-3' (141). In addition, an opposing abasic site or SSBs towards the 3' of the catalytic pocket can greatly reduce OGG1 incision activity (137-139). Furthermore, the position of 8-oxodG in fork substrates can influence OGG1 incision activity (139).

It has been proposed that oxidative DNA damage plays a role in telomere attrition in aging (260). Human cells with long telomeres show increased sensitivity to hydrogen peroxide, but not to etoposide and bleomycin, supporting the notion that telomeres are particularly vulnerable to oxidative damage (102). Several studies have shown that oxidative stress also induces oxidative DNA base damage preferentially at telomeric DNA *in vitro*. For example, oxidative damage is several-fold more efficient in inducing 8-oxodG in oligonucleotides containing telomeric repeats than non-telomeric repeats, even though the latter have similar guanine content (106-108,261). However, it is yet to be determined if telomeric DNA is prone to oxidative damage *in vivo*. Oxidation of guanines can occur at either the 5' or the middle guanine in GGG triplets (106-108). The consequence of oxidative guanine DNA damage has been investigated previously. The presence of 8-oxodG in telomeric nucleotides disrupts telomerase activity (111) and inhibits binding of TRF1 and TRF2 (112), respectively. Our recent studies imply that oxidative guanine damage can arise in telomeres *in vivo*, where it affects telomere length homeostasis, recombination, DNA replication, and DNA breakage repair. We also demonstrated that OGG1 is required for repairing oxidized guanines in telomeres and maintaining telomere integrity in budding yeast and mice (13,262).

Several mechanisms may contribute to the accumulation of oxidative guanine lesions in telomeres. It is possible that telomeric DNA repeats may favor guanine oxidation. In addition, oxidative guanine repair may be impeded by telomere specific factors (*e.g.*, telomere special structures or telomere repeat binding proteins). In this study, we examined if telomeric DNA is prone to oxidative guanine damage *in vivo* and if telomere specific factors can affect OGG1 base incision activity in telomeres. Our data suggest that triplet guanines in telomeric repeats significantly contribute to the preferential accumulation of oxidative guanine damage in telomeres and the repair of oxidative guanine lesions in some telomere configurations can be problematic.

5.2 Experimental Procedures

Cell culture, induction of oxidative DNA damage, and genomic DNA isolation

U2OS osteosarcoma cells were maintained in DMEM (Dulbecco's modified Eagle's Medium) growth medium supplemented with 10% fetal bovine serum (FBS) at 37ºC in a 5% CO_2 atmosphere. To induce oxidative DNA damage *in vivo*, cells were treated with 1 mM of menadione (Sigma Aldrich) in serum-free DMEM growth medium for 30 min, washed with PBS and incubated for additional 6 hours in serum-free DMEM growth medium before being collected (238). DNA isolation was performed as previously described (13,236,262). Briefly, freshly minced mouse kidney (C57BL/6 genetic background) or U2OS cell pellets were incubated with DNA lysis buffer (10 mM Tris, pH 7.5, 400 mM NaCl, 1 mM EDTA, 0.5 % SDS, and 0.1mg/ml proteinase-K) over-night at 37°C. DNA was isolated using standard high salt extraction (6M NaCl with

vigorous shaking, followed by ethanol precipitation), treated with 100 μg/ml of RNase A (for 3 hours, followed by ethanol precipitation), and re-suspended in TE buffer (10 mM Tris, 1 mM EDTA, pH 7.2). For *in vitro* oxidative DNA damage induction, isolated mouse kidney DNA was treated with various concentrations of H_2O_2 and Cu^{2+}, followed by ethanol precipitation of the DNA as previously described (13).

Measurement of oxidative base lesions

Identification of oxidative base lesions in both telomeric and non-telomeric DNA was performed as described (13,236,262). In brief, 2 μg of DNA was treated with 10 units each of *HindfI* and *RsaI* restriction enzymes (New England Biolabs) at 37°C for 3 hours. Enzymes were inactivated by heating at 60°C for 20 minutes. Samples were treated with 8 units of *E. coli* formamidopyrimidine-DNA glycosylase (FPG) (New England Biolabs) at 37°C for 1 hour. Duplicate samples were treated with a mock buffer. FPG was inactivated by heating at 60°C for 15 minutes. Genomic single-stranded DNA fragments treated with FPG or mock buffer were separated on 0.8 % alkaline agarose gel and detected by Southern blot using ^{32}P-labeled $(AATCCC)_4$ or $(CA)_{12}$ probes and visualized by autoradiography. ImageQuant software was applied in quantifying DNA cleavage in FPG-treated and untreated samples. The mean length (ML) was calculated as a center of mass and expressed in kilobase. $ML=\Sigma (MWi \times ODi)/ \Sigma (ODi)$. MWi is the length of the DNA at each row, and ODi is the densitometer output at each row. The frequency of FPG-sensitive lesions was calculated as (ML untreated /ML treated) -1.

Enzyme and purified proteins

Recombinant human 8-oxoguanine DNA glycosylase, OGG1 (α isoform, New England Biolabs) was used in the oligonucleotide incision assay. Recombinant histidine-tagged human TRF1 and TRF2 proteins were purified using a baculovirus/insect cell expression system as previously described (112).

Oligonucleotides

Oligonucleotides used in this study are shown in Table 5.1 (Midland Certified, Midland TX). To construct duplex substrates, 8-oxoguanine modified oligonucleotides were first 5' end labeled using [γ-^{32}P] ATP (3000 Ci/mmol) with T4 polynucleotide kinase (New England Biolabs) and annealed to the template oligonucleotides in a 1:2 molar ratio. Alternatively, 8-oxoguanine modified oligonucleotides were 3' end labeled using [α-^{32}P] ddATP (3000 Ci/mmol) with terminal deoxynucleotidyl transferase (New England Biolabs) and annealed to the template oligonucleotides in a 1:2 molar ratio. Annealing reactions were incubated at 95°C for 5 minutes and cooled to room temperature for 30 minutes. The D-loop substrate was prepared as described (263). Briefly, labeling the 5' end of oligonucleotides (C3/C4) was conducted in the presence of [γ-^{32}P] ATP (3000 Ci/mmol) and T4 polynucleotide kinase. Labeled oligonucleotides (C3/C4) was incubated with the complementary strand (C1) at 95°C for 5 minutes and cooled down stepwise (1.2°C/min) to 60°C, followed by addition of oligonucleotides (C2) and incubated at 60°C for 1 hour, which was cooled down stepwise (1.2°C /min) to 25°C.

Table 5.1 – Oligonucleotides used in this study. Telomeric repeats are underlined and 7,8-dihydro-8-oxogaunine modification is marked with bold X.

Name	Sequence (5' → 3')
Non-telomeric DNA	
A1	GTGGATCCGTACTCTG**X**GTACGTGTCAACACGAATTCGA
A2	GTGGATCCGTACTCTC**X**ATACGTGTCAACACGAATTCGA
A3	TCGAATTCGTGTTGACACGTACCCAGAGTACGGATCCAC
A4	TCGAATTCGTGTTGACACGTATCGAGAGTACGGATCCAC
Telomeric DNA	
B1	GTGGATCCGTACTTAG**X**GTTAGGGTTAACACGAATTCGA
B2	GTGGATCCGTACTTA**XXX**TTAGGGTTAACACGAATTCGA
B3	GTGGATCCGTACACACGAATTCGATGCTTAGGGTTAG**X**G
B4	GTGGATCCGTACTTAG**X**GTTAGGGTTAACACGAATTCGATCTGTGTCTGTGTCTGTG
B5	GTGGATCCGTACACACGAATTCGATGCTTAGGGTTAG**X**GTTATCTGTGTCTGTGTCT
B6	TCGAATTCGTGTTAACCCTAACCCTAAGTACGGATCCAC
B7	CCCTAACCCTAAGCATCGAATTCGTGTGTACGGATCCAC
B8	CACAGACACAGACACAGATCGAATTCGTGTTAACCCTAACCCTAAGTACGGATCCAC
B9	AGACACAGACACAGATAACCCTAACCCTAAGCATCGAATTCGTGTGTACGGATCCAC
B10	TTTTTTTTTTTTTTTTTTTCGAATTCGTGTTAACCCTAACCCTAAGTACGGATCCAC
B11	TTTTTTTTTTTTTTTCTTCCCTAACCCTAAGCATCGAATTCGTGTGTACGGATCCAC
Telomeric D-loop	
C1	TCAAGCTCGGTCTGCAGTCAGGATGATTGTGAGCGTTAACCCTAACCCTAACCCTAACCCTAATCTGCACTCGAGACTCACGTCCTGGTCACG
C2	CGTGACCAGGACGTGAGTCTCGAGTGCAGACCTTTTTTTTTTTTTTTTTTTTTTTTTTTTTTACAATCATCCTGACTGCAGACCGAGCTTGA
C3	CACCATCCAGTTCTCTTTTGAGAACTGGATGGTGTTAG**X**GTTAGGGTTAGGGTTAGGGTTAACGCTC
C4	CACCATCCAGTTCTCTTTTGAGAACTGGATGGTGTTAGGGTTAGGGTTAGGGTTAG**X**GTTAACGCTC

Electrophoretic mobility shift assay (EMSA)

EMSA was performed as previously described with minor modification (112,212). The reaction was conducted in a reaction mixture (10 μl) containing 1x Tel buffer (20 mM HEPES, pH 7.9, 150 mM KCl, 1 mM $MgCl_2$, 0.1 mM EDTA, 0.5 mM DTT, 5% glycerol, 0.1% NP-40 and 100 μg/ml BSA) or 1x NEB #2 buffer (10 mM Tris-HCI, 50 mM NaCl, 10 mM $MgCl_2$, 1 mM DTT and 100 μg/ml BSA). The reactions were incubated with increasing amounts of TRF1 in ice for 20 minutes. Samples were resolved by electrophoresis on a 4.5% native polyacrylamide gel (acylamide/bis 37.5:1). Gels were visualized by Phosphor-Imager and analyzed using the ImageQuant software (GE Bioscience).

Incision Assays

OGG1 incision assays were performed in a reaction mixture (10 μl) containing 1x NEB #2 buffer (10 mM Tris-HCI, 50 mM NaCl, 10 mM $MgCl_2$, 1 mM DTT and 100 μg/ml BSA). The reactions were incubated at 37°C for 15 min and terminated by addition of equal volume of 2x formamide loading buffer (95% (v/v) formamide, 20 mM EDTA, 0.1% (w/v) bromophenol blue and xylene cyanol). Alternatively, reactions were incubated at 37°C for the time points indicated and terminated by adding equal volume of 2x formamide loading buffer. Substrates were allowed to denature at 95^{o}C for 10 min, followed by incubation in ice for 2 min. Samples were resolved by electrophoresis on a 15% Polyacrylamide/7 M urea gel (National Diagnostic Inc.). Gels were visualized by

Phosphor-Imager and analyzed using the ImageQuantTM software (GE Bioscience). The percentage of incision was calculated as the amount of radioactivity present in the product band relative to the total radioactivity. For shelterin protein's effect on hOGG1's incision activity, incision assays were conducted in a reaction mixture (10 μl) containing 1x Tel buffer (20 mM HEPES, pH 7.9, 150 mM KCl, 1 mM $MgCl_2$, 0.1 mM EDTA, 0.5 mM DTT, 5% glycerol, 0.1% NP-40 and 100 μg/ml BSA). Purified TRF1 was first added to the reaction mixture and incubated at room temperature for 20 minutes, followed by addition of hOGG1 and further incubation at 37°C for 15 minutes. 500 μg/μl of tRNA (Roche) was added to each reaction prior to adding TRF1 to neutralize the non-specific exonuclease activity.

5.3 Results

Telomeres are prone to oxidative guanine damage

Evidence indicates that oxidative stress induces oxidative guanine damage preferentially in oligonucleotides with telomere repeats *in vitro* (106-108,261). To further investigate if telomeric DNA is also prone to oxidative DNA damage *in vivo*, the level of guanine oxidation was measured by examining Fpg-sensitive sites in telomeric (TTAGGG) and minisatellite (TG) regions of genomic DNA isolated from mouse kidney. Fpg excises oxidative guanine lesions and resulting abasic sites are further processed to single-strand-breaks via AP-lyase activity of Fpg (264). The extent of DNA fragmentation caused by Fpg reflects the frequency of oxidative DNA lesions, which appear as smaller molecular weight fragments after Fpg treatment (Figure 5.1). The mean

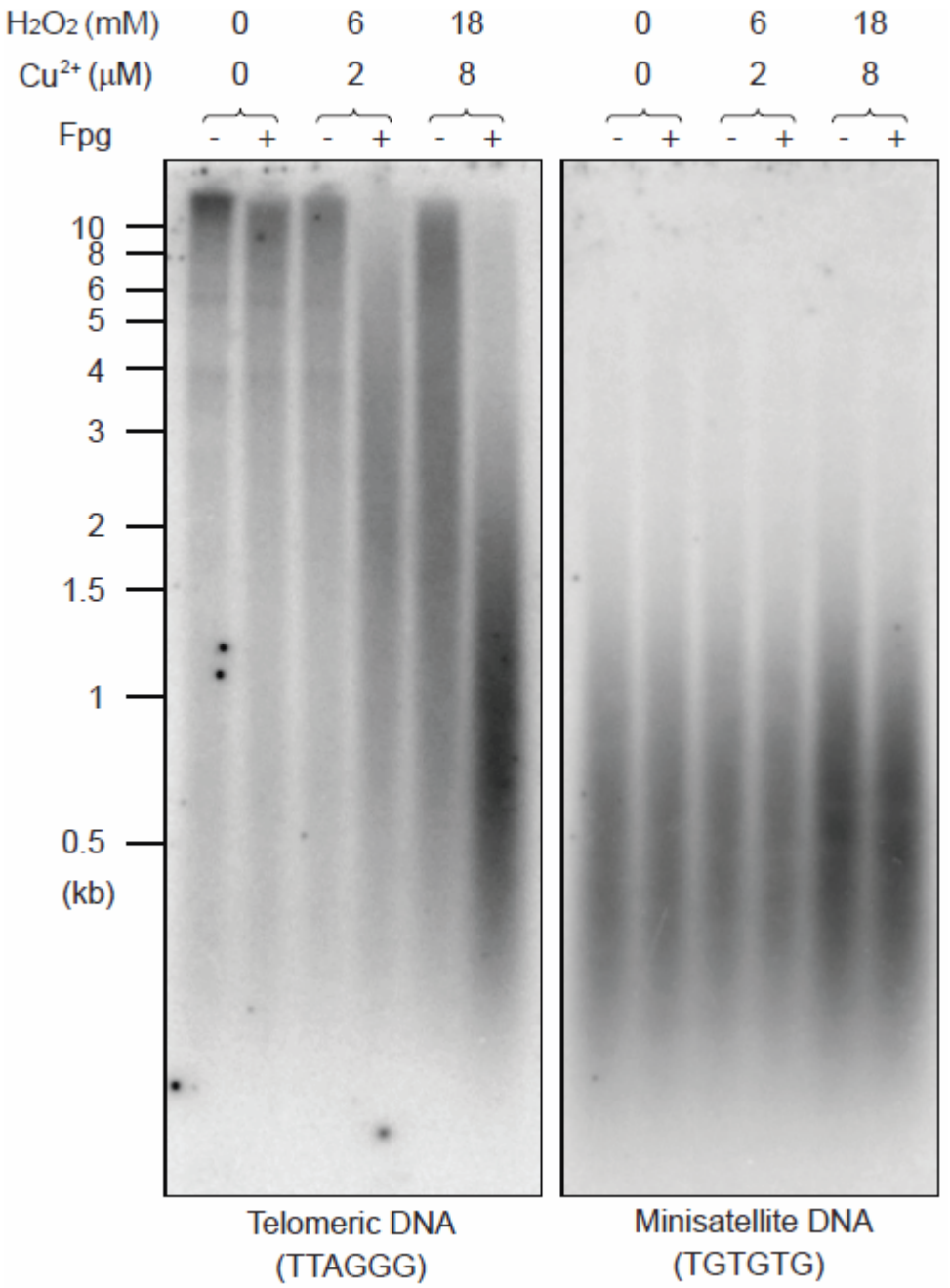

Figure 5.1 – *In vitro* exposure to increasing amount of oxidants leads to an increase in oxidative guanine damage preferentially in telomeres.
Isolated genomic DNA was treated with indicated amounts of H_2O_2/Cu^{2+}, and subsequently with Fpg. Treated samples were separated using alkaline gel, and telomeric and non-telomeric DNA fragments were detected by Southern blot analysis using radiolabelled telomere or CA repeat probes. After the Fpg treatment, telomeric DNA migrated as smaller fragments proportionally to the amount of oxidative stress induced while modest difference in migration was observed in non-telomeric DNA fragments.

values of DNA fragments in Fpg-treated (+) and mock-treated (-) samples were applied to estimate the frequencies of oxidative DNA lesions in telomeric and TG minisatellite regions (236). More Fpg-sensitive sites were found in telomeric than in minisatellite DNA (approximately 45.36 ± 7.4 and 20.76 ± 1.36 sites/10^6 bp in telomeres and minisatellites, respectively) (Table 5.2). Similarly, a human cell line, U2OS displayed more Fpg-sensitive lesions in telomeric TTAGGG repeats compared to TG minisatellites (approximately 5.72 ± 0.51 and 3.76 ± 1.11 sites/10^6 bp in telomeres and minisatellites, respectively) (Table 5.2). Although both types of repeats harbor similar contents of guanines (50%), the fact that more oxidative guanine lesions were detected in telomeric DNA suggest that either triple guanines of telomeric DNA repeats or simply the repeat sequences themselves are prone to oxidation. More guanine damages in telomeres could also reflect that OGG1-initiated BER repair may be less effective in telomeres.

To examine if telomeric DNA repeat sequences are more sensitive to oxidative stress, naked mouse kidney DNA was treated with increasing amounts of H_2O_2 and Cu^{2+} *in vitro* (13), and the level of oxidized guanines (*i.e.*, Fpg-sensitive sites) was examined for both telomeric and minisatellite regions of genomic DNA. Higher doses of H_2O_2 and Cu^{2+} treatment caused Fpg-dependent increase of shorter telomere DNA fragments (Figure 5.1, Left panel), whereas TG minisatellite DNA fragments displayed a moderate shortening under the same treatment conditions (Figure 5.1, Right panel). Accordingly, H_2O_2 and Cu^{2+} treatment increased the frequencies of Fpg-sensitive sites in telomeric DNA fragments significantly more than in TG minisatellite DNA fragments (approximately 303.04 ± 53.41 and 81.57 ± 11.88 sites/10^6 bp at high exposure in

Table 5.2 – The frequencies of FPG-sensitive sites/10^6 bp in telomeric (TTAGGG) and minisatellite (TG) regions of mouse kidney and U2-OS cells.

	Mouse Kidney	U2-OS
Telomeric DNA	45.36 ± 7.4*	5.72 ± 0.51
Minisatellite DNA	20.76 ± 1.36	3.76 ± 1.11

*Because of semi-quantitative nature of the method, the frequency does not represent the absolute values of base lesions in these genomic regions. The values were derived from three independent experiments.

telomeres and TG minisatellites, respectively) (Table 5.3). This observation suggests that telomere repeat sequences (possibly triple guanines or telomeric DNA repeats as a whole) can contribute to preferential guanine damage in telomeric DNA.

To determine if there was differential oxidative guanine damage repair in telomeric DNA and TG minisatellites *in vivo*, U2OS cells were briefly treated with 1 mM of menadione, to induce high incidences of oxidative DNA damage, and allowed to recover for 6 hours according to previously described protocol (238). The level of oxidative DNA lesions was examined for both telomeric and TG minisatellite regions. The starting frequencies of Fpg-sensitive sites in telomeric DNA fragments and TG minisatellite were comparable immediately after the menadione treatment (approximately 7.72 ± 1.75 and 9.56 ± 6.22 respectively) (Table 5.4). However, after 6 hours of recovery time, the Fpg-sensitive sites were undetectable in TG minisatellite while even higher frequencies of Fpg-sensitive sites were detected in telomeric DNA fragments (Not detected and approximately 14.25 ± 1.21 sites/10^6 bp in minisatellites and telomeres, respectively) (Table 5.4). These data suggest that OGG1-initiated BER may be less effective in telomeres *in vivo*, and thus oxidative DNA damage can accumulate in telomeres over time.

The incision activity of α-hOGG1 is comparable in telomeric and non-telomeric double-stranded substrates

Telomere special factors (*e.g.*, telomeric DNA repeat sequences, telomere special structures, or telomere binding proteins) may affect the repair of oxidative guanine

Table 5.3 – The frequencies of FPG-sensitive sites/10^6 bp in telomeric (TTAGGG) and minisatellite (TG) regions of mouse kidney DNA after *in vitro* induction of oxidative stress.

H_2O_2 (mM)	6	18
Cu^{2+} (μM)	2	8
Telomeric DNA	137.88 ± 17.71*	303.04 ± 53.41
Minisatellite DNA	68.69 ± 31.74	81.57 ± 11.88

*Because of semi-quantitative nature of the method, the frequency does not represent the absolute values of base lesions in these genomic regions. The values were derived from three independent experiments.

Table 5.4 – The frequencies of FPG-sensitive sites/10^6 bp in telomeric (TTAGGG) and minisatellite (TG) regions of U2OS cells after menadione treatment plus 6 hours of recovery time.

	0 hour	6 hours
Telomeric DNA	7.72 ± 1.75*	14.25 ± 1.21
Minisatellite DNA	9.56 ± 6.22	ND

*Because of semi-quantitative nature of the method, the frequency does not represent the absolute values of base lesions in these genomic regions. ND= Not detectable. The values were derived from three independent experiments.

damage in telomeres and contribute to differential repair of oxidative guanine damage in telomeric and non-telomeric regions. To examine if triple guanines of telomeric DNA repeats or repeat sequences themselves affect oxidative guanine repair, we employed an *in vitro* α-hOGG1-incision assay. The α-hOGG1 enzyme is primarily responsible for removing 8-oxodG in the nucleus of human cells and its incision activity was examined on 8-oxodG containing double-stranded oligonucleotide substrates, with telomeric or non-telomeric DNA repeats harboring either one or triple guanines. Specifically, in telomeric-duplex-1 (TD1), the middle guanine of one of the telomere repeats was modified with 8-oxoguanine, whereas in non-telomeric-duplex-1 (NTD1) and non-telomeric-duplex-2 (NTD2) 8-oxoguanine modification was surrounded by non-telomeric sequences (Table 5.1, Figure 5.2). Notably, NTD1 had two guanines flanking the 8-oxodG to mimic triple guanines of telomeric DNA, whereas NTD2 was flanked by cytosine and adenine to mimic single 8-oxodG condition. These duplexes (0.5 nM) were incubated with serial dilutions (16, 32, 64, 128, or 256 nM) of α-hOGG1 and the percentage of incision product was measured and compared between telomeric and non-telomeric DNA repeats containing oligonucleotide substrates. 16 nM (lowest concentration of enzyme) of α-hOGG1 was able to efficiently excise the substrates and the percentages of excised products increased with increase in enzyme concentration (Figure 5.3). The percentage of excised products from telomeric duplex TD1 (Lanes 1-6) were equivalent to non-telomeric duplex NTD1 (Lanes 7-12), which suggests that α-hOGG1 can excise 8-oxodG from a triple guanine repeat (G8G, 8 refers to 8-oxodG) of a non-telomeric or telomeric duplex with similar efficiency. Moreover, the percentage of

Designation	Top + Bottom	Nucleotide Sequence
Non-Telomeric-Duplex-1	A1 + A2	5'-GTGGATCCGTACTCTG**X**GTACGTGTCAACACGAATTCGA-3' 3'-CACCTAGGCATGAGACCCATGCACAGTTGTGCTTAAGCT-5'
Non-Telomeric-Duplex-2	A3 + A4	5'-GTGGATCCGTACTCTC**X**ATACGTGTCAACACGAATTCGA-3' 3'-CACCTAGGCATGAGAGCTATGCACAGTTGTGCTTAAGCT-5'
Telomeric-Duplex-1	B1 + B6	5'-GTGGATCCGTACTTAG**X**GTTAGGGTTAACACGAATTCGA-3' 3'-CACCTAGGCATGAATCCCAATCCCAATTGTGCTTAAGCT-5'
Telomeric-Duplex-2	B2 + B6	5'-GTGGATCCGTACTTA**XXX**TTAGGGTTAACACGAATTCGA-3' 3'-CACCTAGGCATGAATCCCAATCCCAATTGTGCTTAAGCT-5'
Telomeric-Duplex-3	B3 + B7	5' GTGGATCCGTACACACGAATTCGATGCTTAGGGTTAGX**G**-3' 3' CACCTAGGCATGTGTGCTTAAGCTACGAATCCCAATCCC-5'
Telomeric-Duplex-4	B4 + B8	5' GTGGATCCGTACTTAG**X**GTTAGGGTTAACACGAATTCGATCTGTGTCTGTGTCTGTG-3' 3' CACCTAGGCATGAATCCCAATCCCAATTGTGCTTAAGCTAGACACAGACACAGACAC-5'
Telomeric-Duplex-5	B5 + B9	5' GTGGATCCGTACACACGAATTCGATGCTTAGGGTTAG**X**GTTATCTGTGTCTGTGTCT-3' 3' CACCTAGGCATGTGTGCTTAAGCTACGAATCCCAATCCCAATAGACACAGACACAGA-5'
Telomeric-3'-Overhang-1	B4 + B6	5' GTGGATCCGTACTTAG**X**GTTAGGGTTAACACGAATTCGATCTGTGTCTGTGTCTGTG-3' 3' CACCTAGGCATGAATCCCAATCCCAATTGTGCTTAAGCT-5'
Telomeric-3'-Overhang-2	B5 + B7	5' GTGGATCCGTACACACGAATTCGATGCTTAGGGTTAG**X**GTTATCTGTGTCTGTGTCT-3' 3' CACCTAGGCATGTGTGCTTAAGCTACGAATCCCAATCCC-5'
Telomeric-Fork-1	B4 + B10	5' GTGGATCCGTACTTAG**X**GTTAGGGTTAACACGAATTCGATCTGTGTCTGTGTCTGTG-3' 3' CACCTAGGCATGAATCCCAATCCCAATTGTGCTTAAGCTTTTTTTTTTTTTTTTTT-5'
Telomeric-Fork-2	B5 + B11	5' GTGGATCCGTACACACGAATTCGATGCTTAGGGTTAG**X**GTTATCTGTGTCTGTGTCT-3' 3' CACCTAGGCATGTGTGCTTAAGCTACGAATCCCAATCCCTTCTTTTTTTTTTTTTT-5'

Figure 5.2 – Double-stranded oligonucleotide substrates.
Oligonucleotides modified with 8-oxodG were either 5' end-labeled or 3' end-labeled and annealed to the corresponding complementary strands. The bold X denotes the 8-oxodG modifications.

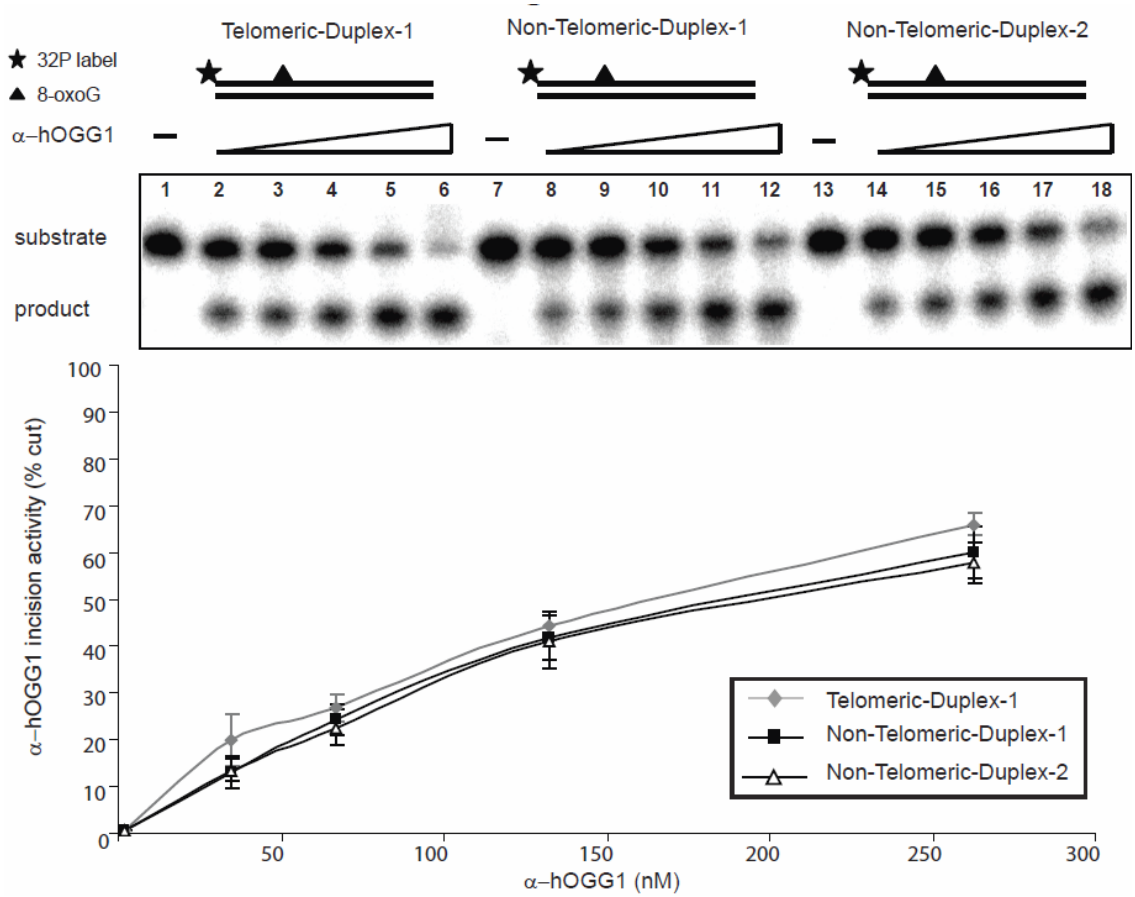

Figure 5.3 – α-hOGG1 incision activity is comparable between telomeric and non-telomeric DNA repeats containing double-stranded substrates.
Substrates (0.5 nM) were incubated alone (lanes 1, 7, and 13) or together with increasing concentrations of OGG1 (16, 32, 64, 128, or 256 nM, lanes 2-6, 8-12, and 14-18). No significant difference in incision activity was observed among these substrates. The percentage cut was plotted against -hOGG1 concentrations. Values and error bars represent the mean and SE from three independent experiments.

excised products was comparable between telomeric substrate TD1 and non-telomeric substrate (NTD2) with a single guanine (Lanes 13-18). Taken together, these studies suggest that triple guanines of telomeric DNA repeats and repeat sequences themselves do not impact OGG1 incision activity.

α-hOGG1 prefers to excise the middle 8-oxodG base lesion in telomeric triplet guanines

Our data suggest that a single 8-oxodG in telomeric substrates can be efficiently excised by α-hOGG1 *in vitro*. It is unclear whether multiple 8-oxodG base lesions in telomeric DNA substrates affect α-hOGG1 incision. The incision activity of α-hOGG1 was examined on telomeric double-stranded oligonucleotide substrates with either single or triple 8-oxodG base modifications. Specifically, all the three guanines in one of the telomeric repeats was replaced by 8-oxodG in telomeric-duplex-2 (TD2) as opposed to one guanine in telomeric duplex TD1 (Table 5.1, Figure 5.2). α-hOGG1 was incubated with 0.5 nM of TD1 or TD2 duplexes in serial dilutions (16, 32, 64, 128, or 256 nM) and the percentage of incision product was measured between the two substrates. Our data indicate that the percentage of incision products was comparable between single and triple 8-oxodG containing substrates (Figure 5.4), which suggest that the number of 8-oxodG within GGG of telomeric DNA repeats do not impact α-hOGG1 incision activity *in vitro.*

Interestingly, the incision products of the triple 8-oxodG containing substrate TD2 appeared more diffuse compared to that of the single 8-oxodG substrate (Figure 5.4, lanes

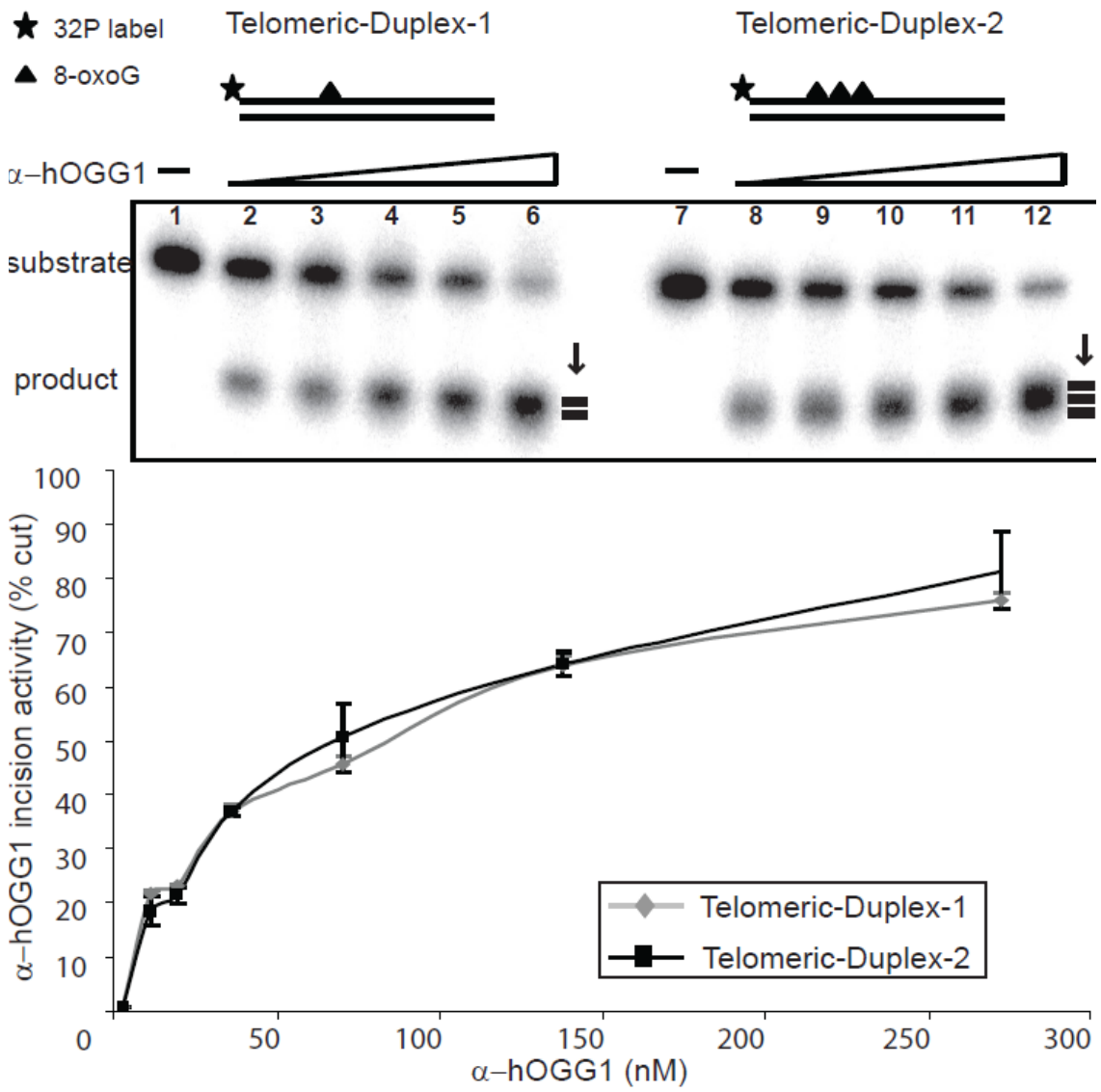

Figure 5.4 – α-hOGG1 incision activity is comparable between single and triple 8-oxodG containing double-stranded telomeric substrates.
Substrates (0.5 nM) were incubated alone (lanes 1 and 7) or together with increasing concentrations of -hOGG1 (16, 32, 64, 128, or 256 nM, lanes 2-6 and 8-12). The incision products of triple 8-oxodG containing substrate was more diffused than single 8-oxodG containing substrate, indicated by three bars as opposed to two bars (arrows). Collectively, these incision products were similar between the two substrates. The percentage cut was plotted against -hOGG1 concentrations. Values and error bars represent the mean and SE from three independent experiments.

6 and 12). This suggests that more than one of triple 8-oxodG was being excised, but it was unclear if there was a preferential incision of 8-oxodG at different positions of the telomeric triple G (GGG) repeat. Previous studies indicated that guanines in a telomeric DNA substrate are not equally susceptible to oxidative damage and that oxidative stress can induce base damage preferentially at 5' or at the middle G in GGG of telomeric DNA repeats (107,108). Thus, we examined if there was preferential incision of 8-oxodG at the 5', the middle or the 3' position in GGG of telomeric DNA repeats by α-hOGG1. To better visualize the incision products, the TD2 substrate was either 5' labeled with γ-^{32}P-dATP or 3' labeled with α-^{32}P-ddATP. To observe sequential incision of 8-oxodG in telomeric GGG, the TD2 substrate was incubated with a fixed amount (8 nM) of α-hOGG1 enzyme. The reactions were stopped and collected at different time points (15 sec, 30 sec, 1 min, 2 min, 4 min, and 8 min), and the incision products were separated to obtain a 1 bp difference. Three individual excised products were observed in 5'- and 3'-labeled substrates at the indicated positions (Figure 5.5, A and B). With 5'-end labeling, the middle 8-oxodG in telomeric GGG was being excised initially, followed by 8-oxodG on the 5'-site, and subsequently 8-oxodG on the 3'-site. After the initial incision of middle 8-oxodG, 8-oxodGs on the 5'-site was efficiently excised, however fewer 8-oxodG at the 3'-site was removed (Figure 5.5C). Similarly, experiments with the 3' labeled substrate also showed that the middle 8-oxodG in telomeric GGG was being excised initially, followed by 8-oxodG on the 5'-site, and subsequently 8-oxodG on the 3'-site (Figure 5.5D). Taken together, these results suggest that there is preferential incision of 8-oxodG by α-hOGG1 at different positions in the telomeric DNA repeat.

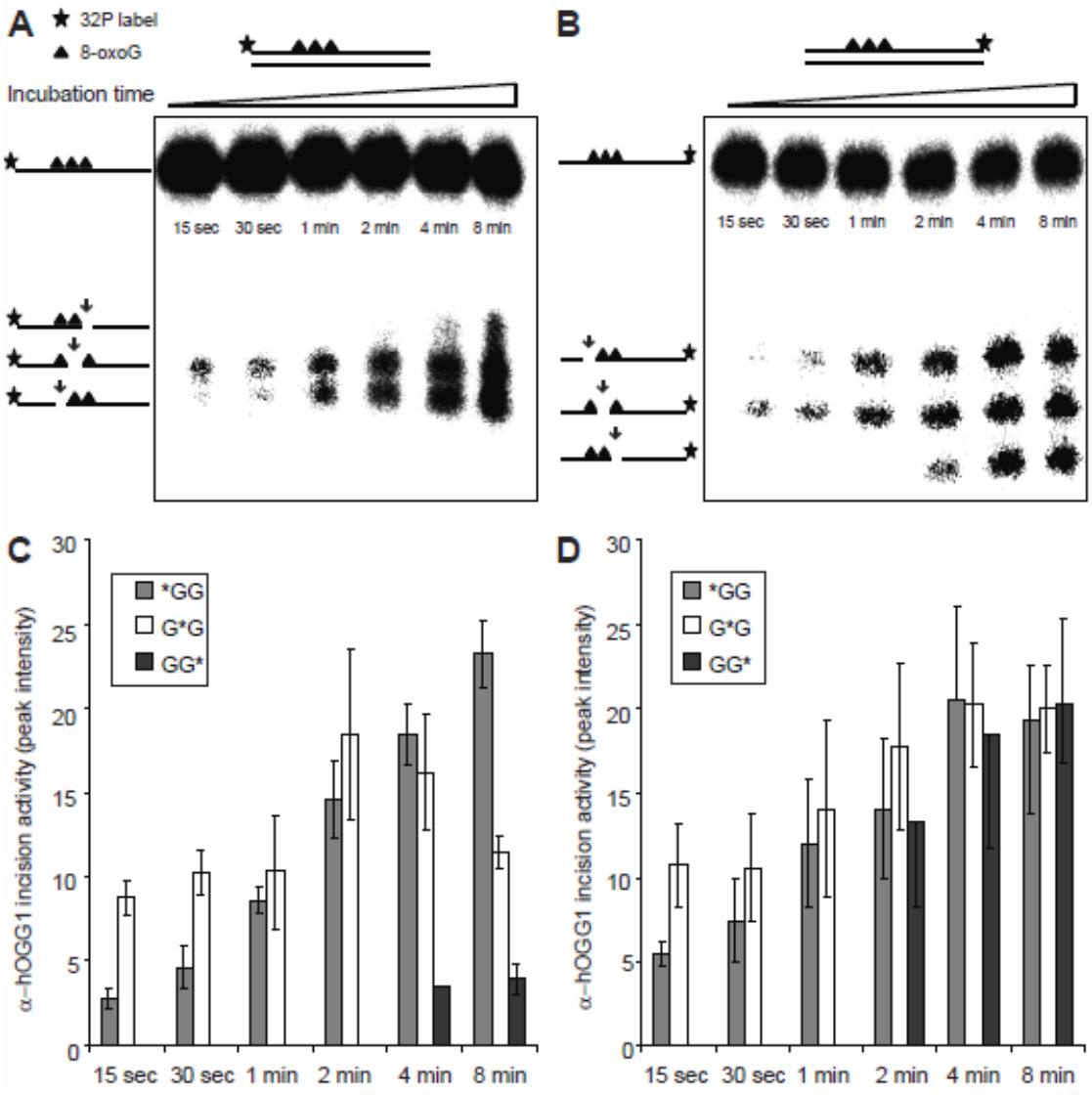

Figure 5.5 – α-hOGG1 prefers to excise middle 8-oxodG base lesion in telomeric DNA repeats. Substrates (0.5 nM) were incubated with fixed concentration of -hOGG1 (8 nM) and collected at different time points (15 sec, 30 sec, 1 min, 2 min, 4 min, and 8 min, lanes 1-6 and 7-12). The middle 8-oxodG in telomeric GGG was excised initially, followed by 8-oxodG on the 5'-site, and subsequently 8-oxodG on the 3'-site in both 5' labeled (A and C) substrate and 3' labeled (B and D) substrates. Arrows – The position of excised 8-oxodG. The peak -hOGG1 incision activity was plotted against time points. Values and error bars represent the mean and SE from three independent experiments.

The position of the 8-oxodG lesion affects α-hOGG1 incision activity on a telomeric double-stranded substrate with a 3'-overhang

Mammalian telomeres have unique structural features such as a 3'-overhang. The single-stranded nature of the 3'-overhang of the G-strand displaces the upstream G-strand and then base pairs with the C-strand creating a displacement loop or D-loop, which creates a circular structure known as the t-loop (3,22). T-loop structure is known to mask the 3'-overhang from triggering DNA damage signaling and DNA repair (3). This telomeric structure may regulate the access or the function of BER proteins at telomeres. We examined the α-hOGG1 incision activity on 8-oxodG containing telomeric double-stranded oligonucleotide substrates with or without a 3'-overhang, namely telomeric-overhang-1 (TOH1) and telomeric-duplex-4 (TD4). TOH1 has 39-mer duplex region followed by an 18 bp 3'-overhang. The duplex region contains an 8-oxodG lesion 12 bp away from the opening of the single-stranded 3'-overhang (Table 5.1, Figure 5.2). α-hOGG1 was incubated with 0.5 nM of substrates in serial dilutions and the percentage of incision products were measured between two substrates. When TOH1 was incubated with 16 nM enzyme, the incision product was visible and increased up to 60% with 256 nM enzyme (Figure 5.6A, lanes 2-7). The TD4 substrate showed a similar trend upon the same enzymatic treatment (Figure 5.6A, lanes 9-14). This result suggests that α-hOGG1 can efficiently excise a guanine lesion that is distant from 3'-overhang.

The junction between the single-stranded 3'-overhang and the duplex DNA appears to be essential in preserving the integrity of the 3'-overhang, hence the formation of the t-loop (29,33). TRF2 binds to the junction sites, where it is essential in t-loop

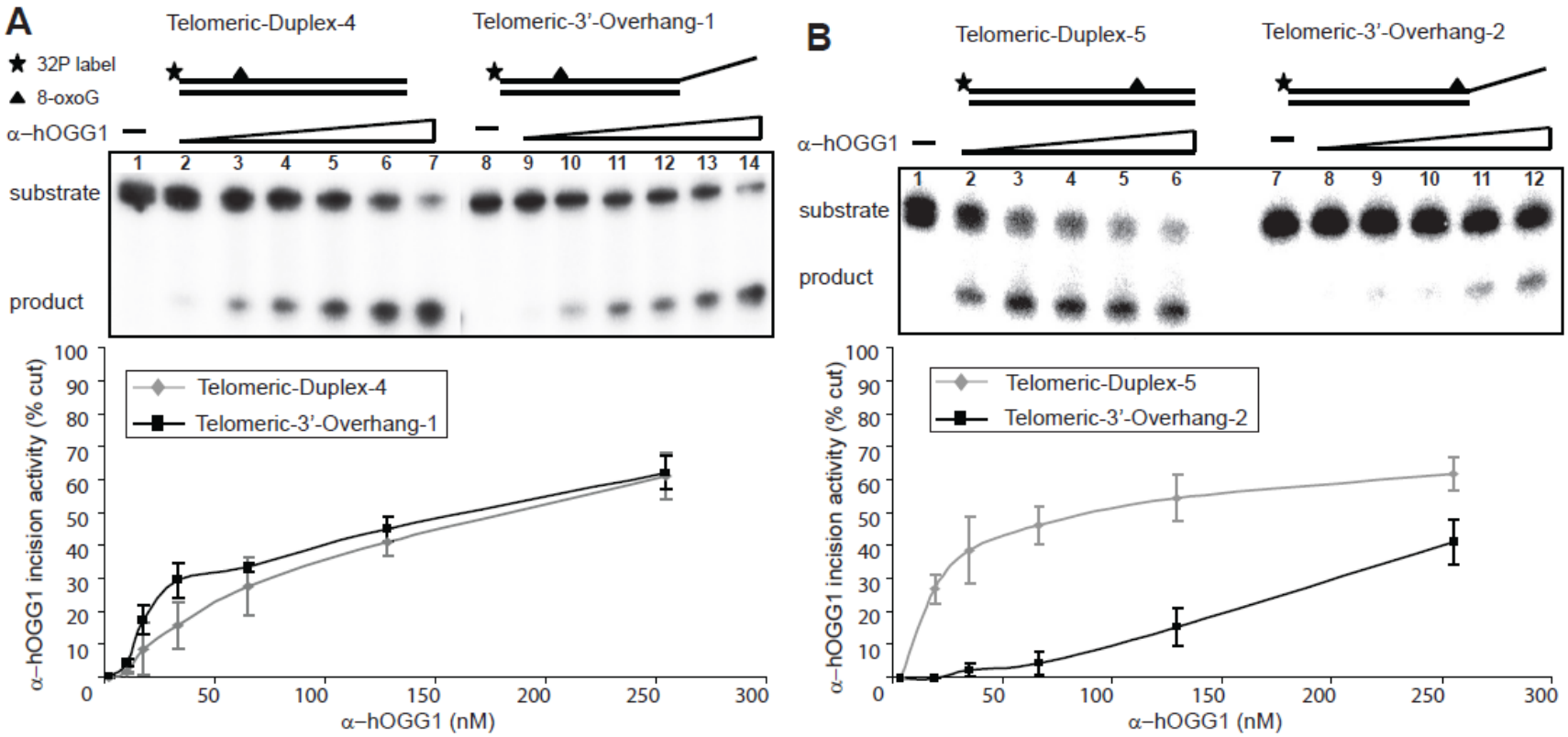

Figure 5.6 – The position of 8-oxodG base lesion affects α-hOGG1 incision activity on telomeric substrates with 3' overhang.
(A) Substrates (0.5 nM) were incubated alone (lanes 1 and 8) or together with increasing concentrations of -hOGG1 (8, 16, 32, 64, 128, or 256 nM, lanes 2-7 and 9-14). The incision activity on telomeric duplex substrate with 3'-overhang was comparable to duplex without 3' over-hang. (B) Substrates (0.5 nM) were incubated alone (lanes 1 and 7) or together with increasing concentrations of OGG1 (16, 32, 64, 128, or 256 nM, lanes 2-6 and 8-12). 8-oxodG modification near opening of 3'-overhang greatly reduced the -hOGG1's incision activity. The percentage cut was plotted against -hOGG1 concentrations. Values and error bars represent the mean and SE from three independent experiments.

formation (33). Since oxidative guanine damage can disrupt the binding by telomere repeat binding factors (112), the repair of oxidative guanine lesions at the junction sites is critical for telomere capping. We thus examined if 8-oxodG modification at the ssDNA/dsDNA junction could be efficiently removed by α-hOGG1 using TOH2 and TD5. TOH2 has 8-oxodG modification one base pair away from the first base of the 3'-overhang. TD5 has the same sequence as TOH2 except with complimentary strand extended the 3'-overhang region to complete the duplex. Interestingly, the α-hOGG1 incision activity was greatly reduced on the overhang substrate TOH2. 16 nM of α-hOGG1 was able to initiate the incision (35% product) on the duplex substrate TD5, whereas 64 nM of enzyme was required to initiate product formation (only 5% product) from the overhang substrate TOH2 (Figure 5.6B, lanes 2-6 and 8-12). The difference in the percentage of incision products was as high as ~15-fold. Together, these results suggest that the telomeric structure (3'-overhang) has differential effects on the *in vitro* incision activity of α-hOGG1, which is dependent on the position of the guanine base lesions.

Telomeric D-loop formation does not impair α-hOGG1 incision activity

To further examine the effects of telomeric structures on oxidative damage repair at telomeres, we examined α-hOGG1 incision activity on *in vitro* assembled D-loop structures DL1 & DL2 (Table 5.1, Figure 5.7). These substrates consist of a bubble structure with two 30 bp duplex arms separated by a 33 nt ssDNA melted region, one strand of which is annealed to an invading ssDNA. The melted region and the invading

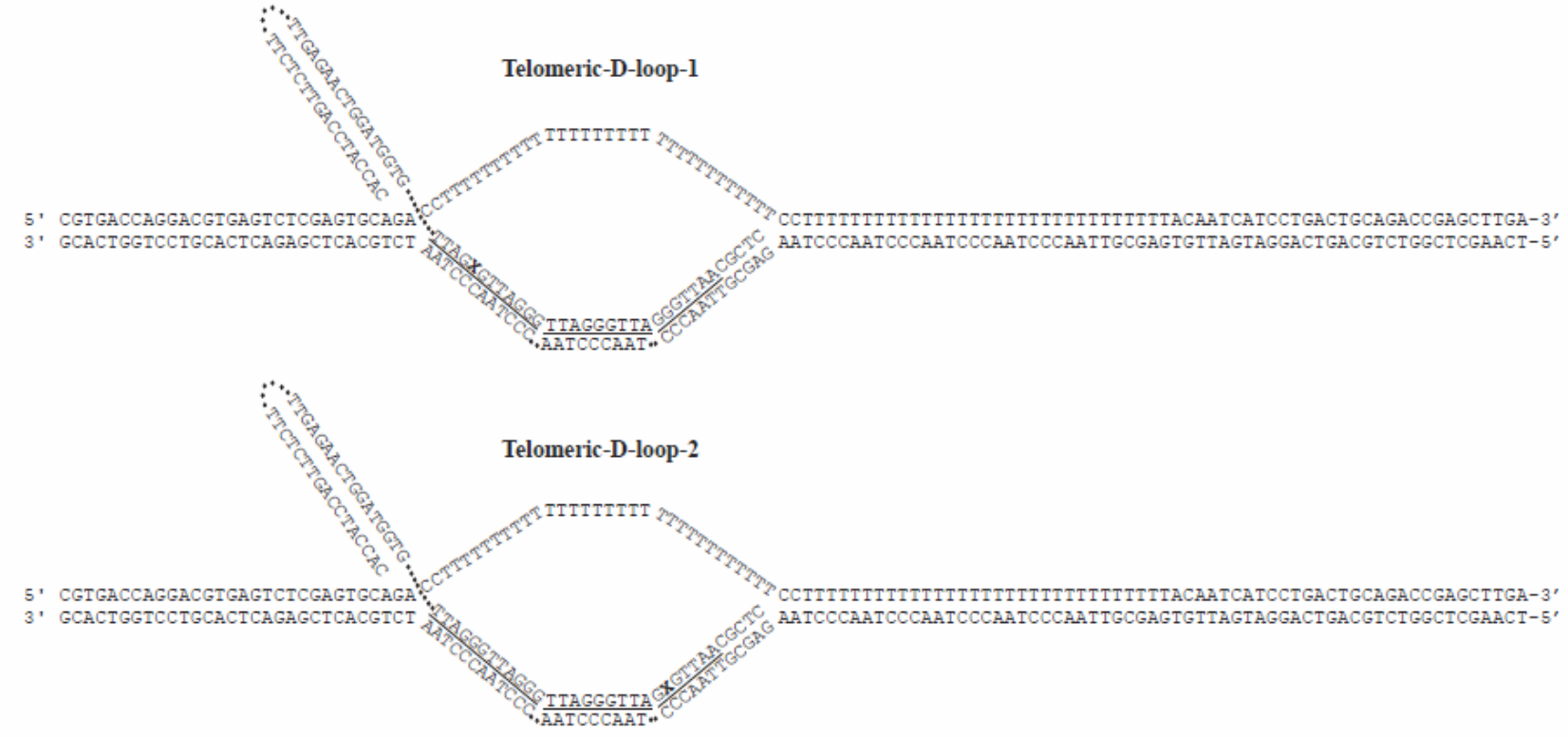

Figure 5.7 – Representation of assembled of telomeric D-loop substrate. X in bold indicates 8-oxodG modifications.

ssDNA carry four telomeric repeats, such that the DNA substrate mimics a telomeric D-loop. The invading telomeric strand contains a 8-oxodG lesion in place of the middle guanine of the first (DL1) or the last (DL2) of four telomeric repeats (263). α-hOGG1 was incubated in serial dilutions with 0.5 nM of substrates and the incision activity was compared between one of the D-loop substrates (DL1) and the double-stranded telomeric substrate TD1. α-hOGG1 excised the lesion from the *in vitro* assembled D-loop substrate DL1 slightly more efficiently than the duplex substrate TD1 using higher concentrations (>64 nM) of α-hOGG1 (Figure 5.8A, lanes 1-6 and 7-12). We also tested the effect of the position of the 8-oxodG lesion on α-hOGG1 incision activity on the damaged telomeric D-loop substrate. Similarly to the observation on double-stranded oligonucleotides with 3'-overhang, 8-oxodG positioned closer to 5' site (DL2) was excised slightly more efficiently (Figure 5.8B, lanes 1-6 and 7-12) than the one close to 3'-end (DL1). Collectively, these results suggest that a telomeric D-loop structure does not impair α-hOGG1 incision activity and that the position of the 8-oxodG lesion may dictate the enzymatic efficiency on oxidatively damaged telomeric D-loops *in vitro*.

An 8-oxodG near a telomeric fork ssDNA/dsDNA junction reduces α-hOGG1 incision activity

The binding of telomere repeat factors to telomere DNA is sequence specific (15,25,265). Unrepaired 8-oxodG can be highly mutagenic after DNA replication (122) and may therefore be detrimental to the binding of telomere repeat binding factors. Thus, we examined if 8-oxodG in a telomeric replication fork context can be efficiently incised

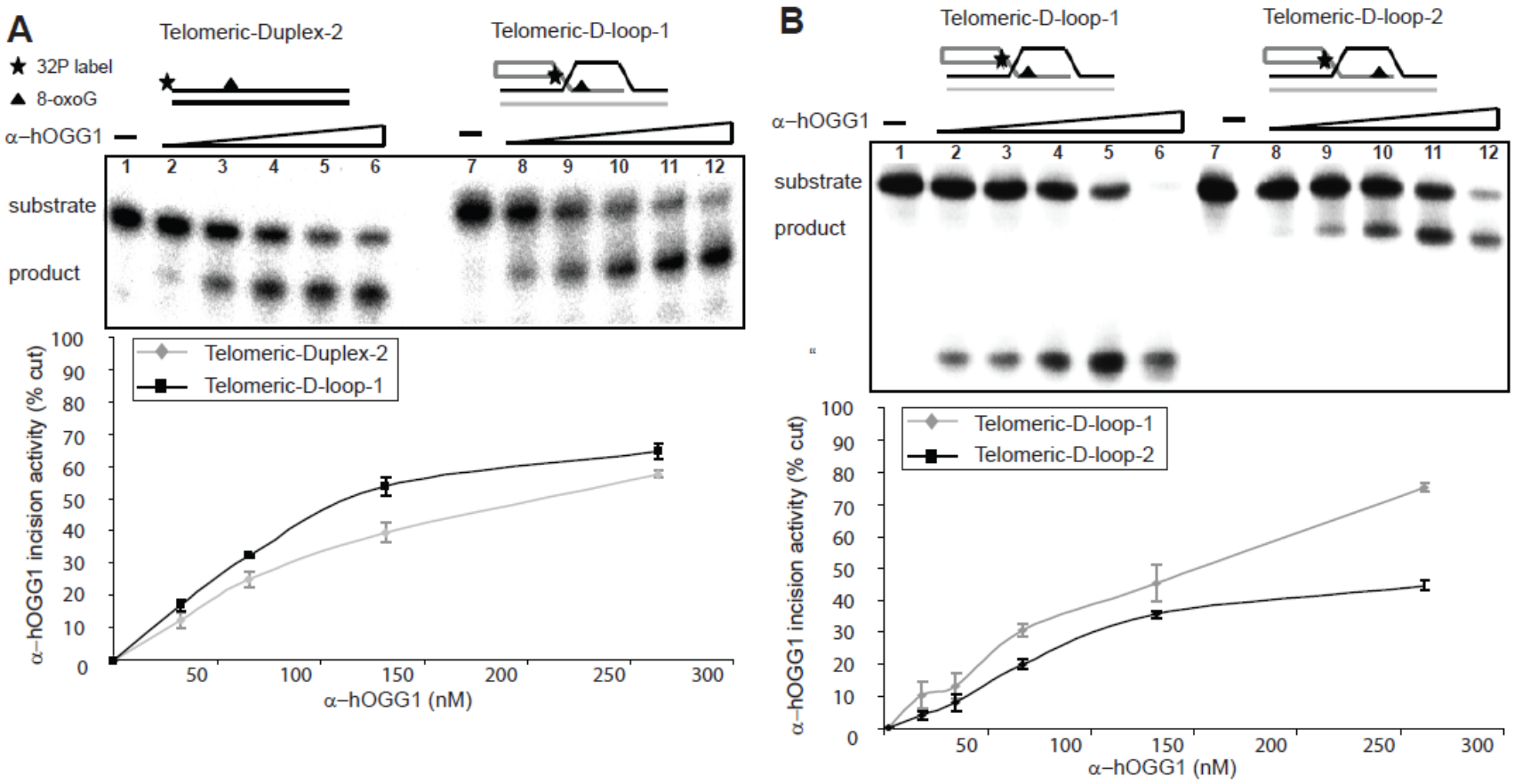

Figure 5.8 – α-hOGG1 incision activity is influenced by position of 8-oxodG base lesion on d-loop substrates.
Substrates (0.5 nM) were incubated alone (lanes 1 and 7) or together with increasing concentrations of OGG1 (16, 32, 64, 128, or 256 nM, lanes 2-6 and 8-12). (A) *In vitro* assembled d-loop substrate was excised slightly more efficiently than double-stranded telomeric substrate. (B) The d-loop substrate with 8-oxodG modification closer to 5' end was excised slightly more efficiently than the D-loop substrate with 8-oxodG modification closer to 3' end. The percentage cut was plotted against -hOGG1 concentrations. Values and error bars represent the mean and SE from three independent experiments.

by α-hOGG1. Since the position of the 8-oxodG may dictate α-hOGG1 incision activity, two 8-oxodG containing telomeric fork substrates, TF1 and TF2, were constructed for this purpose. TF1 contains 8-oxodG 12 bp away from the fork region (resembles an unreplicated region), while TF2 has 8-oxodG next to the fork ssDNA/dsDNA junction (Table 5.1, Figure 5.2). α-hOGG1 was incubated in serial dilutions with 0.5 nM substrate and the incision activity was compared between telomeric fork substrates and its corresponding double-stranded telomeric substrates (TF1 & TD4, and TF2 & TD5, respectively). By using substrates TF1 and TD4, the incision products were visible after addition of 16 nM enzyme and increased up to 60% with 256 nM enzyme at similar rates in both substrates (Figure 5.9A, lanes 1-7 and 8-14). However, α-hOGG1 was unable to efficiently excise 8-oxodG from the other fork substrate TF2 in which the lesion is next to the fork region. While 64 nM of the enzyme was able to generate more than 50% incision product from a similar telomeric duplex substrate (TD5), a large excess (256 nM) of enzyme was required to generate only about 20% incision product using the telomeric fork TF2 (Figure 5.9B, lanes 1-7 and 8-14). The difference in percentage of incision products was as high as ~16-fold. Together, these results imply that α-hOGG1 can efficiently excise a guanine lesion that is distant from the telomeric fork, but its ability to excise a telomeric 8-oxodG lesion next to a fork ssDNA/dsDNA junction is severely compromised.

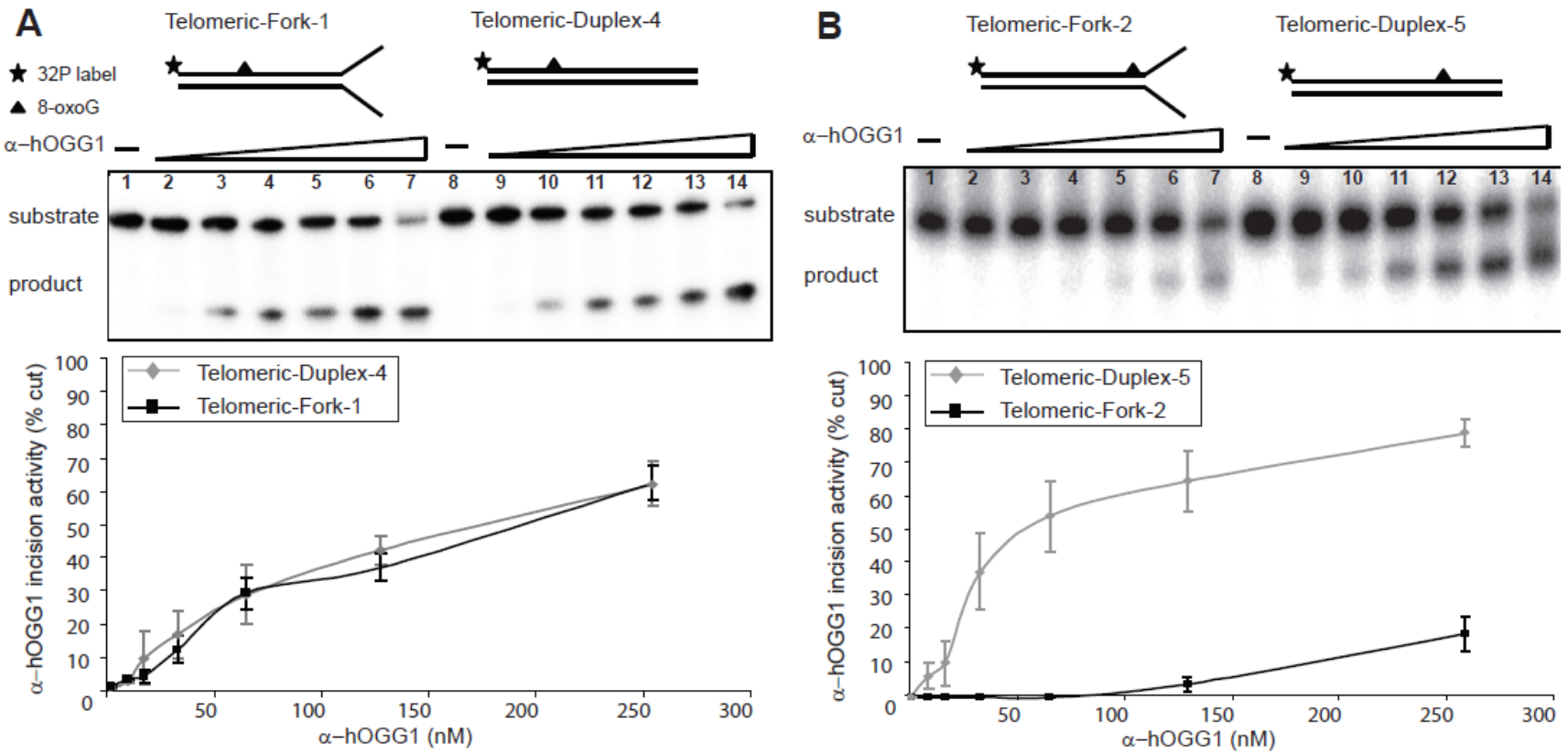

Figure 5.9 – The telomeric substrate with 8-oxodG base lesion near fork-opening greatly affects α-hOGG1 incision activity.
Substrates (0.5 nM) were incubated alone (lanes 1 and 8) or together with increasing concentrations of -hOGG1 (8, 16, 32, 64, 128, or 256 nM, lanes 2-7 and 9-14). (A) 8-oxodG modification away from fork-opening did not affect -hOGG1's incision activity. (B) 8-oxodG modification near the fork-opening significantly reduced -hOGG1's incision activity. The percentage cut was plotted against -hOGG1 concentrations. Values and error bars represent the mean and SE from three independent experiments.

Telomere binding proteins do not impede α-hOGG1 incision activity on telomeric duplex substrates

Shelterin protein complex functions to mask the ends of linear chromosomes from DNA repair at telomeres (3). Additionally, over-expression of shelterin protein TRF2 can lead to inefficient SSB repair at telomeres (266). We hypothesized that shelterin proteins such as TRF1 and TRF2 would affect α-hOGG1 incision activity, when bound to telomeres. To evaluate the effect of shelterin proteins on α-hOGG1 incision activity, we examined activity on a double-stranded telomeric oligonucleotide substrate bound by either TRF1 or TRF2. To ensure that TRF1 is bound to the substrate with 8-oxodG modification in one of telomeric repeats, EMSA was performed using the same experimental conditions as for α-hOGG1 incision assay. Under these experimental conditions, purified TRF1 was detectable at telomeric substrate TD1 (data not shown) and TRF1 alone did not excise the substrate (Figure 5.10, lanes 9-13). When the substrate TD1 was pre-incubated with 16 nM purified TRF1 prior to α-hOGG1 (4 nM) treatment, the incision activity did not change compared to α-hOGG1 treatment alone (Figure 5.10, lanes 2 and 3). However, with gradual increase in TRF1 concentration, a slight increase in incision activity was observed in large excess (256 nM) of TRF1 (Figure 5.10, lanes 3-8). To examine if this minor stimulation was dependent on TRF1's ability to bind to oligonucleotide substrate containing telomeric DNA repeats, the same assay was performed on oligonucleotide substrates containing non-telomeric DNA repeats. Interestingly, we found that in presence of a large excess of TRF1, it can also weakly enhance α-hOGG1 glycosylase activity on non-telomeric substrates NTD1 and NTD2

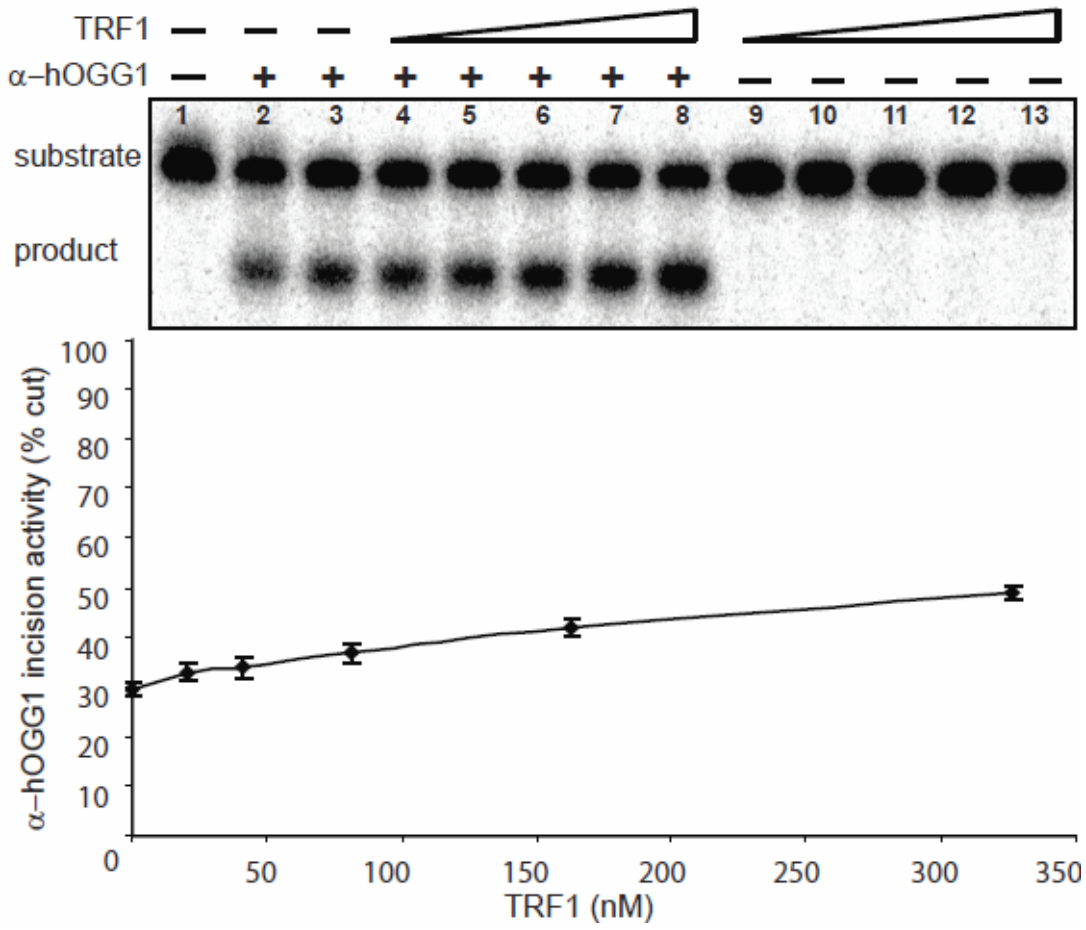

Figure 5.10 – The shelterin protein TRF1 does not greatly affect α-hOGG1 incision activity.
Substrate (0.2 nM) was incubated alone (lane 1) or together with fixed amount of -hOGG1 (4 nM, lanes 2-8) and increasing concentrations of TRF1 (16, 32, 64, 128, or 256 nM, lanes 4-8 and 9-13). The percentage of incision products was plotted against TRF1 concentrations. Values and error bars represent the mean and SE from three independent experiments.

(data not shown), even though EMSA showed no binding of TRF1 to these substrates (data not shown). These data indicate that TRF1 binding does not have any effect on the activity of α-hOGG1. We also tested if TRF2 had any effect on α-hOGG1 incision activity. Under the same experimental condition, TRF2 did not enhance α-hOGG1 incision activity (Figure 5.11). These results indicate that large excess of TRF1, but not TRF2 can weakly stimulate α-hOGG1 incision activity on 8-oxodG containing oligonucleotide substrates, which was independent of TRF1's ability to bind to the substrates. Together, our results suggest that α-hOGG1 is able to proficiently excise 8-oxodG containing oligonucleotide substrates bound by telomere binding proteins *in vitro*.

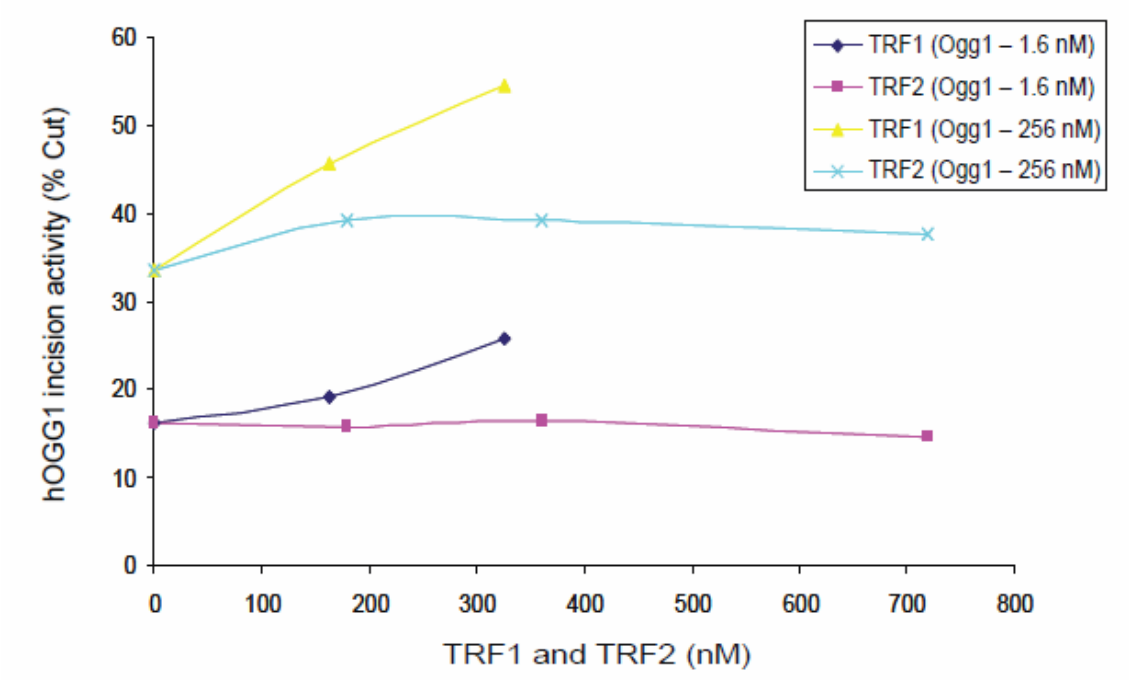

Figure 5.11 – TRF1 and not TRF2 moderately stimulate α-hOGG1 glycosylase activity.
The percentage of incised products was plotted against -hOGG1concentrations.

5.4 Discussion

Due to its low oxidation potential, guanine succumbs to oxidation more than other DNA nucleobases (122,267,268). Additionally, studies indicate that 5‘ guanine of stacked GG and GGG sequences oxidize more easily than a lone guanine in DNA and that the 5‘ guanine of GGG oxidizes more easily than the 5‘ guanine of GG (246,267,269). Telomere tracks consisting of GGG repeats may greatly increase this oxidation potential when compared to the other repeats with single G. In fact, human cells with long telomeres show increased sensitivity to hydrogen peroxide, but not to etoposide and bleomycin, supporting that telomeres are particularly vulnerable to oxidative damage (102). Here, we provide evidence that telomeric DNA is prone to oxidative guanine damage than minisatellite TG repeats *in vivo*. In agreement with our findings, previous oligonucleotide-based *in vitro* studies yielded similar results (106-108). Furthermore, *in vitro* exposure to oxidants on naked DNA displayed more Fpg-sensitive lesions in telomeres than minisatellite TG repeats. These observations suggest that the nature of TTAGGG in telomeres could be the primary driving force behind the preferential accumulation of oxidative guanine damage.

Alternatively, telomere unique factors *i.e.* telomere-specific binding proteins, repeat sequences, and telomere secondary structures may influence guanine oxidation and/or repair at telomeres and in turn promote accumulation of oxidative guanine damage in telomeres. The fact that there is preferential guanine damage in telomere than non-telomeric G-rich DNA and that UV-induced damage at telomeres was more pronounced compared to other genomic regions (236) suggest that DNA damage repair at telomeres is

less effective than in non-telomeric regions. In this study, we demonstrated that acute oxidant exposure causes high incidences of Fpg-sensitive sites in TG minisatellite and telomeric DNA fragments. However, Fpg-sensitive sites were nearly undetectable in TG minisatellites whereas these lesions persist at higher level in telomeres after 6 hours of recovery time. These observations suggest that repair of oxidative DNA damage may be less effective in telomeres *in vivo*, which could be influenced by telomere associated unique factors.

α-hOGG1 is the primary glycosylase that removes 8-oxodG and me-Fapy with comparable efficiencies (141). Here, we evaluated telomere special factors (*i.e.*, telomeric DNA repeat sequences, telomeric structures or telomere binding proteins) in influencing telomeric 8-oxodG removal by α-hOGG1. Initially, we investigated the impact of telomere repeat sequences in the α-hOGG1 incision activity. The sequence-dependent repair efficiency of α-hOGG1 has been reported, even though the study was conducted using me-Fapy as the substrate (141). It shows that α-hOGG1 incision activity on me-Fapy was affected by the flanking sequences, with preference for 5'-(C/G)me-FapyC-3'. Nevertheless, α-hOGG1 incision activities on the telomeric and non-telomeric sequence contexts were similar.

Previous studies demonstrate that oxidant exposure increases 8-oxodG content in the DNA fragment containing the telomeric sequences *in vitro*. In addition, more than one guanine in GGG of telomeric are oxidized (107,108). In this study, we demonstrated that substrates containing single and triple 8-oxodG lesions were excised equally by α-hOGG1, showing no preference for either substrate. In addition, α-hOGG1 appears to

favor incising middle and 5' 8-oxodG in GGG of telomeric DNA. In agreement with our findings, a previous report showed that α-hOGG1 preferred to excise 5' me-Fapy on guanine doublets (141). It is possible that this preference could be a structurally conserved mechanism since oxidative damage induces 8-oxodG preferentially at the 5' site of 5'-GGG-3' sequence (107,108). It has been proposed that optimal DNA twisting plays an important role in lesion recognition (140). Flipping middle 8-oxodG by OGG1 may be preferred since DNA torsional rigidity near the 8-oxodG greatly affects the α-hOGG1 recognition and incision activity (140,270). In addition, it is possible that α-hOGG1 may prefer to work in a certain direction to favor 5' site incision since α-hOGG1 works in a processive mode (140). For instance, single-strand-breaks (SSBs) toward 3' of α-hOGG1 catalytic pocket hinders its incision activity, whereas no adverse effect is observed when SSB is situated at the 5' of α-hOGG1 catalytic pocket (138,139). α-hOGG1 may therefore work in 3' to 5' direction to accommodate for this possible pitfall, which could consequently result in more excision products towards 5' site 8-oxodG. α-hOGG1's preference in excising 5'- and middle 8-oxodG in GGG of telomeric DNA repeats may also explain the frequent appearance of SSBs at 5' guanine in the telomere repeats after oxidative stress (107,108).

One of the unique structural features that shape telomeres is the 3'-overhang, also known as the G-rich overhang. It is important in the t-loop formation and plays a vital part in the initiation process (3). Here, we demonstrated that α-hOGG1 was unable to efficiently excise 8-oxodG near a 3' overhang opening. Previous studies have shown that an opposing abasic site greatly reduced α-hOGG1 incision activity (137). In addition, a

SSB 3' of the catalytic pocket hinders α-hOGG1 glycosylase activity (138,139). An 8-oxodG near the 3' overhang completely lacks the complementary strand, and it is therefore possible that α-hOGG1 is significantly compromised in repairing oxidative damages in the presence of strand breaks near its active site pocket. If these base lesions are not repaired, this may pose a problem since it has been previously shown that 8-oxodG perturbs TRF1 and TRF2 from binding to telomeric DNA repeats (112), and the junction between the telomeric duplex and the 3' opening plays an important role in telomere length maintenance. For instance, TRF2 is implicated in t-loop formation by binding to the junction site (15,23). Disruption of TRF2 binding to the junction region can lead to truncation of 3' overhang, telomere uncapping, and telomere fusion mediated by nonhomologous end-joining (29,30,33).

The t-loop helps to protect the ends of linear chromosome from being recognized as broken DNA (3). The d-loop, as a result of t-loop formation, is the secondary structure formed when the tip of G-rich strand binds to C-rich strand via strand invasion (3). Our data showed that 8-oxodG in a d-loop can be excised by α-hOGG1 with differential efficiency, depending upon its position. Similarly to the observation on 8-oxodG containing oligonucleotides with 3' overhang, embedded 8-oxodG in the d-loop was less effectively excised by α-hOGG1 when it was close to the terminal end. Although α-hOGG1 is not active on single-stranded substrates, it may excise 8-oxodG when the 3' overhang is formed in a d-loop with double-stranded telomere DNA. This incision activity may play an important part in telomere length maintenance since it was

previously shown that 8-oxodG at single telomeric nucleotides disrupt telomerase activity (111).

Efficient repair prior to DNA replication is critical in preventing 8-oxodG mutagenesis (122). In this study, we showed that 8-oxodG at telomeric fork opening led to inefficient α-hOGG1 excision activity. In agreement with this finding, a previous study shows that α-hOGG1 can excise fork substrates and increase the incision efficiencies by positioning the 8-oxodG up to 3 nucleotides away from the opening (139). The fact that a SSB 3' of the catalytic pocket in α-hOGG1 hinders its incision activity also supports this notion (138). Oxidative guanine damage, 8-oxodG, disrupts binding of shelterin proteins (112), which has been shown to be involved for proper replication at telomeres (221,222). It is possible that oxidative DNA damage can have undesired consequences during replication if not readily repaired. Furthermore, adenine will be incorrectly incorporated if 8-oxodG is not promptly repaired, (122), which can impede the binding of TRF1 and TRF2 to telomeres, consequently affecting their regulation on telomere length regulation and telomere capping (112).

Shelterin caps the ends of chromosomes to prevent from spurious DNA repair. A previous study has shown that over-expression of TRF2 leads to inefficient SSB repair at telomeres (266). It is possible that TRF1 and TRF2 may hinder the access of BER proteins to repair base lesions. However, α-hOGG1 can efficiently excise 8-oxodG in the telomere oligonucleotides pre-bound with TRF1 or TRF2, suggesting that shelterin does not inhibit the BER function in telomeres. Interestingly, TRF1, but not TRF2, mildly stimulated α-hOGG1 incision activity. In addition, this stimulation was observed on DNA

substrates that are unable to bind TRF1; excluding the possibility that TRF1 may recruit α-hOGG1 to the damaged sites. It is still unclear how TRF1 weakly promotes α-hOGG1 glycosylase activity at telomere.

In this study, we demonstrate that telomeres are prone to the accumulation of oxidative guanine lesions and 8-oxodG removal by OGG1 could be affected by its position in different telomere structures (*e.g.*, fork-opening, 3'- overhang, and d-loop). Telomere shortening has been linked to human aging, bone marrow failure syndromes and cancer development (271), and oxidative DNA damage is a contributing factor (272). We recently demonstrated that telomere shortening occurs in *Ogg1* deficient mice experiencing high degrees of oxidative stress (262). Telomere guanine damage associated telomere attrition may thus contribute to premature aging and cancer formation.

References

1. Greider, C. W., and Blackburn, E. H. (1996) *Sci Am* **274**(2), 92-97
2. Blackburn, E. H. (2001) *Cell* **106**(6), 661-673
3. de Lange, T. (2005) *Genes Dev* **19**(18), 2100-2110
4. Longhese, M. P. (2008) *Genes Dev* **22**(2), 125-140
5. Gilley, D., Herbert, B. S., Huda, N., Tanaka, H., and Reed, T. (2008) *Mech Ageing Dev* **129**(1-2), 27-34
6. Kappei, D., and Londono-Vallejo, J. A. (2008) *Mech Ageing Dev* **129**(1-2), 17-26
7. Savage, S. A., and Alter, B. P. (2008) *Mech Ageing Dev* **129**(1-2), 35-47
8. Ye, J. Z., Donigian, J. R., van Overbeek, M., Loayza, D., Luo, Y., Krutchinsky, A. N., Chait, B. T., and de Lange, T. (2004) *J Biol Chem* **279**(45), 47264-47271
9. Giannone, R. J., McDonald, W. H., Hurst, G. B., Huang, Y., Wu, J., Liu, Y., and Wang, Y. (2007) *Biotechniques* **43**(3), 296, 298, 300 passim
10. de Lange, T. (2001) *Science* **292**(5519), 1075-1076
11. Cooper, J. P., Watanabe, Y., and Nurse, P. (1998) *Nature* **392**(6678), 828-831
12. Chikashige, Y., and Hiraoka, Y. (2001) *Curr Biol* **11**(20), 1618-1623
13. Lu, J., and Liu, Y. (2009) *Embo J* **29**(2), 398-409
14. Liu, D., O'Connor, M. S., Qin, J., and Songyang, Z. (2004) *J Biol Chem* **279**(49), 51338-51342
15. Court, R., Chapman, L., Fairall, L., and Rhodes, D. (2005) *EMBO Rep* **6**(1), 39-45
16. Ye, J. Z., Hockemeyer, D., Krutchinsky, A. N., Loayza, D., Hooper, S. M., Chait, B. T., and de Lange, T. (2004) *Genes Dev* **18**(14), 1649-1654
17. Houghtaling, B. R., Cuttonaro, L., Chang, W., and Smith, S. (2004) *Curr Biol* **14**(18), 1621-1631
18. Sfeir, A., Kabir, S., van Overbeek, M., Celli, G. B., and de Lange, T. (2010) *Science* **327**(5973), 1657-1661
19. Li, B., Oestreich, S., and de Lange, T. (2000) *Cell* **101**(5), 471-483
20. Barrientos, K. S., Kendellen, M. F., Freibaum, B. D., Armbruster, B. N., Etheridge, K. T., and Counter, C. M. (2008) *Molecular and cellular biology* **28**(17), 5251-5264
21. Loayza, D., Parsons, H., Donigian, J., Hoke, K., and de Lange, T. (2004) *J Biol Chem* **279**(13), 13241-13248
22. Griffith, J. D., Comeau, L., Rosenfield, S., Stansel, R. M., Bianchi, A., Moss, H., and de Lange, T. (1999) *Cell* **97**(4), 503-514
23. Stansel, R. M., de Lange, T., and Griffith, J. D. (2001) *Embo J* **20**(19), 5532-5540
24. Bianchi, A., Smith, S., Chong, L., Elias, P., and de Lange, T. (1997) *Embo J* **16**(7), 1785-1794
25. Bianchi, A., Stansel, R. M., Fairall, L., Griffith, J. D., Rhodes, D., and de Lange, T. (1999) *Embo J* **18**(20), 5735-5744
26. Kim, S. H., Beausejour, C., Davalos, A. R., Kaminker, P., Heo, S. J., and Campisi, J. (2004) *J Biol Chem* **279**(42), 43799-43804
27. Kim, S. H., Han, S., You, Y. H., Chen, D. J., and Campisi, J. (2003) *EMBO Rep* **4**(7), 685-691
28. van Steensel, B., Smogorzewska, A., and de Lange, T. (1998) *Cell* **92**(3), 401-413

29. Zhu, X. D., Niedernhofer, L., Kuster, B., Mann, M., Hoeijmakers, J. H., and de Lange, T. (2003) *Mol Cell* **12**(6), 1489-1498
30. Deng, Y., Guo, X., Ferguson, D. O., and Chang, S. (2009) *Nature* **460**(7257), 914-918
31. Hockemeyer, D., Sfeir, A. J., Shay, J. W., Wright, W. E., and de Lange, T. (2005) *Embo J* **24**(14), 2667-2678
32. Lei, M., Podell, E. R., and Cech, T. R. (2004) *Nat Struct Mol Biol* **11**(12), 1223-1229
33. Yang, Q., Zheng, Y. L., and Harris, C. C. (2005) *Molecular and cellular biology* **25**(3), 1070-1080
34. Sfeir, A. J., Chai, W., Shay, J. W., and Wright, W. E. (2005) *Mol Cell* **18**(1), 131-138
35. Marcand, S., Brevet, V., and Gilson, E. (1999) *Embo J* **18**(12), 3509-3519
36. Loayza, D., and De Lange, T. (2003) *Nature* **423**(6943), 1013-1018
37. Kelleher, C., Kurth, I., and Lingner, J. (2005) *Molecular and cellular biology* **25**(2), 808-818
38. Marcand, S., Gilson, E., and Shore, D. (1997) *Science* **275**(5302), 986-990
39. Ancelin, K., Brunori, M., Bauwens, S., Koering, C. E., Brun, C., Ricoul, M., Pommier, J. P., Sabatier, L., and Gilson, E. (2002) *Molecular and cellular biology* **22**(10), 3474-3487
40. Zhang, P., Furukawa, K., Opresko, P. L., Xu, X., Bohr, V. A., and Mattson, M. P. (2006) *J Neurochem* **97**(2), 567-581
41. Celli, G. B., and de Lange, T. (2005) *Nat Cell Biol* **7**(7), 712-718
42. Karlseder, J., Broccoli, D., Dai, Y., Hardy, S., and de Lange, T. (1999) *Science* **283**(5406), 1321-1325
43. Takai, H., Smogorzewska, A., and de Lange, T. (2003) *Curr Biol* **13**(17), 1549-1556
44. Bakkenist, C. J., and Kastan, M. B. (2003) *Nature* **421**(6922), 499-506
45. Karlseder, J., Hoke, K., Mirzoeva, O. K., Bakkenist, C., Kastan, M. B., Petrini, J. H., and de Lange, T. (2004) *PLoS Biol* **2**(8), E240
46. Cesare, A. J., and Griffith, J. D. (2004) *Molecular and cellular biology* **24**(22), 9948-9957
47. Poulet, A., Buisson, R., Faivre-Moskalenko, C., Koelblen, M., Amiard, S., Montel, F., Cuesta-Lopez, S., Bornet, O., Guerlesquin, F., Godet, T., Moukhtar, J., Argoul, F., Declais, A. C., Lilley, D. M., Ip, S. C., West, S. C., Gilson, E., and Giraud-Panis, M. J. (2009) *Embo J* **28**(6), 641-651
48. Nora, G. J., Buncher, N. A., and Opresko, P. L. (2010) *Nucleic acids research* **2010**, 9
49. Wang, R. C., Smogorzewska, A., and de Lange, T. (2004) *Cell* **119**(3), 355-368
50. Bailey, S. M., Brenneman, M. A., and Goodwin, E. H. (2004) *Nucleic acids research* **32**(12), 3743-3751
51. San Filippo, J., Sung, P., and Klein, H. (2008) *Annual review of biochemistry*
52. Cesare, A. J., and Reddel, R. R. (2008) *Mech Ageing Dev* **129**(1-2), 99-108
53. Shore, D., and Bianchi, A. (2009) *Embo J* **23**, 23

54. Smogorzewska, A., and de Lange, T. (2004) *Annual review of biochemistry* **73**, 177-208
55. Collado, M., Blasco, M. A., and Serrano, M. (2007) *Cell* **130**(2), 223-233
56. Yeager, T. R., and Reddel, R. R. (1999) *Current opinion in biotechnology* **10**(5), 465-469
57. Shay, J. W. (1997) *Journal of cellular physiology* **173**(2), 266-270
58. Cerone, M. A., Autexier, C., Londono-Vallejo, J. A., and Bacchetti, S. (2005) *Oncogene* **24**(53), 7893-7901
59. Bryan, T. M., Englezou, A., Gupta, J., Bacchetti, S., and Reddel, R. R. (1995) *Embo J* **14**(17), 4240-4248
60. Henson, J. D., Neumann, A. A., Yeager, T. R., and Reddel, R. R. (2002) *Oncogene* **21**(4), 598-610
61. Fasching, C. L., Neumann, A. A., Muntoni, A., Yeager, T. R., and Reddel, R. R. (2007) *Cancer research* **67**(15), 7072-7077
62. Tokutake, Y., Matsumoto, T., Watanabe, T., Maeda, S., Tahara, H., Sakamoto, S., Niida, H., Sugimoto, M., Ide, T., and Furuichi, Y. (1998) *Biochemical and biophysical research communications* **247**(3), 765-772
63. Yeager, T. R., Neumann, A. A., Englezou, A., Huschtscha, L. I., Noble, J. R., and Reddel, R. R. (1999) *Cancer research* **59**(17), 4175-4179
64. Wu, G., Lee, W. H., and Chen, P. L. (2000) *J Biol Chem* **275**(39), 30618-30622
65. Grobelny, J. V., Godwin, A. K., and Broccoli, D. (2000) *Journal of cell science* **113 Pt 24**, 4577-4585
66. Cesare, A. J., and Reddel, R. R. (2010) *Nature reviews* **2010**, 30
67. Dunham, M. A., Neumann, A. A., Fasching, C. L., and Reddel, R. R. (2000) *Nature genetics* **26**(4), 447-450
68. Bechter, O. E., Shay, J. W., and Wright, W. E. (2004) *Cell cycle (Georgetown, Tex* **3**(5), 547-549
69. Londono-Vallejo, J. A., Der-Sarkissian, H., Cazes, L., Bacchetti, S., and Reddel, R. R. (2004) *Cancer research* **64**(7), 2324-2327
70. Jiang, W. Q., Zhong, Z. H., Henson, J. D., Neumann, A. A., Chang, A. C., and Reddel, R. R. (2005) *Molecular and cellular biology* **25**(7), 2708-2721
71. Potts, P. R., and Yu, H. (2007) *Nat Struct Mol Biol* **14**(7), 581-590
72. Harley, C. B., Futcher, A. B., and Greider, C. W. (1990) *Nature* **345**(6274), 458-460
73. Shay, J. W., and Wright, W. E. (2002) *Cancer cell* **2**(4), 257-265
74. Lin, S. Y., and Elledge, S. J. (2003) *Cell* **113**(7), 881-889
75. Oh, H., Taffet, G. E., Youker, K. A., Entman, M. L., Overbeek, P. A., Michael, L. H., and Schneider, M. D. (2001) *Proceedings of the National Academy of Sciences of the United States of America* **98**(18), 10308-10313
76. Wiemann, S. U., Satyanarayana, A., Tsahuridu, M., Tillmann, H. L., Zender, L., Klempnauer, J., Flemming, P., Franco, S., Blasco, M. A., Manns, M. P., and Rudolph, K. L. (2002) *Faseb J* **16**(9), 935-942
77. Samani, N. J., Boultby, R., Butler, R., Thompson, J. R., and Goodall, A. H. (2001) *Lancet* **358**(9280), 472-473

78. Cawthon, R. M., Smith, K. R., O'Brien, E., Sivatchenko, A., and Kerber, R. A. (2003) *Lancet* **361**(9355), 393-395
79. Mitchell, J. R., Wood, E., and Collins, K. (1999) *Nature* **402**(6761), 551-555
80. Vulliamy, T. J., Marrone, A., Knight, S. W., Walne, A., Mason, P. J., and Dokal, I. (2006) *Blood* **107**(7), 2680-2685
81. Yamaguchi, H., Calado, R. T., Ly, H., Kajigaya, S., Baerlocher, G. M., Chanock, S. J., Lansdorp, P. M., and Young, N. S. (2005) *The New England journal of medicine* **352**(14), 1413-1424
82. Armanios, M. Y., Chen, J. J., Cogan, J. D., Alder, J. K., Ingersoll, R. G., Markin, C., Lawson, W. E., Xie, M., Vulto, I., Phillips, J. A., 3rd, Lansdorp, P. M., Greider, C. W., and Loyd, J. E. (2007) *The New England journal of medicine* **356**(13), 1317-1326
83. Blasco, M. A. (2005) *Nature reviews* **6**(8), 611-622
84. Blasco, M. A., Funk, W., Villeponteau, B., and Greider, C. W. (1995) *Science* **269**(5228), 1267-1270
85. Blasco, M. A., Lee, H. W., Hande, M. P., Samper, E., Lansdorp, P. M., DePinho, R. A., and Greider, C. W. (1997) *Cell* **91**(1), 25-34
86. Yuan, X., Ishibashi, S., Hatakeyama, S., Saito, M., Nakayama, J., Nikaido, R., Haruyama, T., Watanabe, Y., Iwata, H., Iida, M., Sugimura, H., Yamada, N., and Ishikawa, F. (1999) *Genes Cells* **4**(10), 563-572
87. Liu, Y., Snow, B. E., Hande, M. P., Yeung, D., Erdmann, N. J., Wakeham, A., Itie, A., Siderovski, D. P., Lansdorp, P. M., Robinson, M. O., and Harrington, L. (2000) *Curr Biol* **10**(22), 1459-1462
88. Blasco, M. A. (2005) *Embo J* **24**(6), 1095-1103
89. Herrera, E., Samper, E., Martin-Caballero, J., Flores, J. M., Lee, H. W., and Blasco, M. A. (1999) *Embo J* **18**(11), 2950-2960
90. Leri, A., Franco, S., Zacheo, A., Barlucchi, L., Chimenti, S., Limana, F., Nadal-Ginard, B., Kajstura, J., Anversa, P., and Blasco, M. A. (2003) *Embo J* **22**(1), 131-139
91. Samper, E., Fernandez, P., Eguia, R., Martin-Rivera, L., Bernad, A., Blasco, M. A., and Aracil, M. (2002) *Blood* **99**(8), 2767-2775
92. Gonzalez-Suarez, E., Samper, E., Flores, J. M., and Blasco, M. A. (2000) *Nature genetics* **26**(1), 114-117
93. Rudolph, K. L., Millard, M., Bosenberg, M. W., and DePinho, R. A. (2001) *Nature genetics* **28**(2), 155-159
94. Greenberg, R. A., Chin, L., Femino, A., Lee, K. H., Gottlieb, G. J., Singer, R. H., Greider, C. W., and DePinho, R. A. (1999) *Cell* **97**(4), 515-525
95. Franco, S., van de Vrugt, H. J., Fernandez, P., Aracil, M., Arwert, F., and Blasco, M. A. (2004) *Blood* **104**(13), 3927-3935
96. Lebel, M., Spillare, E. A., Harris, C. C., and Leder, P. (1999) *J Biol Chem* **274**(53), 37795-37799
97. Chester, N., Kuo, F., Kozak, C., O'Hara, C. D., and Leder, P. (1998) *Genes Dev* **12**(21), 3382-3393

98. Chang, S., Multani, A. S., Cabrera, N. G., Naylor, M. L., Laud, P., Lombard, D., Pathak, S., Guarente, L., and DePinho, R. A. (2004) *Nature genetics* **36**(8), 877-882
99. Du, X., Shen, J., Kugan, N., Furth, E. E., Lombard, D. B., Cheung, C., Pak, S., Luo, G., Pignolo, R. J., DePinho, R. A., Guarente, L., and Johnson, F. B. (2004) *Molecular and cellular biology* **24**(19), 8437-8446
100. Wong, K. K., Maser, R. S., Bachoo, R. M., Menon, J., Carrasco, D. R., Gu, Y., Alt, F. W., and DePinho, R. A. (2003) *Nature* **421**(6923), 643-648
101. von Zglinicki, T., Petrie, J., and Kirkwood, T. B. (2003) *Nature biotechnology* **21**(3), 229-230
102. Rubio, M. A., Davalos, A. R., and Campisi, J. (2004) *Experimental cell research* **298**(1), 17-27
103. Parrinello, S., Samper, E., Krtolica, A., Goldstein, J., Melov, S., and Campisi, J. (2003) *Nat Cell Biol* **5**(8), 741-747
104. Espejel, S., and Blasco, M. A. (2002) *Experimental cell research* **276**(2), 242-248
105. von Zglinicki, T., Pilger, R., and Sitte, N. (2000) *Free radical biology & medicine* **28**(1), 64-74
106. Henle, E. S., Han, Z., Tang, N., Rai, P., Luo, Y., and Linn, S. (1999) *J Biol Chem* **274**(2), 962-971
107. Kawanishi, S., Oikawa, S., Murata, M., Tsukitome, H., and Saito, I. (1999) *Biochemistry* **38**(51), 16733-16739
108. Oikawa, S., and Kawanishi, S. (1999) *FEBS Lett* **453**(3), 365-368
109. Petersen, S., Saretzki, G., and von Zglinicki, T. (1998) *Experimental cell research* **239**(1), 152-160
110. Sitte, N., Saretzki, G., and von Zglinicki, T. (1998) *Free radical biology & medicine* **24**(6), 885-893
111. Szalai, V. A., Singer, M. J., and Thorp, H. H. (2002) *J Am Chem Soc* **124**(8), 1625-1631
112. Opresko, P. L., Fan, J., Danzy, S., Wilson, D. M., 3rd, and Bohr, V. A. (2005) *Nucleic acids research* **33**(4), 1230-1239
113. Maynard, S., Schurman, S. H., Harboe, C., de Souza-Pinto, N. C., and Bohr, V. A. (2009) *Carcinogenesis* **30**(1), 2-10
114. Hakem, R. (2008) *Embo J* **27**(4), 589-605
115. Memisoglu, A., and Samson, L. (2000) *Mutat Res* **451**(1-2), 39-51
116. Mol, C. D., Parikh, S. S., Putnam, C. D., Lo, T. P., and Tainer, J. A. (1999) *Annu Rev Biophys Biomol Struct* **28**, 101-128
117. Loeb, L. A. (1985) *Cell* **40**(3), 483-484
118. Hazra, T. K., Hill, J. W., Izumi, T., and Mitra, S. (2001) *Prog Nucleic Acid Res Mol Biol* **68**, 193-205
119. Hegde, M. L., Hazra, T. K., and Mitra, S. (2008) *Cell Res* **18**(1), 27-47
120. Shibutani, S., Takeshita, M., and Grollman, A. P. (1991) *Nature* **349**(6308), 431-434
121. Brieba, L. G., Eichman, B. F., Kokoska, R. J., Doublie, S., Kunkel, T. A., and Ellenberger, T. (2004) *Embo J* **23**(17), 3452-3461

122. Neeley, W. L., and Essigmann, J. M. (2006) *Chem Res Toxicol* **19**(4), 491-505
123. Lindahl, T. (1993) *Nature* **362**(6422), 709-715
124. Klaunig, J. E., and Kamendulis, L. M. (2004) *Annu Rev Pharmacol Toxicol* **44**, 239-267
125. Boiteux, S., and Radicella, J. P. (2000) *Arch Biochem Biophys* **377**(1), 1-8
126. Thayer, M. M., Ahern, H., Xing, D., Cunningham, R. P., and Tainer, J. A. (1995) *Embo J* **14**(16), 4108-4120
127. Arai, K., Morishita, K., Shinmura, K., Kohno, T., Kim, S. R., Nohmi, T., Taniwaki, M., Ohwada, S., and Yokota, J. (1997) *Oncogene* **14**(23), 2857-2861
128. Nishioka, K., Ohtsubo, T., Oda, H., Fujiwara, T., Kang, D., Sugimachi, K., and Nakabeppu, Y. (1999) *Mol Biol Cell* **10**(5), 1637-1652
129. Takao, M., Aburatani, H., Kobayashi, K., and Yasui, A. (1998) *Nucleic acids research* **26**(12), 2917-2922
130. Croteau, D. L., ap Rhys, C. M., Hudson, E. K., Dianov, G. L., Hansford, R. G., and Bohr, V. A. (1997) *J Biol Chem* **272**(43), 27338-27344
131. Rosenquist, T. A., Zharkov, D. O., and Grollman, A. P. (1997) *Proceedings of the National Academy of Sciences of the United States of America* **94**(14), 7429-7434
132. Radicella, J. P., Dherin, C., Desmaze, C., Fox, M. S., and Boiteux, S. (1997) *Proceedings of the National Academy of Sciences of the United States of America* **94**(15), 8010-8015
133. Dhenaut, A., Boiteux, S., and Radicella, J. P. (2000) *Mutat Res* **461**(2), 109-118
134. Roldan-Arjona, T., Wei, Y. F., Carter, K. C., Klungland, A., Anselmino, C., Wang, R. P., Augustus, M., and Lindahl, T. (1997) *Proceedings of the National Academy of Sciences of the United States of America* **94**(15), 8016-8020
135. Bjoras, M., Seeberg, E., Luna, L., Pearl, L. H., and Barrett, T. E. (2002) *J Mol Biol* **317**(2), 171-177
136. Bruner, S. D., Norman, D. P., and Verdine, G. L. (2000) *Nature* **403**(6772), 859-866
137. Barone, F., Dogliotti, E., Cellai, L., Giordano, C., Bjoras, M., and Mazzei, F. (2003) *Nucleic acids research* **31**(7), 1897-1903
138. Rogacheva, M. V., Saparbaev, M. K., Afanasov, I. M., and Kuznetsova, S. A. (2005) *Biochimie* **87**(12), 1079-1088
139. Parsons, J. L., Zharkov, D. O., and Dianov, G. L. (2005) *Nucleic acids research* **33**(15), 4849-4856
140. Sidorenko, V. S., and Zharkov, D. O. (2008) *Biochemistry* **47**(34), 8970-8976
141. Asagoshi, K., Yamada, T., Terato, H., Ohyama, Y., Monden, Y., Arai, T., Nishimura, S., Aburatani, H., Lindahl, T., and Ide, H. (2000) *J Biol Chem* **275**(7), 4956-4964
142. Fromme, J. C., Banerjee, A., Huang, S. J., and Verdine, G. L. (2004) *Nature* **427**(6975), 652-656
143. Minowa, O., Arai, T., Hirano, M., Monden, Y., Nakai, S., Fukuda, M., Itoh, M., Takano, H., Hippou, Y., Aburatani, H., Masumura, K., Nohmi, T., Nishimura, S., and Noda, T. (2000) *Proceedings of the National Academy of Sciences of the United States of America* **97**(8), 4156-4161

144. Klungland, A., Rosewell, I., Hollenbach, S., Larsen, E., Daly, G., Epe, B., Seeberg, E., Lindahl, T., and Barnes, D. E. (1999) *Proceedings of the National Academy of Sciences of the United States of America* **96**(23), 13300-13305
145. Sakumi, K., Tominaga, Y., Furuichi, M., Xu, P., Tsuzuki, T., Sekiguchi, M., and Nakabeppu, Y. (2003) *Cancer research* **63**(5), 902-905
146. Osterod, M., Hollenbach, S., Hengstler, J. G., Barnes, D. E., Lindahl, T., and Epe, B. (2001) *Carcinogenesis* **22**(9), 1459-1463
147. Xie, Y., Yang, H., Cunanan, C., Okamoto, K., Shibata, D., Pan, J., Barnes, D. E., Lindahl, T., McIlhatton, M., Fishel, R., and Miller, J. H. (2004) *Cancer research* **64**(9), 3096-3102
148. Dokal, I. (2006) *Br Med Bull* **77-78**, 37-53
149. Shimamura, A. (2006) *Hematology Am Soc Hematol Educ Program*, 63-71
150. Pang, Q., and Andreassen, P. R. (2009) *Mutat Res* **668**(1-2), 42-53
151. Auerbach, A. D. (1993) *Exp Hematol* **21**(6), 731-733
152. Wang, W. (2007) *Nature reviews* **8**(10), 735-748
153. Meetei, A. R., Levitus, M., Xue, Y., Medhurst, A. L., Zwaan, M., Ling, C., Rooimans, M. A., Bier, P., Hoatlin, M., Pals, G., de Winter, J. P., Wang, W., and Joenje, H. (2004) *Nature genetics* **36**(11), 1219-1224
154. Kennedy, R. D., and D'Andrea, A. D. (2005) *Genes Dev* **19**(24), 2925-2940
155. Meetei, A. R., Medhurst, A. L., Ling, C., Xue, Y., Singh, T. R., Bier, P., Steltenpool, J., Stone, S., Dokal, I., Mathew, C. G., Hoatlin, M., Joenje, H., de Winter, J. P., and Wang, W. (2005) *Nature genetics* **37**(9), 958-963
156. Matsushita, N., Kitao, H., Ishiai, M., Nagashima, N., Hirano, S., Okawa, K., Ohta, T., Yu, D. S., McHugh, P. J., Hickson, I. D., Venkitaraman, A. R., Kurumizaka, H., and Takata, M. (2005) *Mol Cell* **19**(6), 841-847
157. Wang, X., Andreassen, P. R., and D'Andrea, A. D. (2004) *Molecular and cellular biology* **24**(13), 5850-5862
158. Niedzwiedz, W., Mosedale, G., Johnson, M., Ong, C. Y., Pace, P., and Patel, K. J. (2004) *Mol Cell* **15**(4), 607-620
159. Nakanishi, K., Yang, Y. G., Pierce, A. J., Taniguchi, T., Digweed, M., D'Andrea, A. D., Wang, Z. Q., and Jasin, M. (2005) *Proceedings of the National Academy of Sciences of the United States of America* **102**(4), 1110-1115
160. Shen, X., Jun, S., O'Neal, L. E., Sonoda, E., Bemark, M., Sale, J. E., and Li, L. (2006) *J Biol Chem* **281**(20), 13869-13872
161. Saadatzadeh, M. R., Bijangi-Vishehsaraei, K., Hong, P., Bergmann, H., and Haneline, L. S. (2004) *J Biol Chem* **279**(16), 16805-16812
162. Uziel, O., Reshef, H., Ravid, A., Fabian, I., Halperin, D., Ram, R., Bakhanashvili, M., Nordenberg, J., and Lahav, M. (2008) *Br J Haematol* **142**(1), 82-93
163. Carreau, M., Alon, N., Bosnoyan-Collins, L., Joenje, H., and Buchwald, M. (1999) *Mutat Res* **435**(1), 103-109
164. Palom, Y., Suresh Kumar, G., Tang, L. Q., Paz, M. M., Musser, S. M., Rockwell, S., and Tomasz, M. (2002) *Chem Res Toxicol* **15**(11), 1398-1406
165. Povirk, L. F., and Shuker, D. E. (1994) *Mutat Res* **318**(3), 205-226
166. Calado, R. T., and Young, N. S. (2008) *Blood* **111**(9), 4446-4455

167. Adelfalk, C., Lorenz, M., Serra, V., von Zglinicki, T., Hirsch-Kauffmann, M., and Schweiger, M. (2001) *FEBS Lett* **506**(1), 22-26
168. Ball, S. E., Gibson, F. M., Rizzo, S., Tooze, J. A., Marsh, J. C., and Gordon-Smith, E. C. (1998) *Blood* **91**(10), 3582-3592
169. Spardy, N., Duensing, A., Hoskins, E. E., Wells, S. I., and Duensing, S. (2008) *Cancer research* **68**(23), 9954-9963
170. Fan, Q., Zhang, F., Barrett, B., Ren, K., and Andreassen, P. R. (2009) *Nucleic acids research* **37**(6), 1740-1754
171. Patel, K. J., and Joenje, H. (2007) *DNA Repair (Amst)* **6**(7), 885-890
172. Strathdee, C. A., Gavish, H., Shannon, W. R., and Buchwald, M. (1992) *Nature* **358**(6385), 434
173. Hirano, S., Yamamoto, K., Ishiai, M., Yamazoe, M., Seki, M., Matsushita, N., Ohzeki, M., Yamashita, Y. M., Arakawa, H., Buerstedde, J. M., Enomoto, T., Takeda, S., Thompson, L. H., and Takata, M. (2005) *Embo J* **24**(2), 418-427
174. Meetei, A. R., Sechi, S., Wallisch, M., Yang, D., Young, M. K., Joenje, H., Hoatlin, M. E., and Wang, W. (2003) *Molecular and cellular biology* **23**(10), 3417-3426
175. Hadjur, S., Ung, K., Wadsworth, L., Dimmick, J., Rajcan-Separovic, E., Scott, R. W., Buchwald, M., and Jirik, F. R. (2001) *Blood* **98**(4), 1003-1011
176. Kruyt, F. A., Hoshino, T., Liu, J. M., Joseph, P., Jaiswal, A. K., and Youssoufian, H. (1998) *Blood* **92**(9), 3050-3056
177. Cumming, R. C., Lightfoot, J., Beard, K., Youssoufian, H., O'Brien, P. J., and Buchwald, M. (2001) *Nat Med* **7**(7), 814-820
178. Rani, R., Li, J., and Pang, Q. (2008) *Cancer research* **68**(23), 9693-9702
179. Liebetrau, W., Budde, A., Savoia, A., Grummt, F., and Hoehn, H. (1997) *Hum Mol Genet* **6**(2), 277-283
180. Liebetrau, W., Runger, T. M., Mehling, B. E., Poot, M., and Hoehn, H. (1997) *Mutagenesis* **12**(2), 69-77
181. Freie, B., Li, X., Ciccone, S. L., Nawa, K., Cooper, S., Vogelweid, C., Schantz, L., Haneline, L. S., Orazi, A., Broxmeyer, H. E., Lee, S. H., and Clapp, D. W. (2003) *Blood* **102**(12), 4146-4152
182. Greider, C. W. (2006) *Cold Spring Harb Symp Quant Biol* **71**, 225-229
183. d'Adda di Fagagna, F., Teo, S. H., and Jackson, S. P. (2004) *Genes Dev* **18**(15), 1781-1799
184. Erdmann, N., Liu, Y., and Harrington, L. (2004) *Proceedings of the National Academy of Sciences of the United States of America* **101**(16), 6080-6085
185. Lee, H. W., Blasco, M. A., Gottlieb, G. J., Horner, J. W., 2nd, Greider, C. W., and DePinho, R. A. (1998) *Nature* **392**(6676), 569-574
186. Rudolph, K. L., Chang, S., Lee, H. W., Blasco, M., Gottlieb, G. J., Greider, C., and DePinho, R. A. (1999) *Cell* **96**(5), 701-712
187. Hathcock, K. S., Hemann, M. T., Opperman, K. K., Strong, M. A., Greider, C. W., and Hodes, R. J. (2002) *Proceedings of the National Academy of Sciences of the United States of America* **99**(6), 3591-3596

188. Hao, L. Y., Armanios, M., Strong, M. A., Karim, B., Feldser, D. M., Huso, D., and Greider, C. W. (2005) *Cell* **123**(6), 1121-1131
189. Leteurtre, F., Li, X., Guardiola, P., Le Roux, G., Sergere, J. C., Richard, P., Carosella, E. D., and Gluckman, E. (1999) *Br J Haematol* **105**(4), 883-893
190. Hanson, H., Mathew, C. G., Docherty, Z., and Mackie Ogilvie, C. (2001) *Cytogenetics and cell genetics* **93**(3-4), 203-206
191. Callen, E., Samper, E., Ramirez, M. J., Creus, A., Marcos, R., Ortega, J. J., Olive, T., Badell, I., Blasco, M. A., and Surralles, J. (2002) *Hum Mol Genet* **11**(4), 439-444
192. Alter, B. P., Baerlocher, G. M., Savage, S. A., Chanock, S. J., Weksler, B. B., Willner, J. P., Peters, J. A., Giri, N., and Lansdorp, P. M. (2007) *Blood* **110**(5), 1439-1447
193. Wang, Y., Giannone, R. J., and Liu, Y. (2005) *Cell cycle (Georgetown, Tex* **4**(10), 1320-1322
194. Wang, Y., Erdmann, N., Giannone, R. J., Wu, J., Gomez, M., and Liu, Y. (2005) *Proceedings of the National Academy of Sciences of the United States of America* **102**(29), 10256-10260
195. Morrish, T. A., and Greider, C. W. (2009) *PLoS genetics* **5**(1), e1000357
196. Laud, P. R., Multani, A. S., Bailey, S. M., Wu, L., Ma, J., Kingsley, C., Lebel, M., Pathak, S., DePinho, R. A., and Chang, S. (2005) *Genes Dev* **19**(21), 2560-2570
197. Celli, G. B., Denchi, E. L., and de Lange, T. (2006) *Nat Cell Biol* **8**(8), 885-890
198. Wu, L., Multani, A. S., He, H., Cosme-Blanco, W., Deng, Y., Deng, J. M., Bachilo, O., Pathak, S., Tahara, H., Bailey, S. M., Deng, Y., Behringer, R. R., and Chang, S. (2006) *Cell* **126**(1), 49-62
199. He, H., Multani, A. S., Cosme-Blanco, W., Tahara, H., Ma, J., Pathak, S., Deng, Y., and Chang, S. (2006) *Embo J* **25**(21), 5180-5190
200. Benetti, R., Gonzalo, S., Jaco, I., Schotta, G., Klatt, P., Jenuwein, T., and Blasco, M. A. (2007) *The Journal of cell biology* **178**(6), 925-936
201. Ameziane, N., Errami, A., Leveille, F., Fontaine, C., de Vries, Y., van Spaendonk, R. M., de Winter, J. P., Pals, G., and Joenje, H. (2008) *Human mutation* **29**(1), 159-166
202. Bridge, W. L., Vandenberg, C. J., Franklin, R. J., and Hiom, K. (2005) *Nature genetics* **37**(9), 953-957
203. Hemann, M. T., and Greider, C. W. (2000) *Nucleic acids research* **28**(22), 4474-4478
204. Blasco, M. A. (2007) *Nature chemical biology* **3**(10), 640-649
205. Chen, M., Tomkins, D. J., Auerbach, W., McKerlie, C., Youssoufian, H., Liu, L., Gan, O., Carreau, M., Auerbach, A., Groves, T., Guidos, C. J., Freedman, M. H., Cross, J., Percy, D. H., Dick, J. E., Joyner, A. L., and Buchwald, M. (1996) *Nature genetics* **12**(4), 448-451
206. Haneline, L. S., Gobbett, T. A., Ramani, R., Carreau, M., Buchwald, M., Yoder, M. C., and Clapp, D. W. (1999) *Blood* **94**(1), 1-8
207. Haneline, L. S., Li, X., Ciccone, S. L., Hong, P., Yang, Y., Broxmeyer, H. E., Lee, S. H., Orazi, A., Srour, E. F., and Clapp, D. W. (2003) *Blood* **101**(4), 1299-1307

208. Haneline, L. S., Broxmeyer, H. E., Cooper, S., Hangoc, G., Carreau, M., Buchwald, M., and Clapp, D. W. (1998) *Blood* **91**(11), 4092-4098
209. Li, X., Plett, P. A., Yang, Y., Hong, P., Freie, B., Srour, E. F., Orschell, C. M., Clapp, D. W., and Haneline, L. S. (2003) *Blood* **102**(6), 2081-2084
210. Rufer, N., Dragowska, W., Thornbury, G., Roosnek, E., and Lansdorp, P. M. (1998) *Nature biotechnology* **16**(8), 743-747
211. Zijlmans, J. M., Martens, U. M., Poon, S. S., Raap, A. K., Tanke, H. J., Ward, R. K., and Lansdorp, P. M. (1997) *Proceedings of the National Academy of Sciences of the United States of America* **94**(14), 7423-7428
212. Gomez, M., Wu, J., Schreiber, V., Dunlap, J., Dantzer, F., Wang, Y., and Liu, Y. (2006) *Mol Biol Cell* **17**(4), 1686-1696
213. Hemann, M. T., and Greider, C. W. (1999) *Nucleic acids research* **27**(20), 3964-3969
214. van Steensel, B., and de Lange, T. (1997) *Nature* **385**(6618), 740-743
215. Smith, S., and de Lange, T. (2000) *Curr Biol* **10**(20), 1299-1302
216. Karlseder, J., Smogorzewska, A., and de Lange, T. (2002) *Science* **295**(5564), 2446-2449
217. Denchi, E. L., and de Lange, T. (2007) *Nature* **448**(7157), 1068-1071
218. Guo, X., Deng, Y., Lin, Y., Cosme-Blanco, W., Chan, S., He, H., Yuan, G., Brown, E. J., and Chang, S. (2007) *Embo J* **26**(22), 4709-4719
219. Crabbe, L., Verdun, R. E., Haggblom, C. I., and Karlseder, J. (2004) *Science* **306**(5703), 1951-1953
220. Atanasiu, C., Deng, Z., Wiedmer, A., Norseen, J., and Lieberman, P. M. (2006) *EMBO Rep* **7**(7), 716-721
221. Tatsumi, Y., Ezura, K., Yoshida, K., Yugawa, T., Narisawa-Saito, M., Kiyono, T., Ohta, S., Obuse, C., and Fujita, M. (2008) *Genes Cells* **13**(10), 1045-1059
222. Sfeir, A., Kosiyatrakul, S. T., Hockemeyer, D., MacRae, S. L., Karlseder, J., Schildkraut, C. L., and de Lange, T. (2009) *Cell* **138**(1), 90-103
223. Oikawa, S., Tada-Oikawa, S., and Kawanishi, S. (2001) *Biochemistry* **40**(15), 4763-4768
224. Dizdaroglu, M., Kirkali, G., and Jaruga, P. (2008) *Free radical biology & medicine* **45**(12), 1610-1621
225. Hu, J., de Souza-Pinto, N. C., Haraguchi, K., Hogue, B. A., Jaruga, P., Greenberg, M. M., Dizdaroglu, M., and Bohr, V. A. (2005) *J Biol Chem* **280**(49), 40544-40551
226. Akbari, M., and Krokan, H. E. (2008) *Mech Ageing Dev* **129**(7-8), 353-365
227. Michaels, M. L., Cruz, C., Grollman, A. P., and Miller, J. H. (1992) *Proceedings of the National Academy of Sciences of the United States of America* **89**(15), 7022-7025
228. Grollman, A. P., and Moriya, M. (1993) *Trends Genet* **9**(7), 246-249
229. Boiteux, S., and Radicella, J. P. (1999) *Biochimie* **81**(1-2), 59-67
230. Nakabeppu, Y., Sakumi, K., Sakamoto, K., Tsuchimoto, D., Tsuzuki, T., and Nakatsu, Y. (2006) *Biological chemistry* **387**(4), 373-379

231. Kunisada, M., Sakumi, K., Tominaga, Y., Budiyanto, A., Ueda, M., Ichihashi, M., Nakabeppu, Y., and Nishigori, C. (2005) *Cancer research* **65**(14), 6006-6010
232. Nakabeppu, Y., Tsuchimoto, D., Furuichi, M., and Sakumi, K. (2004) *Free radical research* **38**(5), 423-429
233. Oka, S., Ohno, M., Tsuchimoto, D., Sakumi, K., Furuichi, M., and Nakabeppu, Y. (2008) *Embo J* **27**(2), 421-432
234. Xie, Y., Yang, H., Miller, J. H., Shih, D. M., Hicks, G. G., Xie, J., and Shiu, R. P. (2008) *Carcinogenesis* **29**(4), 722-728
235. de Souza-Pinto, N. C., Eide, L., Hogue, B. A., Thybo, T., Stevnsner, T., Seeberg, E., Klungland, A., and Bohr, V. A. (2001) *Cancer research* **61**(14), 5378-5381
236. Kruk, P. A., Rampino, N. J., and Bohr, V. A. (1995) *Proceedings of the National Academy of Sciences of the United States of America* **92**(1), 258-262
237. Askree, S. H., Yehuda, T., Smolikov, S., Gurevich, R., Hawk, J., Coker, C., Krauskopf, A., Kupiec, M., and McEachern, M. J. (2004) *Proceedings of the National Academy of Sciences of the United States of America* **101**(23), 8658-8663
238. de Souza-Pinto, N. C., Maynard, S., Hashiguchi, K., Hu, J., Muftuoglu, M., and Bohr, V. (2009) *Molecular and cellular biology*
239. Lomax, M. E., Cunniffe, S., and O'Neill, P. (2004) *DNA Repair (Amst)* **3**(3), 289-299
240. Mourgues, S., Lomax, M. E., and O'Neill, P. (2007) *Nucleic acids research* **35**(22), 7676-7687
241. Thompson, L. H., and West, M. G. (2000) *Mutat Res* **459**(1), 1-18
242. d'Adda di Fagagna, F., Reaper, P. M., Clay-Farrace, L., Fiegler, H., Carr, P., Von Zglinicki, T., Saretzki, G., Carter, N. P., and Jackson, S. P. (2003) *Nature* **426**(6963), 194-198
243. Crabbe, L., Jauch, A., Naeger, C. M., Holtgreve-Grez, H., and Karlseder, J. (2007) *Proceedings of the National Academy of Sciences of the United States of America* **104**(7), 2205-2210
244. Saharia, A., Guittat, L., Crocker, S., Lim, A., Steffen, M., Kulkarni, S., and Stewart, S. A. (2008) *Curr Biol* **18**(7), 496-500
245. Yoshioka, Y., Kitagawa, Y., Takano, Y., Yamaguchi, K., Nakamura, T., and Saito, I. (1999) *J Am Chem Soc* **121**, 8712-8719
246. Saito, I., Nakamura, I., and Nakatani, K. (1998) *J Am Chem Soc* **120**, 12686-12687
247. Brevet, V., Berthiau, A. S., Civitelli, L., Donini, P., Schramke, V., Geli, V., Ascenzioni, F., and Gilson, E. (2003) *Embo J* **22**(7), 1697-1706
248. Pawar, V., Jingjing, L., Patel, N., Kaur, N., Doetsch, P. W., Shadel, G. S., Zhang, H., and Siede, W. (2009) *Mech Ageing Dev*
249. Carson, M. J., and Hartwell, L. (1985) *Cell* **42**(1), 249-257
250. Adams, A. K., and Holm, C. (1996) *Molecular and cellular biology* **16**(9), 4614-4620
251. Vartanian, V., Lowell, B., Minko, I. G., Wood, T. G., Ceci, J. D., George, S., Ballinger, S. W., Corless, C. L., McCullough, A. K., and Lloyd, R. S. (2006)

Proceedings of the National Academy of Sciences of the United States of America **103**(6), 1864-1869
252. Swanson, R. L., Morey, N. J., Doetsch, P. W., and Jinks-Robertson, S. (1999) *Molecular and cellular biology* **19**(4), 2929-2935
253. Palm, W., and de Lange, T. (2008) *Annual review of genetics* **42**, 301-334
254. Wang, F., Podell, E. R., Zaug, A. J., Yang, Y., Baciu, P., Cech, T. R., and Lei, M. (2007) *Nature* **445**(7127), 506-510
255. Dianov, G. L., and Parsons, J. L. (2007) *DNA Repair (Amst)* **6**(4), 454-460
256. Wallace, S. S. (2002) *Free radical biology & medicine* **33**(1), 1-14
257. Dodson, M. L., and Lloyd, R. S. (2002) *Free radical biology & medicine* **32**(8), 678-682
258. Robertson, A. B., Klungland, A., Rognes, T., and Leiros, I. (2009) *Cell Mol Life Sci* **66**(6), 981-993
259. Tchou, J., Kasai, H., Shibutani, S., Chung, M. H., Laval, J., Grollman, A. P., and Nishimura, S. (1991) *Proceedings of the National Academy of Sciences of the United States of America* **88**(11), 4690-4694
260. Richter, T., and von Zglinicki, T. (2007) *Exp Gerontol* **42**(11), 1039-1042
261. Kawanishi, S., and Oikawa, S. (2004) *Ann N Y Acad Sci* **1019**, 278-284
262. Wang, Z., Rhee, D. B., Lu, J., Bohr, C. T., Zhou, F., Vallabhaneni, H., de Souza-Pinto, N. C., and Liu, Y. (2010) *PLoS genetics* **In press**
263. Ghosh, A., Rossi, M. L., Aulds, J., Croteau, D., and Bohr, V. A. (2009) *J Biol Chem* **284**(45), 31074-31084
264. Klungland, A., and Bjelland, S. (2007) *DNA Repair (Amst)* **6**(4), 481-488
265. Hanaoka, S., Nagadoi, A., and Nishimura, Y. (2005) *Protein Sci* **14**(1), 119-130
266. Richter, T., Saretzki, G., Nelson, G., Melcher, M., Olijslagers, S., and von Zglinicki, T. (2007) *Mech Ageing Dev* **128**(4), 340-345
267. Saito, I., Takayama, M., Sugiyama, H., Nakatani, K., Tsuchida, A., and Yamamoto, M. (1995) *Journal of the American Chemical Society* **117**(23), 6406-6407
268. Sugiyama, H., and Saito, I. (1996) *Journal of the American Chemical Society* **118**, 7063−7068
269. Hall, D. B., Holmlin, R. E., and Barton, J. K. (1996) *Nature* **382**(6593), 731-735
270. Barone, F., Lankas, F., Spackova, N., Sponer, J., Karran, P., Bignami, M., and Mazzei, F. (2005) *Biophys Chem* **118**(1), 31-41
271. Sahin, E., and Depinho, R. A. *Nature* **464**(7288), 520-528
272. von Zglinicki, T. (1998) *Ann N Y Acad Sci* **854**, 318-327

Vita

David Beomjin Rhee was born in Seoul, South Korea, where he spent his early and part of his middle childhood until his family immigrated to Arlington, Texas. After moving to Texas, he attended South Davis Elementary School, Crockett Middle School, Boles Junior High School, and James Martin High School where he received his diploma in 1998. Following high school, he enrolled in Baylor University in Waco, Texas as Pre-dental Biology major. However, he soon changed his major after realizing his desire to pursue a career in programming. At that time, Baylor University was one of the few Universities in the United States to offer Bioinformatics as an undergraduate major. Thus, he gladly took the challenge of studying both Biology and Computer Science simultaneously. He went on to earn his Bachelor of Science (B.S.) degree in Informatics, concentrating in Bioinformatics, in 2003. After finishing his college education, he was accepted into the Graduate School of Genome Science and Technology, which is a joint program between the University of Tennessee in Knoxville and the Oak Ridge National Laboratory (ORNL) in 2004. He joined Dr. Yie Liu's group in ORNL to study mammalian telomeres. Shortly after he joined the lab, Dr. Yie Liu's group moved to National Institute on Aging (NIA) in Baltimore, Maryland. He followed his advisor to NIA to continue working on his dissertation, and earned his Doctor of Philosophy (Ph.D.) degree in 2010. Following graduate study, he went on to work as a post-doctoral fellow in Dr. Asa Abeliovich's group in Columbia University in New York.